ABSTRACT

ZHU JIANCHENG. Benzimidazolyl Palladium Complexes as Highly Active Bifunctional Catalysts for Sustainable Cross-Coupling, C–H Functionalization and Hyperpolarization, and Approach to Light-mediated Fluoroethylation of Heteroarenes. (Under the direction of Dr. Vincent Lindsay).

Protic N-heterocyclic carbene (NHC)-metal complexes have received considerable attention from the scientific community because of their structural properties and their interesting potential for catalyzing organic transformations. Current studies about the syntheses and application are far from sufficient. Herein, both the synthesis of a family of 2-benzimidazolyl palladium complexes and their applications in C–H activation and sustainable cross-coupling reactions are reported.

Cyclopropanone, a highly strained ketone, is a promising three carbon building block in organic transformations partially because of the versatile ring-opening or expansion reactions. Cyclopropanone precursors, such as 1-sulfonylcyclopropanols, were found to react with Selectfluor® in aqueous media to generate fluoropropionic acids. By combining this process with a subsequent Minisci-type reaction or cross-electrophile coupling reaction, we have developed the first C–H fluoroethylation of heteroarenes. Although fluorination is a popular topic in synthetic community, no research of fluoroethylation has been reported to the best of our knowledge.

Hyperpolarization processes significantly increase the signal strength of nuclear magnetic resonance (NMR) and magnetic resonance imaging (MRI) thus increase the *in vivo* detectability of bioactive molecules. In collaboration with the Theis group at North Carolina State University, several new NHC iridium complexes that can potentially catalyze hyperpolarization with high efficiency were synthesized. Evaluation of these complexes is underway in the Theis laboratory.

Benzimidazolyl Palladium Complexes as Highly Active Bifunctional Catalysts for Sustainable Cross-Coupling, C–H Functionalization and Hyperpolarization, and Approach to Light-mediated Fluoroethylation of Heteroarenes

by
Jiancheng Zhu

A dissertation submitted to the Graduate Faculty of
North Carolina State University
in partial fulfillment of the
requirements for the degree of
Doctor of Philosophy

Fiber & Polymer Science

Raleigh, North Carolina
2020

APPROVED BY:

Vincent Lindsay Committee Co-Chair	Januka Budhathoki Uprety Committee Co-Chair
Jonathan Lindsey	Wei-Chen Chang
Emily Griffith	

DEDICATION

To my father who passed away one year before my graduation.

BIOGRAPHY

Jiancheng Zhu was born and raised in Tianjin, China. He received his B. A. and B. E. in Chemistry and Chemical Engineering in 2010 from the joint undergraduate program of Nankai University and Tianjin University, respectively. He joined the Chemistry Department at North Carolina State University in August 2011. As a graduate student, he worked on the material chemistry project first, where he grafted the biodegradable oligolactic acids onto device surfaces as polymer brushes for antibiofouling. He then changed his research interest, co-majored in the Fiber and Polymer Science graduate program of the Department of Textile Engineering, Chemistry and Science in 2015 and joined the Lindsay lab in August 2016, where he worked on the organic methodology and organometallics project, including the design, synthesis and application of novel (benz)imidazolyl transition metal complexes.

ACKNOWLEDGMENTS

My research would have been impossible without the support of my advisor, Dr. Vincent Lindsay. His mentorship, diligence, kindness and the good research environment he provided in our laboratory have deeply affected me and will change my life in the future. I thank him for helping me out in my most difficult time.

I would like to thank Dr. Januka Budhathoki-Uprety, Dr. Jonathan Lindsey, Dr. Wei-Chen Chang and Dr. Emily Griffith for being my committee members.

Finally, it is my sincere thanks to my family. Thank you all for the extraordinary support and sacrifice you provided during my Ph.D. life.

TABLE OF CONTENTS

LIST OF FIGURES

LIST OF TABLES

LIST OF SCHEMES

LIST OF ABBREVIATIONS

Ac-Gly-OH	N-acetylglycine
AgOAc	Silver acetate
*n*BuLi	*n*-Butyllithium
*n*BuOH	*n*-Butanol
CN	Isocyanide
CH_3NO_2	Nitromethane
CsF	Cesium fluoride
DMSO	Dimethyl sulfoxide
DCM	Dichloromethane
DMF	*N*,*N*-Dimethylformamide
Et_2O	Diethyl ether
HNO_3	Nitric acid
H_2SO_4	Sulfuric acid
HFIP	Hexafluoro-2-propanol
Ir	Iridium
$[Ir(cod)Cl]_2$	Bis(1,5-cyclooctadiene)diiridium(I) dichloride
KO*t*Bu	Potassium *tert*-butoxide
KPF_6	Potassium hexafluorophosphate
KCl	Potassium chloride
LiHMDS	Lithium bis(trimethylsilyl)amide
LDA	Lithium diisopropylamide
2-MeTHF	2-Methyltetrahydrofuran
MeI	Iodomethane
Me_3OBF_4	Trimethyloxonium tetrafluoroborate
MeCN	Acetonitrile
MeLi	Methyl lithium
MeOH	Methanol
NH_4PF_6	Ammonium hexafluorophosphate
*p*NHC	*Protic* N-heterocyclic carbene
PG	Protecting group
$Pd_2(dba)_3$	Tris(dibenzylideneacetone)dipalladium(0)
$Pd(PPh_3)_4$	Tetrakis(triphenylphosphine)palladium(0)
$Pd(OAc)_2$	Palladium(II) acetate
$PdCl_2$	Palladium(II) chloride
PhMe	Toluene
$[RhCl_2Cp^*]_2$	Pentamethylcyclopentadienylrhodium(III) chloride dimer
rt	Room temperature
THF	Tetrahydrofuran
TFFH	Tetramethylfluoroformamidinium hexafluorophosphate

CHAPTER 1

General Introduction

1.1. Introduction to Green and Sustainable Cross-Coupling Reactions

Because of their excellent reliability and ease, catalytic cross-coupling reactions of organic (pseudo) halides and corresponding coupling partners have been established as a state-of-the-art method for synthetic chemists.[1] As being observed in early 1970s, palladium catalysis showed high efficiency in forming C_{sp2}-C_{sp2}/C_{sp2}-C_{sp3} structure motif.[2] These types of transformations make use of easily available substrates and access to the preparation of substituted (hetero)arenes in a much shorter and more selective way compared to non-catalytic pathways, exhibiting both the chemoselectivity and broad functional group (FG) tolerance. All these advantages led them to the wide application in academia[3] as well as pharmaceutical, agrochemical and fine chemical industries[4]. Among them, Suzuki-Miyaura[2], Heck-Mizoroki[5] and Sonogashira-Hagihara[6] reactions have been especially studied in terms of the mechanism, scope, optimal conditions and applications owing to their contribution to the functionalization of pharma/material-demanded, complex building blocks.

For example, about 12% of all registered compounds in the most modern era of AstraZeneca screening collection contained biphenyl fragments constructed by Suzuki-Miyaura reactions, whereas only 2% over the period of 1982 to 1990, representing a 6-fold increase in use of this approach over the years.[4a] Two examples illustrating the tremendous contribution of cross-couplings to drug molecules are presented in **Figure 1**.[7] The synthesis of the angiotensin II receptor antagonist Losartan and Hepatitis C virus (HCV) inhibitor Ledipasvir can hardly be realized without using the Suzuki-Miyaura reaction. Further investigation on the data set IBEX indicated that *para*-substituted arrangement was 5-6 and 2-3 times more frequent than *meta*- and *ortho*-substitution, respectively, whether in mono- or di-substituted biphenyl compounds (**Figure 2**).[8] As the demand of *meta*- or *ortho*- substituted compounds is commonly seen in a myriad of medicinal chemistry reports, these studies generally summarized the synthetic challenges met by the pharmaceutical industry and highlighted the requirement for the development of more active (Pd) catalysts.

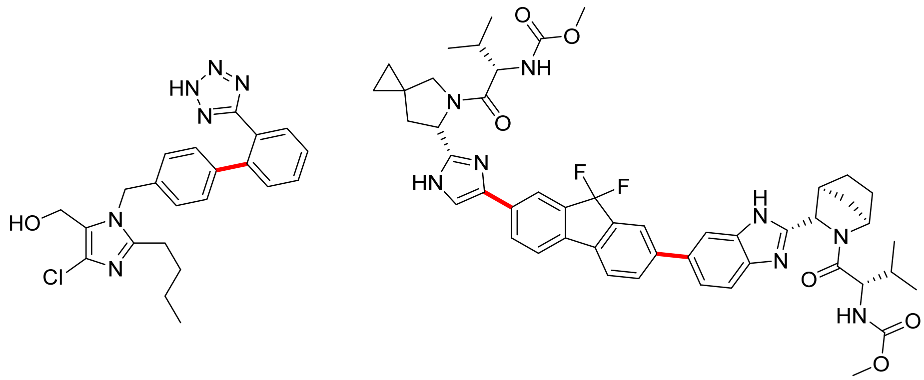

Figure 1: Two examples of drugs with biphenyl motif made via Suzuki-Miyaura reaction.

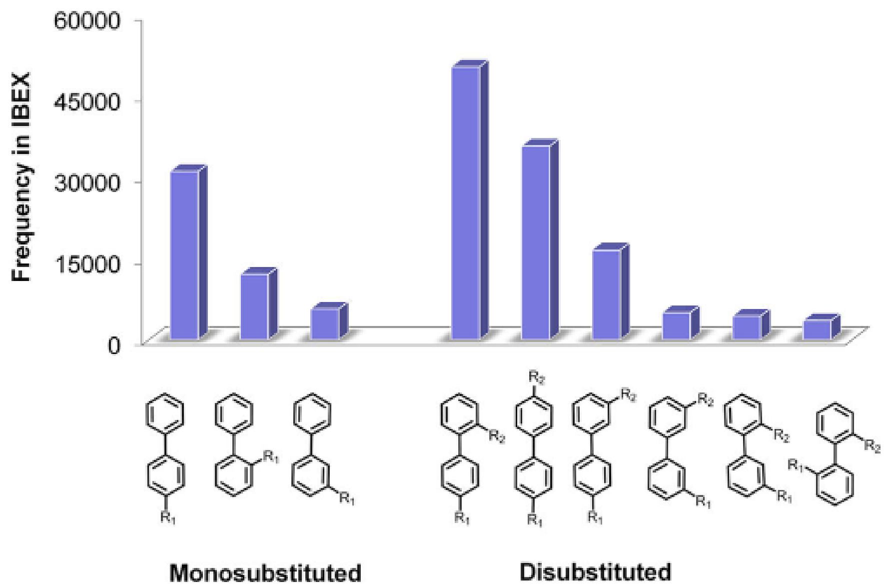

Figure 2: Frequency population of various biphenyl regioisomers in the IBEX.[8]

However, there exists a more intimidating challenge, the need of environmentally benign organic transformations, that synthetic chemist has to face in the 21th century.[9] The biocompatible problem brought by traditional pharmaceutical and fine chemical industry, including toxic byproducts, waste management of organic solvents and byproducts, and invested energy, are known to be enormous.[10] Some industrialized organic transformations, including cross-coupling reactions, have been developed to fit part of the 12 Principles of Green Chemistry in terms of high degree of selectivity and low metal catalyst loading.[9] But the road to further improve this feature is still long in many aspects, such as reducing noble metal catalyst loading to trace amount,[11] replacing petroleum-based solvents with "greener" biomass-derived alternatives and increasing atom economy. For instance, the commonly used phosphine/Palladium ligand/metal catalysis for the three cross-couplings mentioned above are considered as expensive, moisture/air sensitive, bio-incompatible and hard to fully separate from the final product, which hampers the use of these reactions in the late stages of preparation of pharmaceuticals.[12] Over 80% of auxiliary waste and toxic materials produced by the practice of synthetic chemistry worldwide is attributable to a single reaction variable: petroleum-based organic solvents[13]. While a variety of media, such as ionic and supercritical liquid,[13, 14] have been studied as alternatives, water, alcohol and other biomass-derived solvents,[12a] e.g. 2-MeTHF, are merited as inexpensive, biocompatible, abundant and safe-to-use, thus still be the most eco-friendly options. An atom-efficient alternative, C–H activation, does not require pre-installation of FGs on substrates thus eliminates the generation of byproducts formed by transmetalation. All of these challenges drive modern synthetic chemists to design new catalysts with high efficiency while being compatible in green conditions.

1.2. Introduction to C–H Activation and Our *p*NHC-based Catalytic Cycle

Compared with cross-coupling reactions, recent studies on C–H activation have significantly changed the way chemists design the synthesis of pharmaceuticals and natural products. Generally, C–H activation brings fragments together in a convergent manner by coupling C–H bonds to forge the requisite C–C bond of the target compound, where at least one partner is not pre-functionalized.[15] So the more "direct" synthesis achieved through this way constitutes a step-economical transformation. For example, the synthesis of carbazole alkaloids took advantage of the proximity effect in intramolecular C–H coupling (**Scheme 1**).[16] Researchers further use the methodology in the streamlined synthesis of more complex natural products. Gutekunst and Baran reported the total synthesis of Piperarborenine B, a dimeric cyclobutane containing natural product, by sequential C(sp^3)–H arylation with complete regio- and stereoselectivity, on gram scale (**Figure 3**).[17]

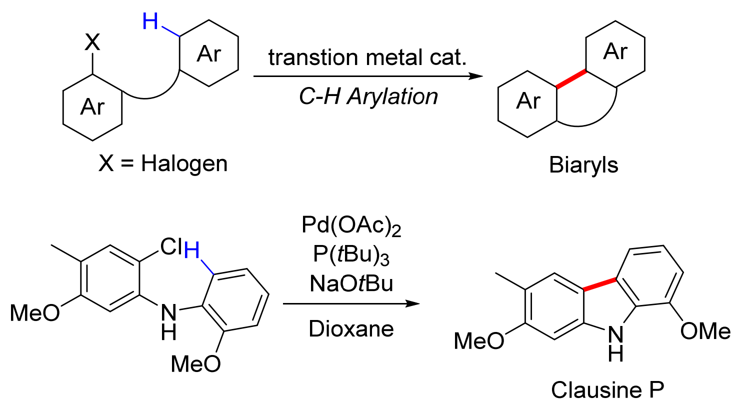

Scheme 1: Metal-catalyzed intramolecular C–H/C–X biaryl coupling scheme representation and application on natural product.

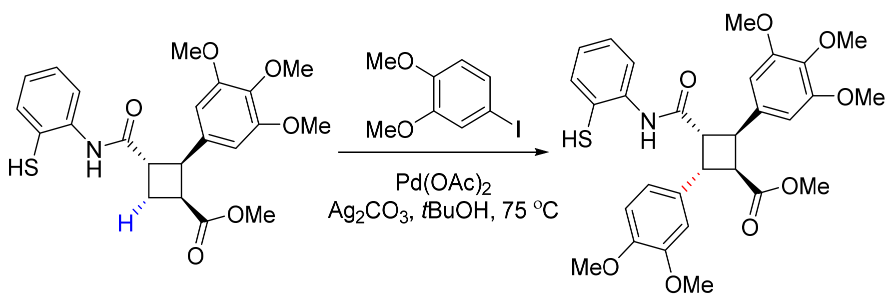

Figure 3: Key directed C–H activation in the synthesis of Piperarborenine B.

The C–H bond is known to be robust (enthalpy equals 413 kJ/mol, 298 K). In order to facilitate the activation process and achieve the regioselectivity, general approaches, which rely on either the electronic/steric properties of the substrate or the use of Directing Groups (DGs) that coordinate to the metal center to direct the activation, have been established.[18] Some literature reports about the preparation and use of special DG templates have even realized *meta*-C–H activation (**Scheme 2**).[19] But they were often plagued by either the challenging preparation of the templates or the use of stoichiometric DG and an extra step of DG deconstruction. Instead of pre-installing stoichiometric DG on the substrate, the "Traceless Directing Group" (TDG) strategy has emerged as another choice to save steps of installation and removal of DGs, where the DG is removed in the same step as the C–H functionalization.[20]

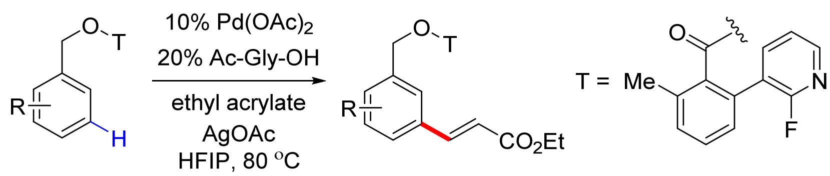

Scheme 2: Remote *meta*-C–H activation DG template.

Our catalytic design combine the metal catalyst with a DG imbedded in the ligand template, in order to realizes a "Catalytic Directing Groups" (CDG) strategy, being overall only one step and using only catalytic amount of the DG. The goal is to use the *protic* NH wingtip of N-heterocyclic carbene (NHC) as a catalytic directing site through equilibrated acylation and deacylation with the substrate (**Scheme 3**). The C-bound imidazolyl ligand is used for reversible binding with the substrate while the metal center serves as the activator of a proximal *ortho* C–H bond.

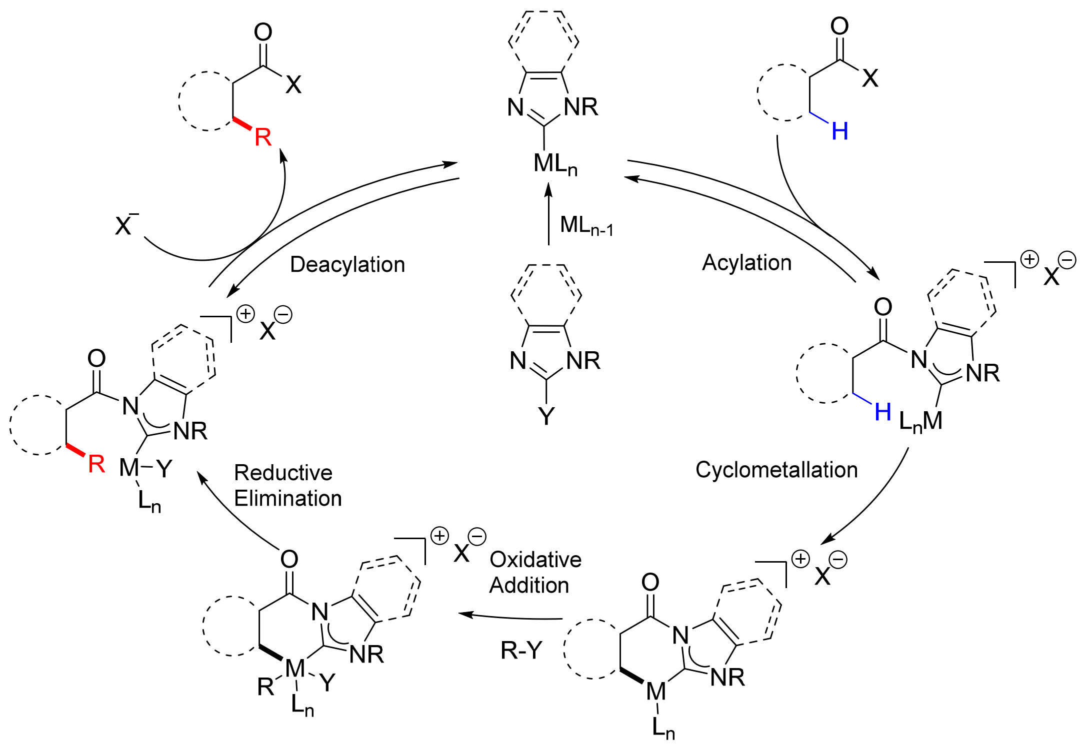

Scheme 3: Mechanism proposed for the imidazolyl-metal complex catalyzed directed C–H activation.

1.3. Introduction to *Protic* NHC-Metal Complexes and Potential Application

NHCs have been developed as a prominent class of efficient ligands in coordination and catalytic chemistry, not only because of their chemical robustness but also the electronic and steric tunability.[21] Classic di-N-substituted ligands, where both N wingtips of NHCs are substituted, are most commonly used. Modification of the bulkiness of substitutions on the ring-nitrogen can exert an important impact on the steric demand in the coordination sphere of a metal atom while structural change on both ring-nitrogen and carbon backbone of the heterocyclic skeleton affects the σ-donor properties of NHCs.[22] All of these factors influence the catalytic activity and selectivity of NHC complexes and give access to chemist to versatile reactions as the classic di-N-substituted NHC-Pd complexes (I) have been employed in a variety of cross-coupling and C–H activation reactions.[23] However, the study of *protic* NHC-metal complexes (*p*NHC) with one or both N left unfunctionalized (II) is still insufficient, let alone the applications.

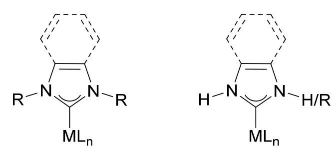

I classic NHC   II *protic* NHC

Our design of the catalytic cycle, including the nucleophilicity of N on NHCs, is supported by the research of Crabtree[24] and Hahn[25] et al. (**Figure 4**). The Brønsted-basicity/nucleophilicity of the N wingtip of *p*NHC ligands has been demonstrated, showing that the lone pair on N is nucleophilic enough to undergo alkylation with the existing (b) or to-be-installed (a) metal centre unaffected. Both the thermo-stability of *N*-acyl protected NHC-metal complex and the suitable proximity of the *ortho*-protons on the phenyl ring with Ir indicated that the lone pair on N can potentially play an important role in catalysis and furnish the catalytic cycle of our proposed C–H activation (**Scheme 3**).

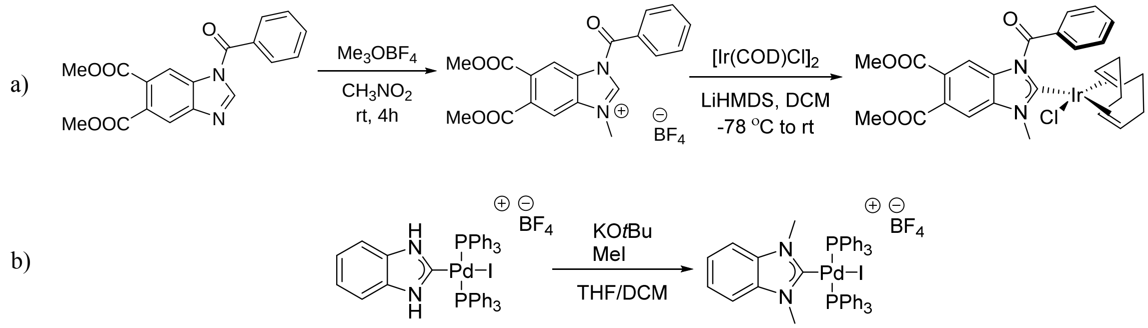

Figure 4: Utilizing the nucleophilicity of N site of NHCs to do acylation and alkylation, (a) Crabtree et al,[24] (b) Hahn et al.[25]

In **part 1**, **2** and **3** of this document, we report the first readily accessible syntheses of four mono- or tri-dentate benzimidazolyl palladium complexes. We further studied their catalytic activity in C–H activation and cross-couplings, including Suzuki, Heck and Sonogashira reactions. These benzimidazolyl-Pd complexes exhibited excellent efficiency of catalysis in water or alcohols with trace amount of catalyst loading (0.01 mol%) for the cross-couplings. To the best of our knowledge, this is the first example of the *p*NHC-Pd (type) complexes used in catalyzing cross-coupling reactions. The free nucleophilic N wingtip on the bifunctional catalyst is proposed to enhance the catalytic activity by an accelerated transmetallation step, explaining the significant efficiency of these new complexes in sustainable cross-coupling reactions.

1.4. Introduction to Visible-Light Photocatalysis in C–H Fluorination

Owing to their low reactivity and high thermodynamic stability, although being ubiquitous in organic compounds, C–H bonds do not seem to be operative FGs.[26] Highly selective C–H functionalization in the laboratory remains a great challenge to accomplish. The C–H activation platform mediated by transition-metal-catalysis, including Pd, Cu, Rh and Au, built up by modern synthetic chemists, significantly improved the atom and step economy for target molecule construction.[15, 26] However, this platform is often plagued by high energy consumption and limited functional group compatibility. Usually, high reaction temperatures are needed, which means the use of exhaustive and nonrenewal fossil fuels for applying the kind of reactions in chemical industry. Also, although this kind of reactions is operative for several FGs on coupling partners, for example, halogens, alkenes, alkynes and heteroatoms, the common FGs, carboxylic acid and esters are often not compatible, which highly limits the application in late-stage modification of material and drug molecules.[27]

The pioneers in this area have also dedicated efforts to convert solar energy into chemical energy for organic transformations. Light-induced organic reactions, including C–H functionalization were not well-recognized, which was attributed to the poor efficiency of light absorption by organic molecules, until a milestone made by MacMillan[28] and Yoon[29] demonstrating the utilization of visible light to form new C–C and C–Heteroatom bonds. Owing to the advantages in environmentally benign features, visible-light-induced photocatalysis has developed rapidly and attracted considerable attention in both academia and industry. Several commonly used photocatalysts are listed in **Figure 5**.[27]

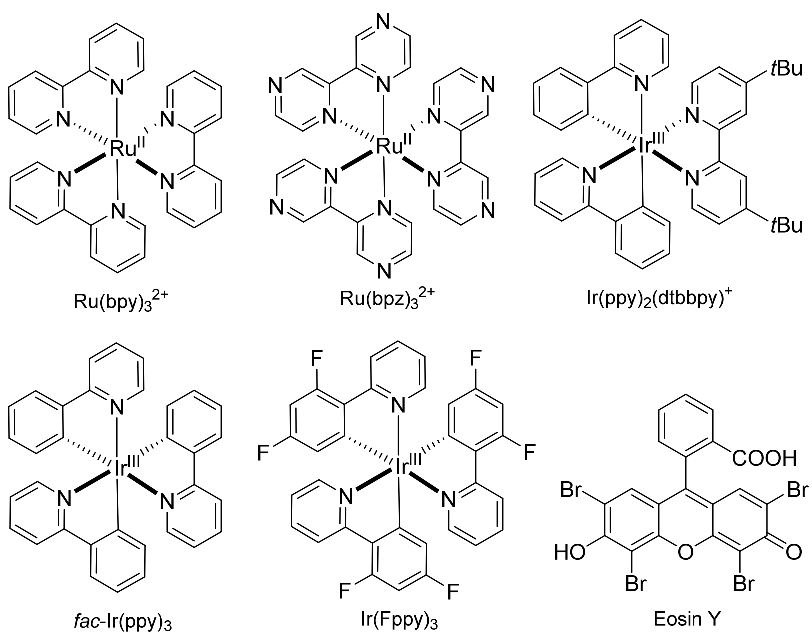

Figure 5: Chemical Structures of typical photocatalysts.

The chemistry of fluorination on bioactive molecules has drawn significant attention from synthetic and medicinal chemists since more than 15 percent of launched drug molecules worldwide over the past 50 years contain at least one fluorine atom.[30] Although the relationship of physiological activity and molecular structure for fluorine-containing compounds still largely depends on experimentation rather than design, (e.g., what kind of fluorine functionalities should be introduced and where should the functionalities be introduced) fluorination chemistry is well recognized as beneficial for altering the properties of antimetabolite, lipophilicity and acidity for drugs because of the unique properties of the fluorine atom.[31]

Fluorine is a small atom with the van der Waals radius of 1.47 Å, which is close to hydrogen atom with the value of 1.20 Å. The influence of fluorine is marginal compared to other halogens in terms of steric effects.[30] However, the electronegativity of fluorine is high (3.98 on the Pauling electronegativity scale) compared to O (3.44), H (2.20) and C (2.55), which makes a highly polarized C–F bond with a strong bond-dissociation energy (481 kJ/mol, 298 K). The strong electron withdrawing nature of fluorine is also evidenced by the effect on the acidity of neighboring FGs. For example, linear and cyclic amines become much less basic with β-, γ-, even δ-fluorine substitution.[30] CF_2H is recognized as a weak lipophilic hydrogen bond donor and the acidity is stronger when it is at a position α to sulfoxide or sulfone.[32]

Synthetic methods in organofluorine chemistry have made huge progress in recent years, especially in the field of C–H fluorination. Using the concept of TDG raised by Yu et al., Chen and Sorensen realized a direct, Pd-catalyzed *ortho* C–H fluorination of benzaldehydes with orthanilic acids as TDGs.[33] In terms of the light-induced C–H fluorination, the research team of Nicewicz developed a mild method for the ^{18}F-fluorination of aromatic C–H bonds by a $[^{18}F]F^-$ salt via organic photocatalysis under blue LED illumination (**Figure 6**).[34] The significance of this work is that the radiolabeled products can serve as diagnostic agents for the development of positron emission tomography (PET) imaging. Although there are more and more scientific reports about Minisci-type light-mediated fluorination to date, most of them focused on di- or trifluoroalkylation and no monofluoroethylation of (hetero)arenes has been reported to the best of our knowledge.

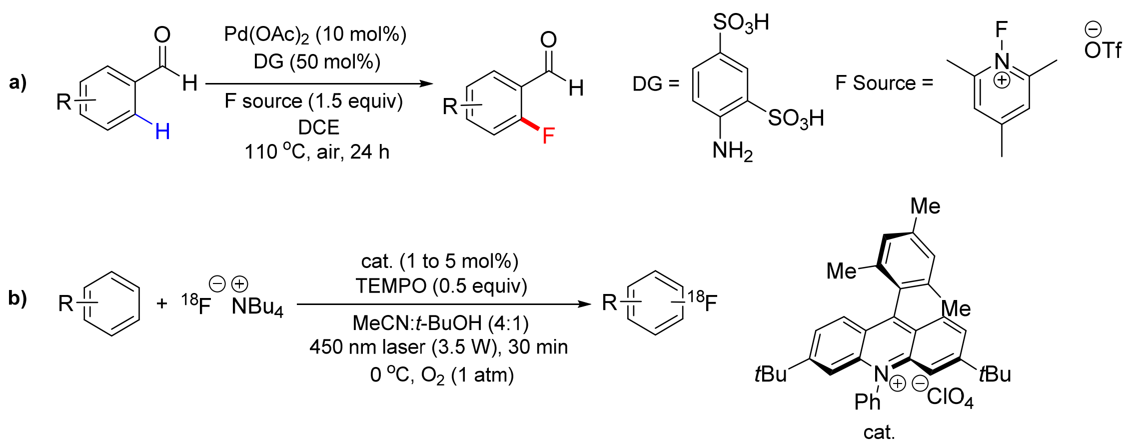

Figure 6: C–H fluorination: (a) TDG of Sorensen et al.,[33] (b) Organophotoredox of Nicewicz et al.[34]

One of the main research topic in the Lindsay group is ring-opening reaction of 1-sulfonylcyclopropanol, the sulfinate adduct of cyclopropanone, and the synthetic method to using the ring-opened product for modification of bioactive molecules. Fluoropropionic acid was generated *in situ* by treating 1-(methylsulfonyl)cyclopropanol with stoichiometric Selectfluor® in aqueous media. In **part 4** of this document, the approach to a decarboxylative, Minisci-type, light-mediated fluoroethylation of (hetero)arenes is described as the application of the fluorocarboxylic acid product of such reaction.

1.5. Introduction to *para*-Hydrogen-Induced Hyperpolarization Processes Mediated by NHC-Ir Complexes

Hyperpolarization methods that can be potentially used for the *in vivo* observation of molecular metabolism can significantly increase the signal strength of nuclear magnetic resonance (NMR) and magnetic resonance imaging (MRI).[35-37] The process transfers the latent magnetism of *para*-hydrogen into a substrate, for example, drug molecules, to improve its NMR detectability at low concentration without changing its chemical identity.[38] Signal amplification by reversible exchange (SABRE) has drawn significant attention from scientific community for this fast growing field of research. The hyperpolarization process, SABRE, transfers the associated non-Boltzmann distribution of spin energies from *para*-hydrogen (p-H_2) to a ligated substrate molecule via the reversible binding to a metal catalyst, which is NHC-Ir complexes in our study (**Figure 7**).

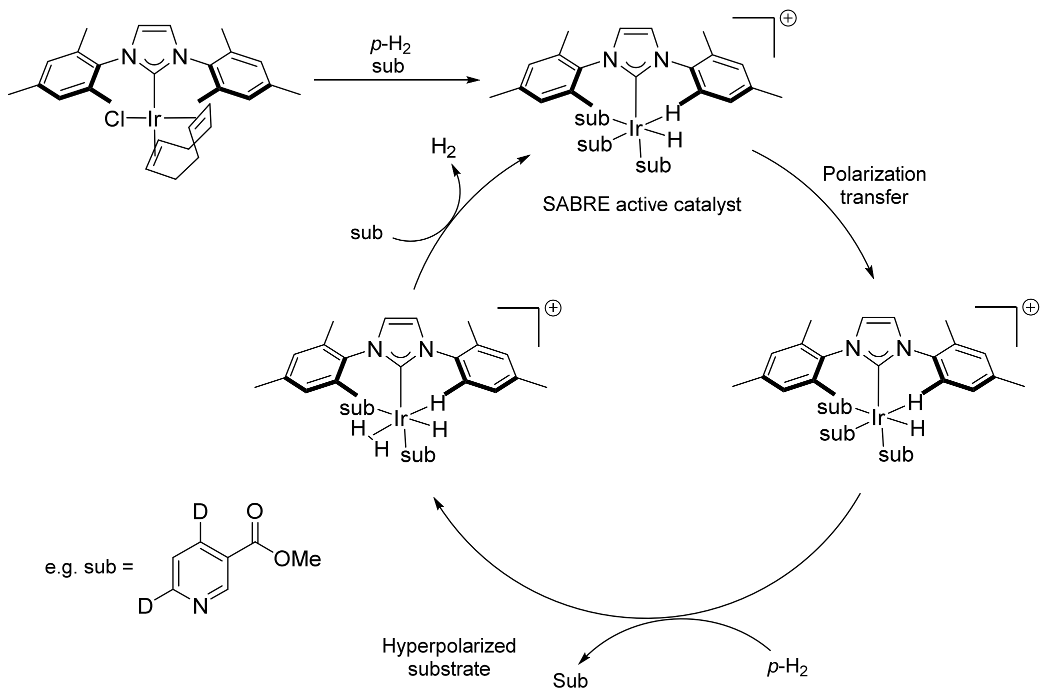

Figure 7: The SABRE catalytic cycle: hyperpolarized substrates concentrate in solution through the reversible binding of substrate (sub) and *p*-H_2.

A thorough study conducted by Duckett and co-workers revealed that the structural differences of NHC-Ir complexes deeply affect the SABRE process. For example, aromatic NHC ligands are more effective mediators of the SABRE process than alkyl NHCs.[38] Further study exhibited that rate of substrate dissociation, buried volumn (%V_{bur}) of complex, Tolman Electronic Parameter (TEP) of NHC ligand and information provided by X-ray crystallography, such as the bond length of C_1–Ir, are other key factors that can affect the SABRE process.[38] In general, complexes with electron withdrawing group (EWG) on the backbone of imidazole have higher hyperpolarization activity. While di-bromo-modified NHC-Ir decomposed to a black precipitate once underwent *p*-H_2 addition, di-chloro-NHC-Ir complex showed the best SABRE effect and stability as demonstrated by Duckett et al.[38] Thus, further investigation focuses on rational design of imidazole ligands with other stable EWGs on the backbone or benzimidazole derivatives.

In **part 5** of this document, the synthesis of several new, electron-deficient mono-and polydentate NHC-Ir complexes is described for building up the library of catalysts. The work of testing the hyperpolarization effects of these complexes is currently in progress in the Theis laboratory.

CHAPTER 2

Design and Syntheses of 2-Benzimidazolyl Palladium Complexes

2.1. Introduction to *Protic* NHC-Metal Complexes: Property, Preparation and Our Design

It is the lone pair on N wingtip of *protic* NHC-metal complexes (II) that serves as the key factor of our strategy of C–H functionalization and cross-coupling reactions. Although the preparation and application on complexes (I) have been widely reported, research relating to its *protic* counterpart (II) is far from sufficient, partially because of the synthetic challenge, where the free N wingtip of the NHC can lead to tautomerization to a N-bound complex.[39] Limited amount of pioneering reports have exhibited not only the syntheses but also the chemical properties, such as nucleophilicity, hydrogen-bond donor/acceptor and catalytic activities of *protic* NHC-metal complexes, although no example about using the lone pair on the deprotonated N wingtip to achieve C–H activation through the acyl adduct, which is the complex synthesized by Crabtree et al., (**Figure 4a**) has been reported.[22] As shown in **Figure 8a**, an alkene with an ester group was reduced two times faster than that without FG, suggesting the bifunctional mode of the catalyst as a H-bond donor in the substrate recognition.[40] Additionally, acetonitrile was bifunctionally activated by the intramolecular nucleophilic attack of the N wingtip to yield an imine-chelated complex (**Figure 8b**).[41]

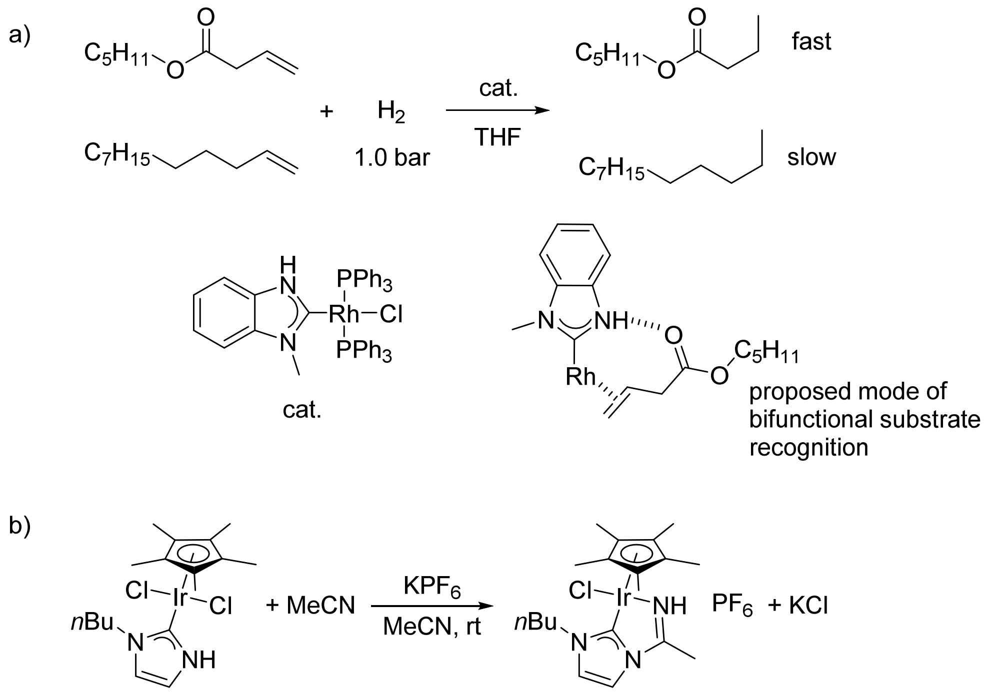

Figure 8: (a) Competitive hydrogenation of alkenes with and without a carbonyl group, catalyzed by a *p*NHC complex;[40] (b) Nucleophilic addition of a *p*NHC ligand at a coordinated nitrile.[41]

Classic synthetic methods to prepare *p*NHC complexes include formal tautomerization of azoles, annulation at a metal template, oxidative addition and chelation-assisted C–H activation. While the first two approaches have been reported only for limited kinds of metal under special conditions (**Figure 9**, **a** and **b**),[42] the last two methods (**Figure 9**, **c** and **d**) were selected to prepare the desired complexes.

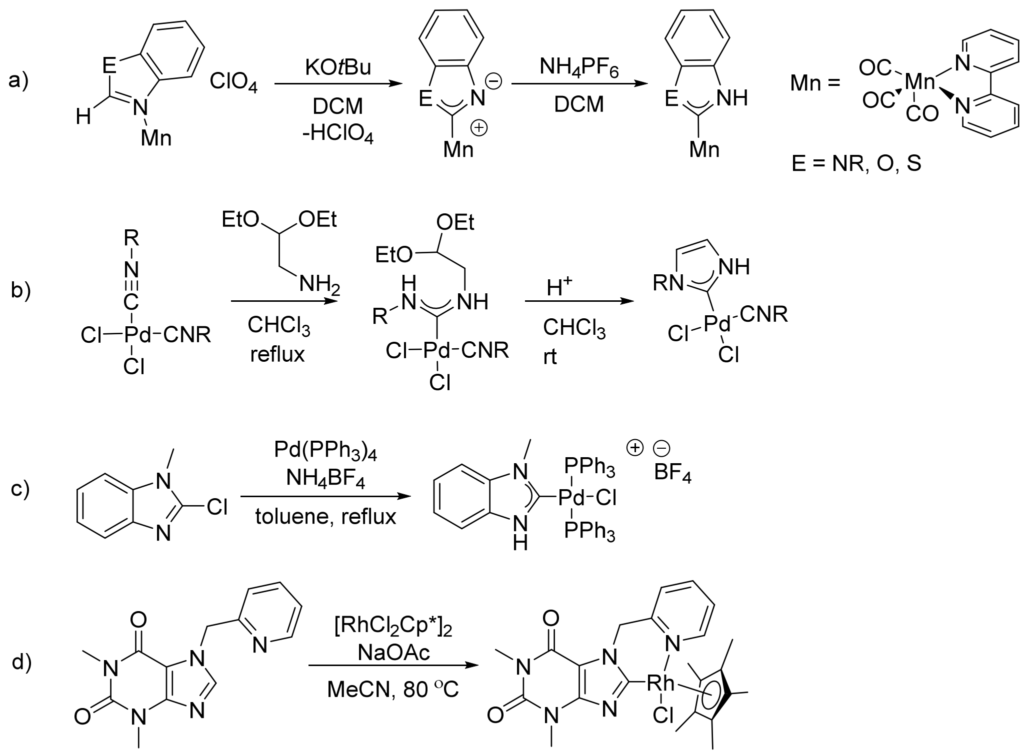

Figure 9: Representative example of *p*NHC-metal complexes syntheses: (a) formal tautomerization of azoles coordinated to manganese; b) Metal template approach from isocyanide complexes and α-aminoacetal; (c) Preparation of *p*NHC-Pd complex via oxidative addition; (d) Preparation of NHC-Rh (III) complex via chelation-directed C–H activation.

Several structural templates of *p*NHC-metal complexes are proposed in **Scheme 4**. They are expected to be acylated in C–H activation and facilitate the transmetallation in cross-coupling reactions using the free N wingtip of *p*NHC. As a starting point, a simple *N*-methyl template (**A**) was used for the complex preparation through oxidative addition.

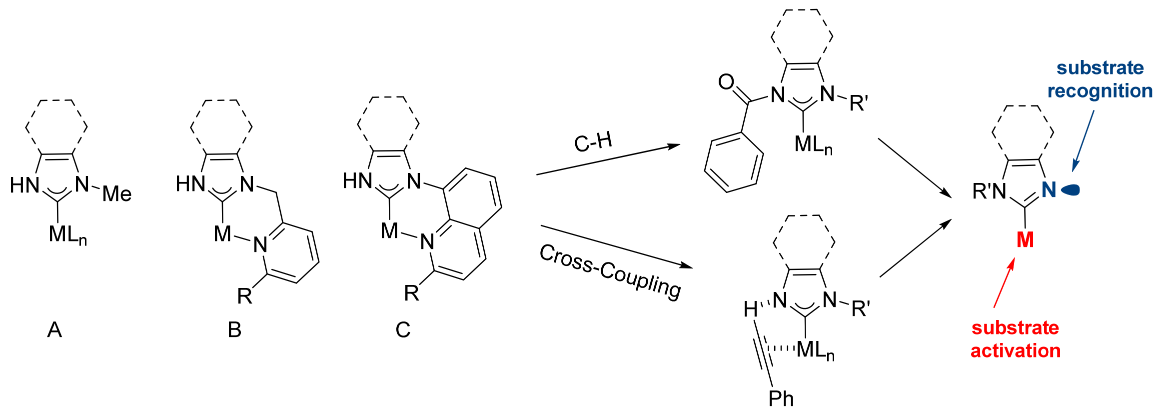

Scheme 4: *p*NHC-metal complexes templates, the potential application and the illustration of bifunctional mode (R = H or 2-pyridine).

Also, notice that pyridine(s) as a common ligand for metal binding will be installed on one N wingtip of NHC (**B** and **C**, **Scheme 4**) as a chelating side-arm, which was expected to lock the metal at C(1) of the NHC then direct the follow-up C–H activation. Another key reason for our choice of the side-arms was originated from the detailed mechanistic study reported by Ananikov and co-workers.[43] Pd (0) species was found to be generated *in-situ* during cross-coupling reactions using NHC-Pd (II) as catalysts in the presence of conventionally engaged bases (**Figure 10a**). Pd sources that functioned in ArX oxidative-addition-dependent reactions were also found to not exist as the presented chemical formula of Pd precatalysts, e.g. $Pd_2(dba)_3$, $Pd(PPh_3)_4$ and NHC-Pd.[44] According to the computational study of leaching/capture pathways and analysis of stabilization energy reported by Ananikov et al., reversible leaching of Pd nanoparticles derived from precatalyst to three destinies (pools): (1) catalytically active Pd nanoparticles with enough surface defects; (2) mono/oligomeric $L[ArPdX]_nL$, the oxidatively added species and (3) irreversibly deactivated Pd (**Figure 10b**).[44] Since the detachment, agglomeration and deactivation of the corresponding NHC catalysts cannot be neglected, we wanted to attach the chelating side-arms covalently onto NHCs through a linker, e.g. CH_2 (**B**, **Scheme 4**) and phenyl (**C**, **Scheme 4**). When the *p*NHC-metal complex functions in reacitions, even if the metal gets detached from NHC moiety, it is still chelated by the (bi)pyridine side-arms and has a chance to reattach to NHC (**Figure 10c**). The special ligands lower the risk of decomposition caused by detachment of ligand with metal.

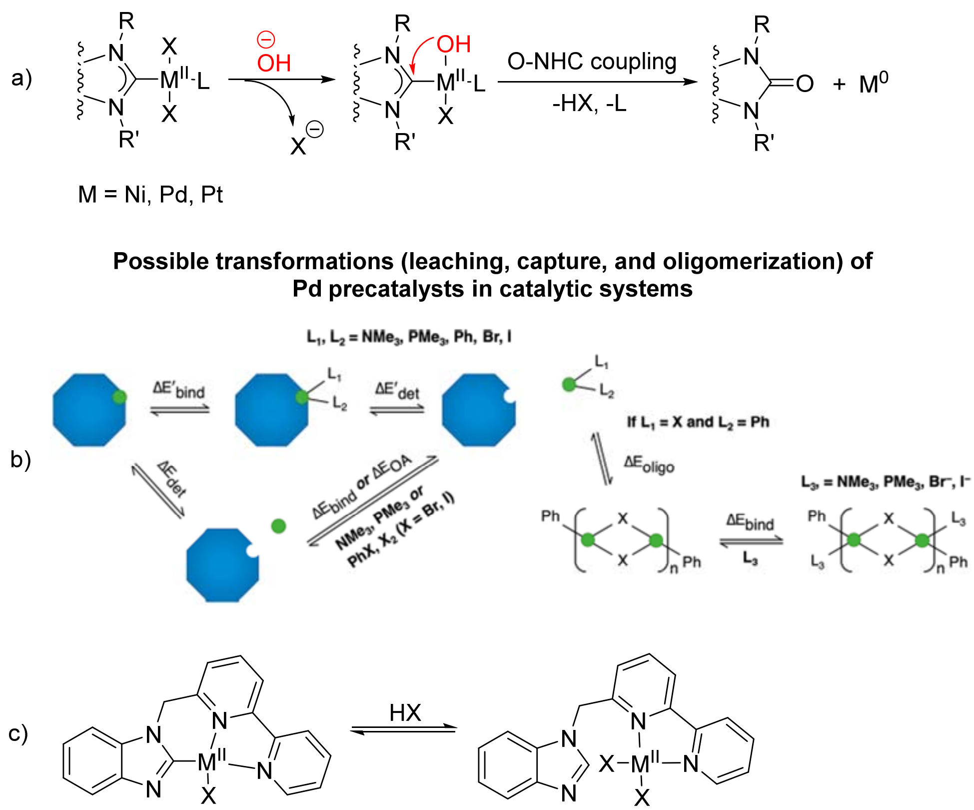

Figure 10: a) Detachment of Metal (Pd) from M/NHC in the presence of bases engaged in cross-coupling reactions; b) Possible leaching, Capture and oligomerization in Pd catalytic system. Nanoparticles: blue; atoms: green.[44] c) Equilibrium between the detachment and reattachment of Metal to NHC.

2.2. Syntheses of Benzimidazolyl Palladium Complexes

The insertion of Pd(0) species into the C(1)-halogen bond through oxidative addition has been well studied. With no transmetalation partner presented, the resulting complex is stable and likely to stay in this state according to the literature reported by Hahn et al.[25] The preparation of ligands thus focused on the introduction of a halogen atom at the C(1) position of benzimidazole (**Scheme 5** and **Figure 11**). 1-Methylbenzimidazole was prepared by treating benzimidazole with NaH and MeI sequentially. Then *n*BuLi was used to deprotonate the C(1) proton followed by iodination with I_2, a typical procedure commonly used to halogenate the C(1) position of imidazole derivatives. Refluxing ligand **1**, $Pd_2(dba)_3$ and 2,2'-bipyridine in THF at 80 °C followed by cooling to room temperature (rt), adding NH_4PF_6 and reheating to 80 °C yielded pale yellow crystals. Interestingly, the structure was identified as the dinuclear form of **2** instead of monomer as evidenced by X-Ray crystallography (**Figure 11**). Similar observation about the preparation of dinuclear complex, where the N wingtip of one moiety coordinates to the metal center of the other, had been observed by Danopoulos et al,[45] suggesting that the nucleophilicity of the N lone pair on the benzimidaolyl motif could potentially be used as a second reactive functional group. The yield was up to 50% when $Pd_2(dba)_3$ was used as received, and dropped dramatically after storing in the glovebox for months, an effect which has been observed and discussed previously (see **Experimental**, **Palladium Complex 2**, vide infra).

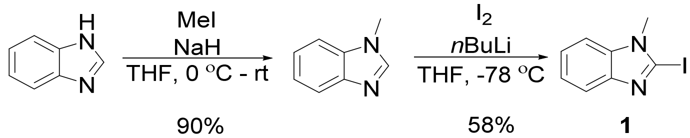

Scheme 5: The synthetic route to monodentate ligand **1**.

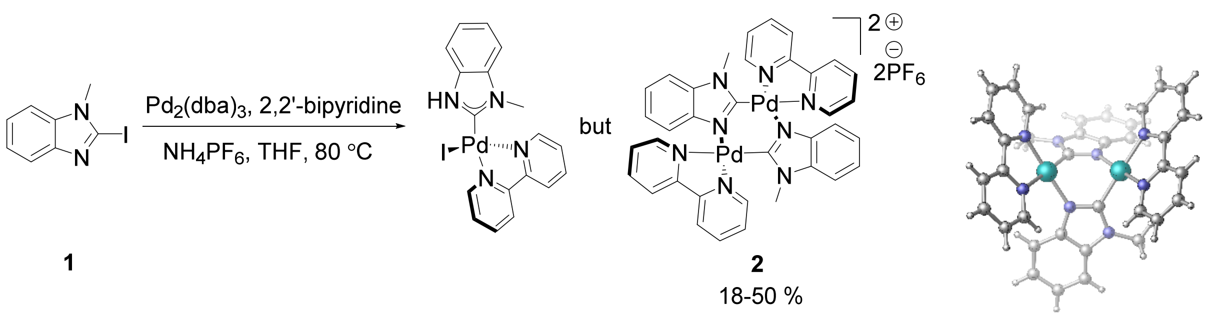

Figure 11: Synthesis of complex **2** and the corresponding X-Ray structure (omitting solvents and anions; Pd = light blue, N = dark blue, C = grey, large, H = grey, small).

Next, three bidentate NHC ligands with pyridine as side-arms were prepared through Buchwald-Hartwig cross-coupling reactions (**3** and **4**, **Scheme 6**) and S_N2 reaction (**5**). The pyridine ligand was expected to chelate Pd (II) and direct it to C(1) for the C–H activation. All of the ligands were prepared successfully except **3**, where 10% yield was obtained at the beginning when conditions such as CuI (cat.), KO*t*Bu (base), benzotriazole (ligand), DMSO (solv.) and 130 °C was employed. The yield was largely promoted to 92% when the conditions were changed to CuI, CsF, 8-hydoxyquinoline, DMSO and 130 °C. However, all attempts on complexing the three ligands with $Pd(OAc)_2$ and/or $PdCl_2$ under different conditions (90/100/110/120 °C, presence of Ag_2O or not, different solvents) via the concerted metallation-deprotonation (CMD) mechanism turned out to be whether decomposition or recovered starting materials (ligands) plus precipitated

Pd black, probably caused by tautomerization from C(1) to the N wingtip of the benzimidazolyl moiety.

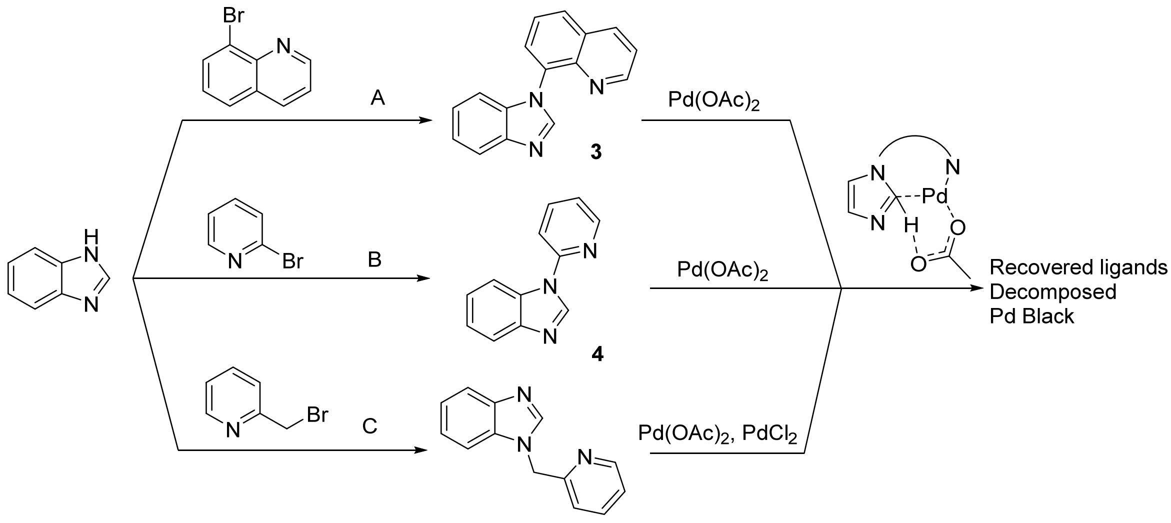

Scheme 6: Syntheses of bidentate NHC-Pyridine ligands **3**, **4**, **5** and Pd complexes via CMD C–H activation.

Pre-activation of the C(1)–H bond by halogenation was attempted to direct Pd(II) to C(1) position. Halogen and pyridine side-arm were expected to cooperate to lock Pd at C(1). However, neither radical halogenation nor typical *n*BuLi/I_2 treatment at low temperature gave the correct product. Only decompositions were observed for all starting materials (**3** and **5**, **Scheme 6**) except **4** (**Scheme 7a**). Unfortunately, oxidative addition of $Pd_2(dba)_3$ with the only available halogen-*p*NHC ligand **4** delivered a decomposed slurry. Interestingly, when the halogenation of **5** was attempted, the ring-closure product was observed (**Scheme 7b**). To resolve this problem, dimethylation on the methylene linker was attempted but no desired product was observed in the last step. The decomposition was potentially caused by the nucleophilic attack of the pyridine to the very electrophilic C(1) of benzimidazole after the introduction of halogen, which demonstrated the inaccessibility of the C(1)-halo-imidazoles template with a pyridine-based side-arm. The strategy of oxidative addition may not be practical for the bidentate ligands (**Scheme 7c**).

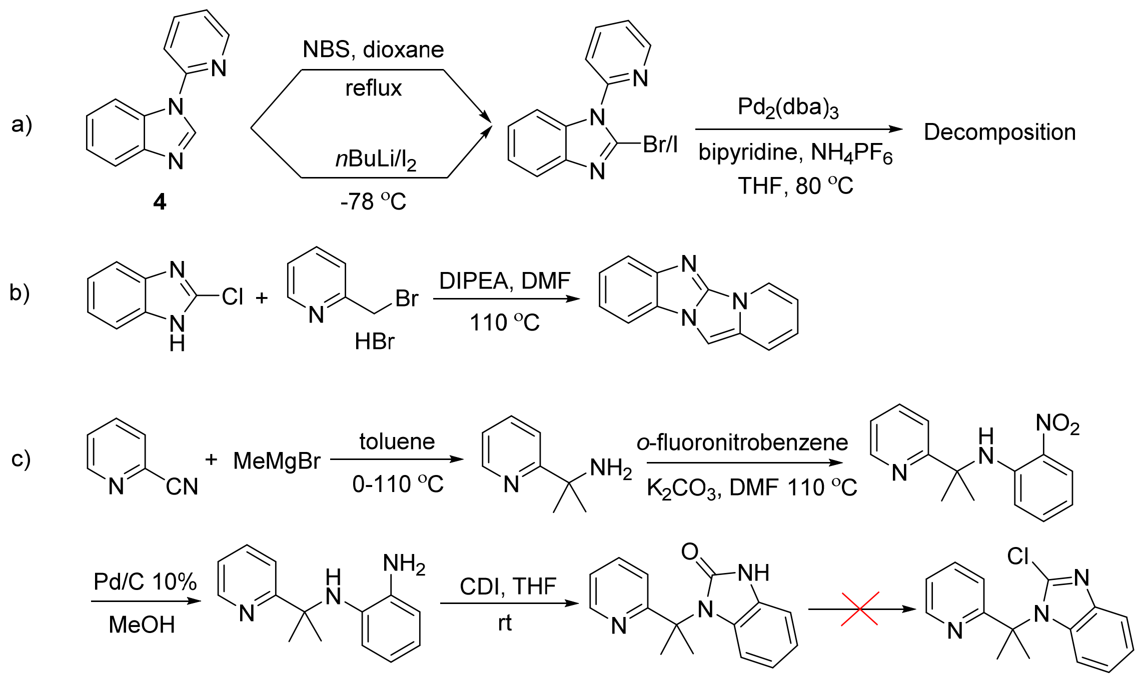

Scheme 7: Failed reactions: a) the only available halogenation of bidentate NHC; b) the ring-closure side reaction; c) synthetic route of di-methylated 2-chloro-NHC-pyridine.

Finally, we focused on the tridentate ligands with 2,2'-bipyridine as the side-arm (R = 2-pyridyl, **Scheme 4**) and the results demonstrated that the di-chelating effect of bipyridine side-arm did override the tautomerization to N wingtip of benzimidazolyl for Pd complexing, thus delivering the desired products. As shown in **Scheme 8**, 3-bromobenzaldehyde was treated with HNO_3/H_2SO_4 to nitrate at the second position with 21% yield. The nitro compound **6** was reduced to an amine using iron powder under acidic, aqueous conditions. Without further purification, 2-acetylpyridine was reacted with the amine through Friedländer annulation under basic condition to yield **7**. Applying the optimal conditions explored for the synthesis of compound **3** on the Buchwald-Hartwig coupling reaction of compound **7** with benzimidazole delivered the desired tridentate ligand **8** in 82% yield.

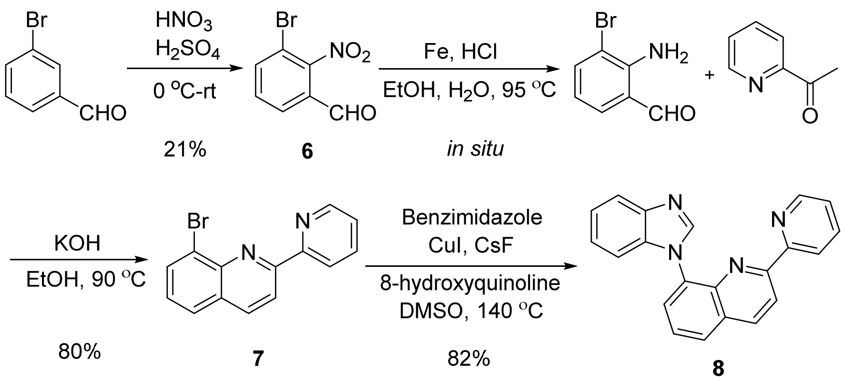

Scheme 8: The synthetic route to tridentate ligand **8.**

Next, 2,2'-bipyridine was treated with MeLi at 0 °C and then refluxed at 40 °C to methylate at the second position in 46% yield (**Scheme 9**). **9** was lithiated at –78 °C and treated with TMSCl in THF to yield the trimethylsilyl intermediate **10** in 82% yield. Subsequent chlorination proceeded high yield (95%) using hexachloroethane and CsF in MeCN at 60 °C. Note that the goal here was to introduce a good leaving group (LG) for the next S_N2 reaction. The direct bromination of compound **9** using NBS was attempted herein but no positive result was obtained. Using benzimidazole and KOH powder generated the nucleophile to react with **11** thus delivered the desired tridentate ligand **12** in 95% yield.

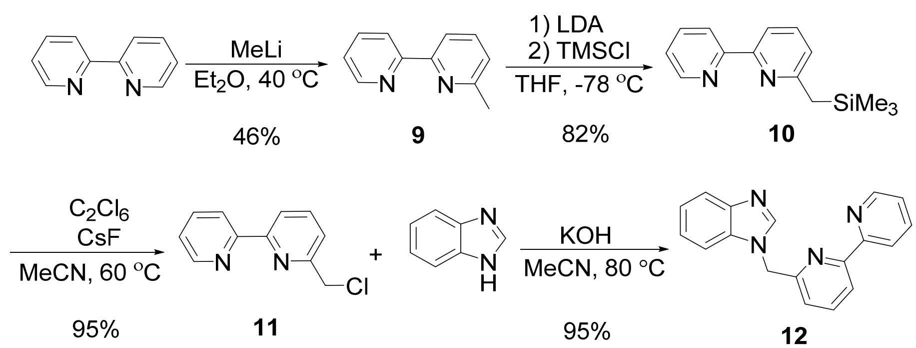

Scheme 9: The synthetic route to tridentate ligand **12**.

After uncovering the excellent catalytic activity of the family of dinuclear complexes for Suzuki, Heck and Sonogashira cross-coupling reactions (**Part 3**, vide infra), the tridentate ligand **16** with *tert*-butyl groups on the *para* positions of the bipyridine side-arm was designed and synthesized (**Scheme 10**). Different electronic effects, i.e. electron donating group (EDG) in this case, are expected to alter the catalytic activity of the explored reactions to provide further insight into the chemical properties of these catalysts. 4,4'-Di-*tert*-butyl-2,2'-dipyridyl was treated with

MeLi at 0 °C in toluene to methylate at C(2) in 48% yield after oxidation with $KMnO_4$. Then **13** was lithiated at –78 °C and treated with TMSCl in THF to yield the trimethylsilyl intermediate **14** in 65% yield. Subsequent chlorination proceeded in high yield (83%) using hexachloroethane and CsF in MeCN at elevated temperature. Finally, benzimidazole was deprotonated and underwent nucleophilic substitution with **15** thus delivered the desired tridentate ligand **16** in 90% yield.

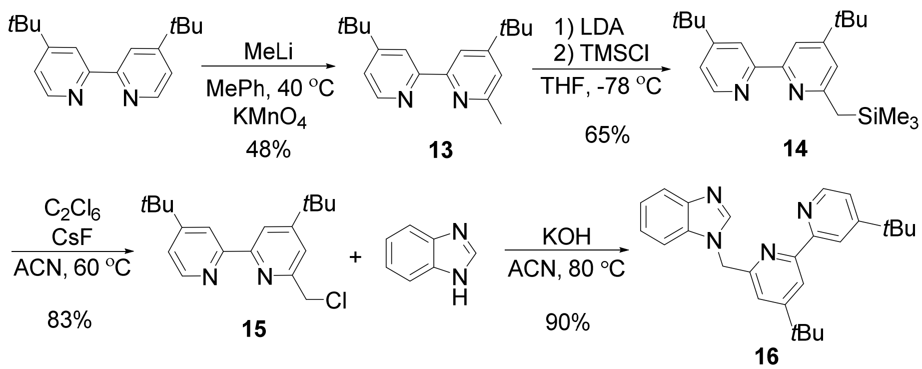

Scheme 10: The synthetic route to tridentate ligand **16**.

Complexation of the tridentate ligands **8**, **12** and **16** prepared with $Pd(OAc)_2$ via bipyridine-directed C–H activation delivered the dinuclear benzimidazolyl-Pd complexes which were structurally similar to complex **2** (**Figure 12**). The complexes were isolated first using basic Al_2O_3 column and the structures were evidenced by ^1H NMR. Although lots of attempts on crystallizing **18** turned out to be just precipitate or microcrystals, crystals of **17** and **19** were readily accessible and refined by recrystallization (MeCN/Hexanes for **17** and DCM/Hexanes for **19**) and analyzed by X-Ray diffraction.

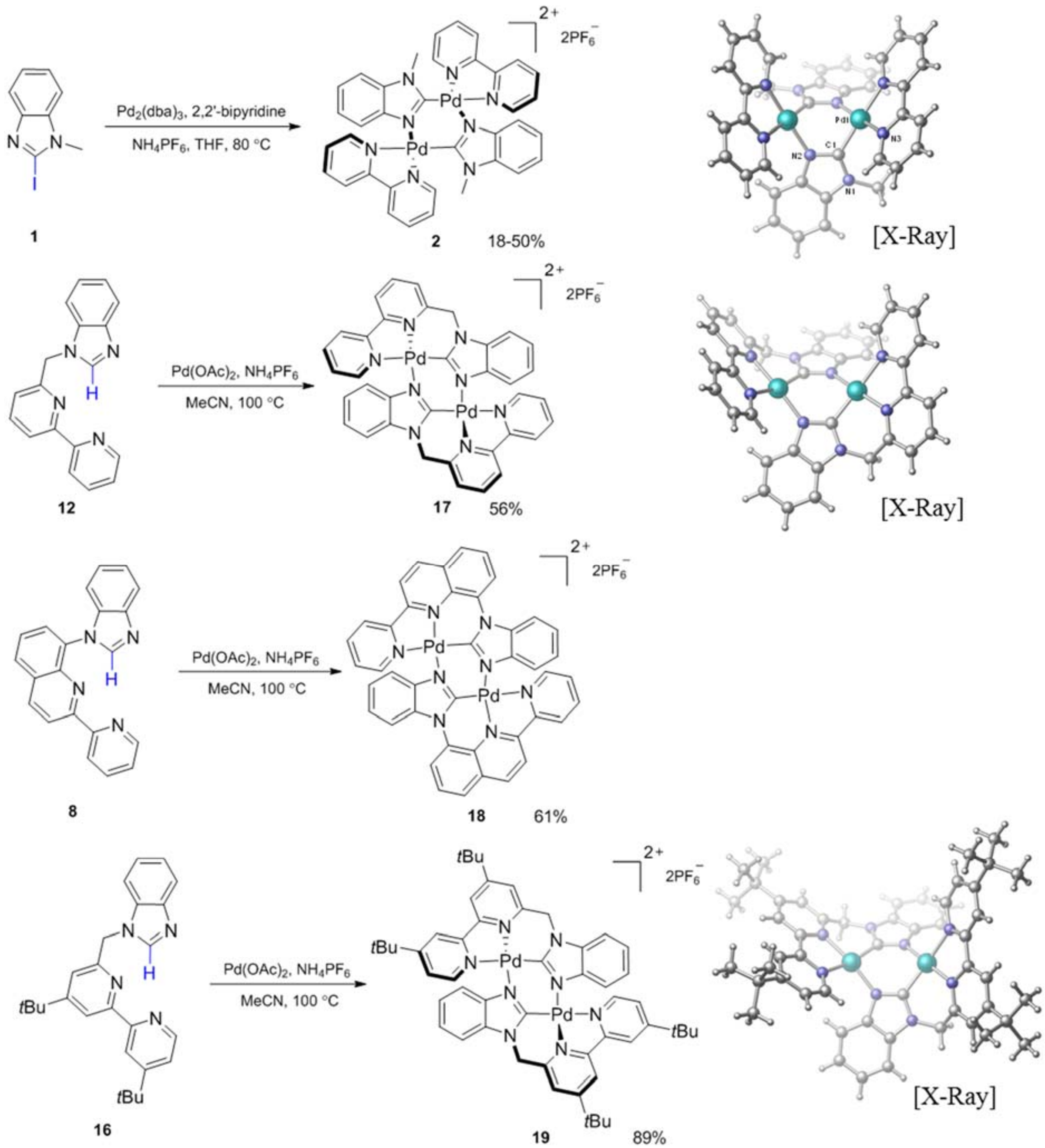

Figure 12: Synthesis of complex **2-19** and the corresponding X-Ray structure of **2**, **17** and **19** (omitting solvents and anions; Pd = light blue, N = dark blue, C = grey, large, H = grey, small).

2.3. Future Work

The preliminary research on complexing **8, 12** and **16** with other transition metals has been conducted in our laboratory in order to broaden the library of the family of dinuclear imidazolyl-metal complexes and to prepare candidates that potentially function in sustainable cross-couplings, C–H activations and other interesting organic transformations. The synthesis of *p*NHC-Ir-bipyridine **20** via C–H insertion by Ir (I) in MeCN at 80 °C formed an interesting structure with hydride, MeCN and chloride ligands attached to the Ir (III) center (**Scheme 11**). However, complex **20** was found to be too polar to dissolve in most organic solvents commonly used in laboratory except DMSO, which may affect its application in the future. Danopoulos et al. observed that a structurally similar *p*NHC-Ir compound can recrystallize from CH_2Cl_2/Hexanes, which indicated that the modification of bipyridine side-arm could influence the physicochemical properties, e.g. solubility in organic solvents.[45] In the future, we will modify R group (**Scheme 4**) to be more lipophilic, such as diphenylphosphine with a CH_2 tether (**21**, **Scheme 11**). Future efforts will also be directed toward the ligation of **12** and **16** to first-row transition metals, e.g. Fe, Cu and Ni, in view of developing more sustainable reactions.

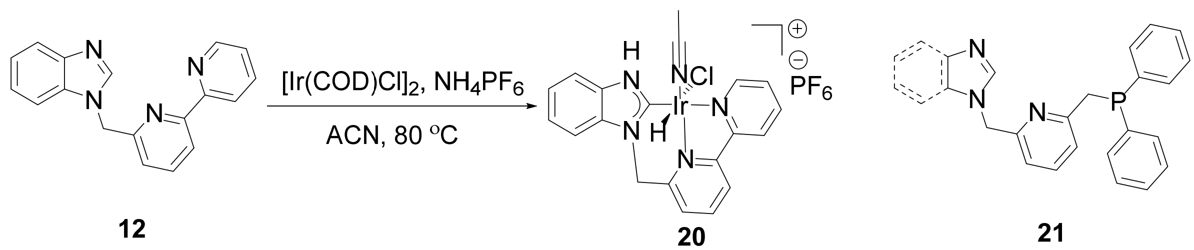

Scheme 11: Synthesis of Ir (III) complex **20** and design of new tridentate ligand **21**.

CHAPTER 3

Approaches to *p*NHC-Pd Catalyzed C–H Activation

3.1. Introduction to DG C–H Activation

Being one of the major foci in molecular synthesis, C–H activation has significantly improved the arsenal for synthetic chemist and realized "green chemistry" in terms of step- and atom-economy and minimizing waste production. Other than the direct C–H activation, which highly depends on the position of the target proton on the substrate and its inherent electronic/steric properties, thus far, the most common approach with good regioselectivity is constituted by chelation of DG (**Scheme 12**).[46] As discussed before, this strategy is hampered by the pre-installation and post-removal of DG on the substrate. On the other hand, the emergence of CDG requires weak coordination of the DG modifier (template) to the FG on substrate. Usually, this strategy is disadvantaged in the requirement of high loading of CDG, e.g. the bifunctional ligand CDG loading was 10-fold higher than $[Rh(coe)Cl]_2$ in the example reported by Dong et al. (**Scheme 13**).[47]

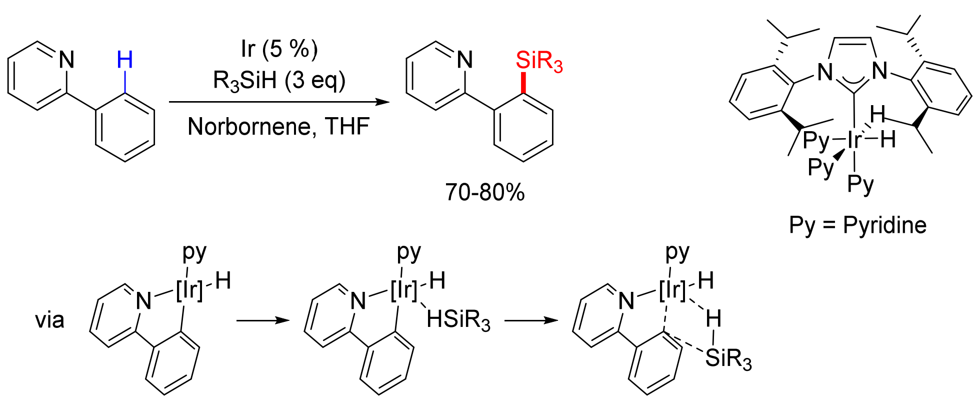

Scheme 12: C–H silylation catalyzed by DG/NHC-Ir.

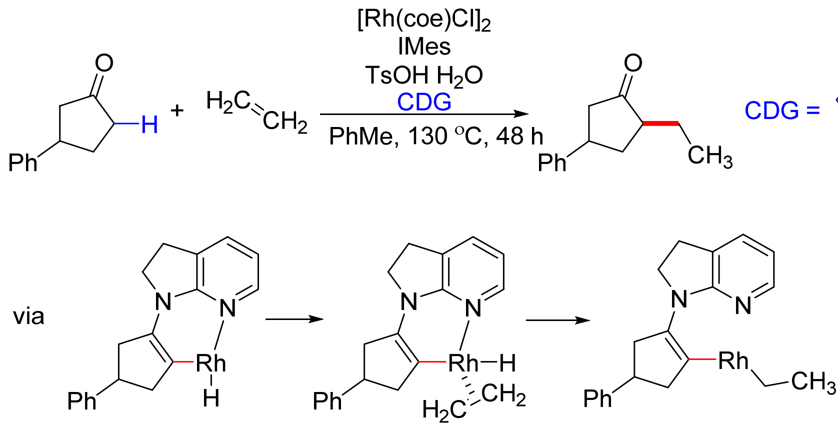

Scheme 13: C–H ethylation catalyzed by CDG/Rh.

To realize the readily accessible CDG strategy, the use of deprotonated *p*NHC-metal complex is proposed for an imbedded DG and a metal activator coexisted in the same motif (**Scheme 3**). With the benzimidazolyl-Pd complexes **2**, **17**, **18** and **19** in our hand, C–H activation was attempted in two ways: 1) optimization of conditions for each intermediate, e.g. acylation, cyclometallation, etc., in each step of the mechanism (**Scheme 3**) then combining the optimal conditions to reach the final goal; 2) screening out the optimal condition for the whole catalysis cycle in one pot.

3.2. Study of the Acylated Intermediate

The preparation and isolation of the *N*-acyl-NHC-Pd intermediate was performed with **2** and benzoyl chloride in THF under N_2 at rt. The homogeneous solution was obtained and the crystal of the desired product **22** was grown from DCM/Hexanes after extraction of solvents and washing by Et_2O for the crude product (**Figure 13**). The observation demonstrated that: (1) the dinuclear complex can break in organic solvent and function as a Nu at room temperature; (2) different from the design of Crabtree (**Figure 4a**), in which case NHC was acylated first and then complexed with the metal (Ir), the lone pair showed good nucleophilicity after the complexation with Pd in our case, which supported our design of the catalysis cycle and the general accessibility of the acylated, hydrolysable organometallic. Note that **22** is highly sensitive to moisture and decomposed easily in THF solution, which was also similar to the observation of Crabtree et al. and made the reproducibility of this reaction poor, but it also demonstrated the viability of the last step of our mechanism involving a de-acylation.

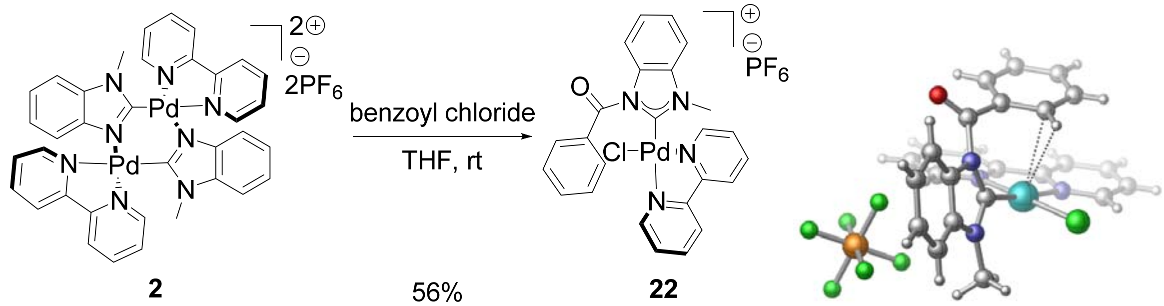

Figure 13: The intermediate of acylated benzimidazolyl-Pd complex **22** and the corresponding X-Ray structure (omitting solvents; Pd = light blue, N = dark blue, O = red, P = yellow, Cl, F = green, C = grey, large, H = grey, small).

Next, we attempted to access a C–H activated intermediate by cyclometallation reaction of **22**, the next step in our proposed mechanism. Different silver salts (e.g. AgOAc and AgTFA) were tested at room or elevated temperature with inert gas protection, to exchange the chloride in **22** with acetate or derivative in order to assist the cyclometallation via a CMD mechanism. The *ortho* proton of the benzoyl group was activated and the structure of the cyclometallated product was confirmed by ^{1}H NMR when AgTFA, CH_2Cl_2 and 60 °C were employed as the optimal condition (**Scheme 14**). Note that both the intermediate **22** and **23** were difficult to handle for purification thus impurities coexisted with the product and the yield of complex **23** could not be determined at this step.

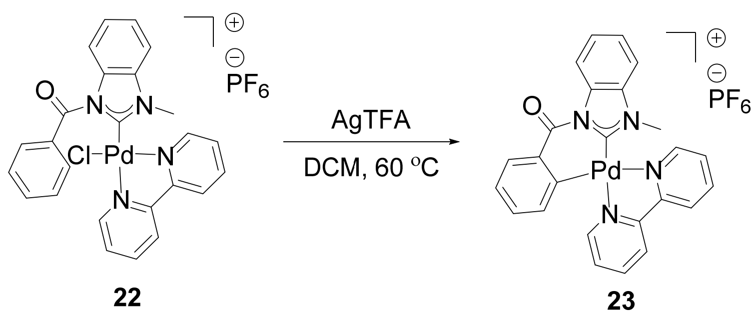

Scheme 14: Synthesis of the cyclometallated intermediate **23**.

Research was also focused on functionalizing the dinuclear complex **17** with *p*-nitrobenzenesulfonyl chloride in THF at elevated temperature. However, the desired product was still easily hydrolyzed and the monomer **17a** was obtained without decomposition based on ^{1}H

NMR analysis (**Scheme 15**). Again, the experiment exhibited that it was the monomer derived from the dinuclear benzimidazolyl-Pd that actually functioned in the reactions.

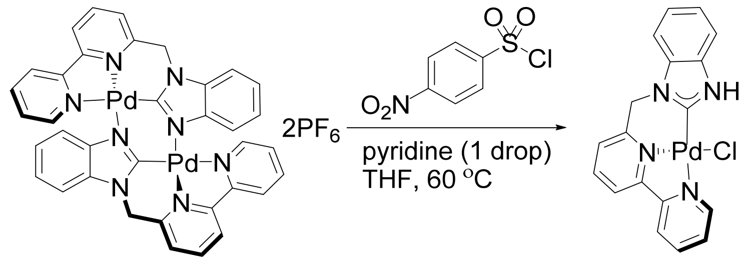

17

17a

Scheme 15: Sulfonylation of complex **17**.

In the meantime, a variety of anhydrous reaction conditions for C–H activation in one pot have also been attempted. To ensure that the acylation step was reversible, which is the key step for a catalytic cycle, the leaving group (X^-) of phenyl acyl should be optimized to be both a good nucleophile and leaving group (**Scheme 3**). The testing reactions with different levels of major factors, such as anhydrous solvents, temperature, substrates (X^-), and silver additives were tested but no positive results were obtained so far for this challenging new catalytic DG strategy.

3.3. Future Work

The syntheses of each intermediates in the catalytic cycle require strictly anhydrous conditions based on the aforementioned discussions. More efforts will be spent on screening the optimal conditions and preparing the key intermediates. Also, considering the instability of the acylated complexes, mild conditions at room temperature using more active metals, such as Ir and Rh, are expected.

CHAPTER 4

Sustainable Cross-Couplings Catalyzed by Benzimidazolyl-Pd Complexes

4.1. Introduction to Cross-Couplings with New Perspectives

Recently, transition-metal-catalyzed cross-coupling reactions with new mechanisms, high efficacy, and difficult substrate/FG derived from the traditional versions have reemerged as a hot research topic in academia. For example, Sanford and co-workers observed the base-free, Ni-catalyzed, decarboxylative Suzuki-type cross-coupling reaction between boronic acid and carboxylic acid (**Scheme 16**).[48] Aryl carboxylic acid was converted to acyl fluoride in 15 minutes and reacted with aryl boronic acid under mild condition with no base engaged.

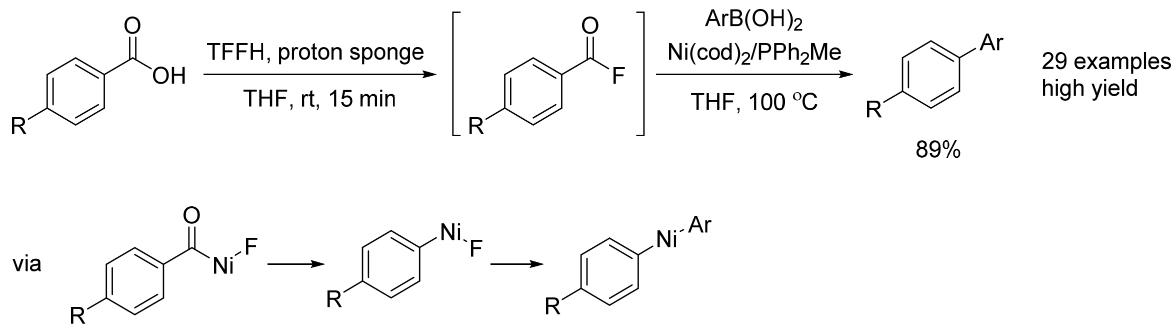

Scheme 16: Base-free, Ni-catalyzed, decarboxylative Suzuki-type cross-coupling reaction.

In this study, the family of benzimidazolyl Pd complexes were expected to catalyze the cross-coupling reactions with high efficiency via the bifunctional-mode-accelerated transmetalation key step. The lone pair on N wingtip of our complexes were proposed to coordinate to the FGs of cross-coupling partners (boronic acid, acetylene) thus the accelerated transmetalation key intermediate could lead high yields and a new mechanism of catalysis (**Scheme 4**).

4.2. Optimization of the *p*NHC-Pd Complexes Catalyzed Cross-Couplings

A preliminary evaluation of the catalytic activity in Suzuki-Miyaura, Heck-Mizoroki and Sonogashira-Hagihara reactions were performed on typical conditions with no sustainable factors involved. Easily accessible substrates, 4-bromoacetophenone (**24**, **Scheme 17**) and coupling partners, phenyl boronic acid, styrene and phenylacetylene, were selected as model substrates. For Suzuki-Miyaura reaction, phenyl bromide reacted with phenylboronic acid (1.5 equiv) in the presence of 5 mol% catalyst **2** and KOH (2.0 equiv) in water (1.5 mL) at 100 °C without inert gas protection (**Scheme 17a**). For Heck-Mizoroki reaction, phenyl bromide reacted with styrene (1.5 equiv) in the presence of 2.5 mol% catalyst **2**, TBAB (1.5 equiv) and K_2CO_3 (2.0 equiv) in DMF (1.2 mL) at 140 °C without inert gas protection (**Scheme 17b** and entry 1, **Table 4**). For Sonogashira-Hagihara reaction, phenyl bromide reacted with phenylacetylene (1.5 equiv) in the presence of 5 mol% catalyst **2** and Cs_2CO_3 (2.0 equiv) in DMF (1.5 mL) at 100 °C without inert gas protection (**Scheme 17c** and entry 1, **Table 3**). Moderate to high yields of the cross-coupled products were obtained for these preliminary testing reactions.

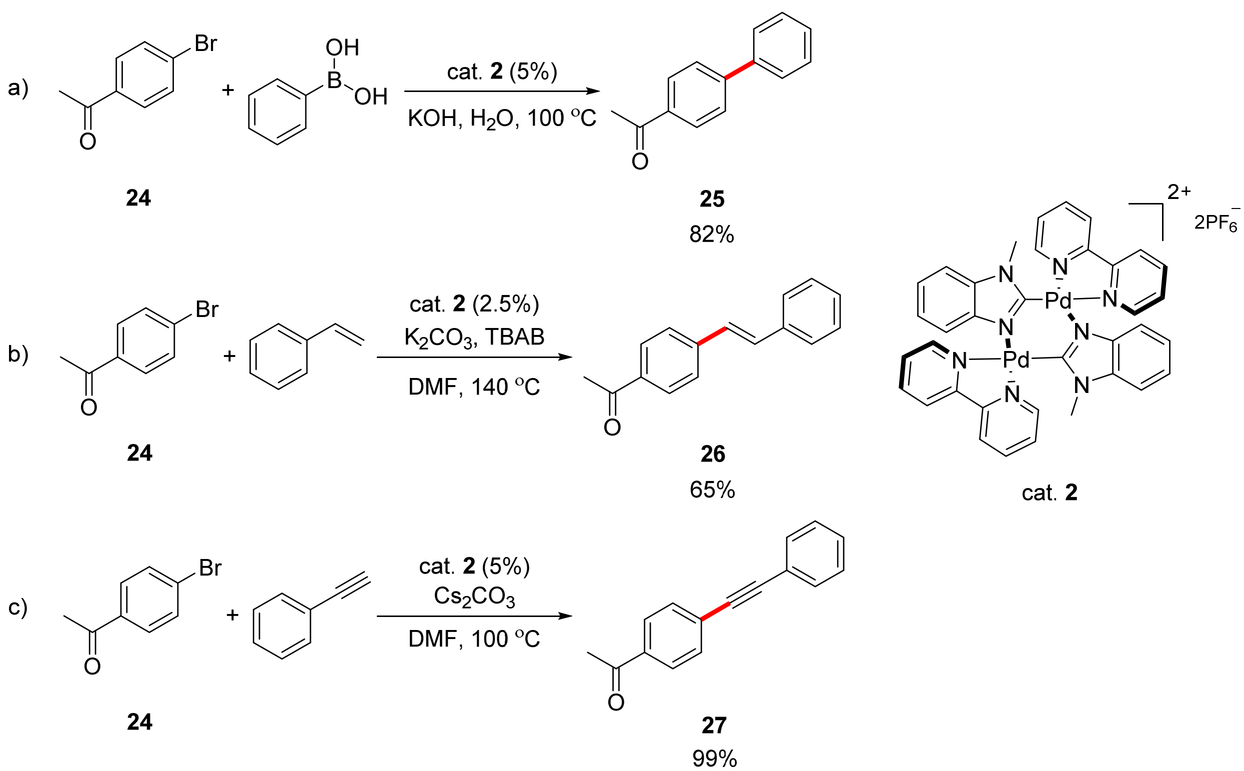

Scheme 17: Preliminary evaluation of complex **2** as catalyst in (a) Suzuki, (b) Heck and (c) Sonogashira reactions.

Then the research was focused on optimizing the three cross-coupling reactions under sustainable conditions. According to the typical features for green cross-coupling reactions reported in literatures and discussion in the **General Introduction** of this document, the goal herein is to reduce the catalyst loading to minute amounts (e.g. 0.01 mol%), using aqueous/alcohol media and mild/cheap bases, being applicable for broad scope of substrates and achieving high to excellent yields.

The Suzuki cross-coupling of 4-bromoanisole (**28**, **Table 1**) and phenylboronic acid was elected as model reaction in order to evaluate the catalytic activity of the new benzimidazolyl-Pd complexes. The control reaction using $Pd(OAc)_2$ and bipyridine confirmed the absence of catalytic activity in aqueous conditions (entry 1). By comparing catalysts **2**, **17** and **18** directly under the same aqueous conditions, a significant difference in catalytic activity was revealed. Pincer complex **17** furnished a quantitative yield (entry 4) while **2** and **18** only resulted the coupled product **29** in low yields (entry 2 and 3). When the catalyst loading of **17** was reduced to 0.25 mol%, the yield was decreased (entry 5). But when alcohol media and mild base was used, **17** afforded high yield with the same loading (entry 6) or even less (0.1 mol%, entry 7 and 0.01 mol%, entry 8). The sustainable condition of entry 7 was identified as the optimal condition of Suzuki coupling for the study of substrate expansion. However, when electron-rich catalyst **19** (obtained later than **17**) was synthesized and used, with the same (0.1 mol%) or lower (0.01 mol%) catalyst loading (entry 9 and 10), quantitative yields under the optimal condition were observed. X-ray structures of the benzimidazolyl-Pd complexes (**Figure 12**) demonstrate that ligands with CH_2 tether (**17** and **19**) or complex **2** have the flexibility of the benzimidazolyl moiety to some level that allows it to stay out of the Pd coordination plane. The flexibility should be limited in complex **18** as the phenyl tether forces the compound to be coplanar. The observations in **Table 1** demonstrated that both the electronic effect and the flexibility of the pincer ligand have big influence on the catalytic activity. By comparing the yields in entry 8 with 10, we can conclude that the electron-rich complex with some flexibility for benzimidazolyl moiety is favored to catalyze Suzuki reaction under sustainable condition. The catalysts with even lower loadings are being investigated in our laboratory and expected to be reported in the due course.

Table 1. Evaluation of bifunctional catalysts using a Suzuki cross-coupling as a model reaction.

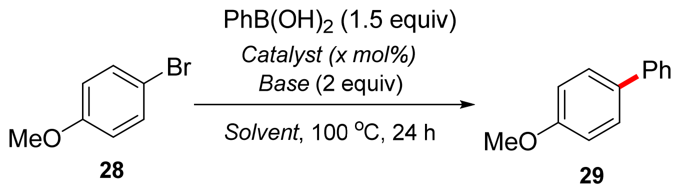

Entry	Cat.	Cat. Loading (mol %)	Base	Solv.	Yield[a] (%)
1	**Pd(OAc)$_2$:bipy (1:1)**	1.00	KOH	H_2O	<5
2	**2**	1.00	KOH	H_2O	34
3	**18**	1.00	KOH	H_2O	12
4	**17**	1.00	KOH	H_2O	>99
5	**17**	0.25	KOH	H_2O	65
6	**17**	0.25	K_2CO_3	EtOH	95
7	**17**	0.10	K_2CO_3	EtOH	89
8	**17**	0.01	K_2CO_3	EtOH	78
9	**19**	0.10	K_2CO_3	EtOH	>99
10	**19**	0.01	K_2CO_3	EtOH	>99

[a] NMR yield determined using 1,3,5-trimethoxybenzene as internal standard.

4.2.1. Optimization of Suzuki-Miyaura Reaction

In order to have further insight of the catalysis mechanism, control reactions were performed. Evaluating the reaction on *p*-bromoanisole without catalyst gave no yield, which means the *p*NHC-Pd catalysts is a necessary factor in Suzuki coupling of bromoanisole and phenylboronic acid (entry 1, **Table 2**). To further demonstrate that it was the mechanism of accelerated transmetalation assisted by the bifunctional mode that afforded such an active catalyst, complex **32** was synthesized with the N wingtip blocked by a methyl group and used for Suzuki coupling under the optimal condition to compare the catalytic activities (**Scheme 18**). To synthesize the classic NHC-Pd complex **32**, **30** was prepared from refluxing *N*-methyl benzimidazole with **11** in MeCN for 2 days. After the anion exchange reaction, **31** was subjected to deprotonation by Ag_2O and subsequent transmetalation to $PdCl_2$ to deliver complex **32** in 60% yield. The inferior result obtained by using **32** under the identical condition for complex **17** (entry 2 and 3, **Table 2**) did confirm the importance of the free N of the monomer form of **17** and the bifunctional mode works in the reaction.

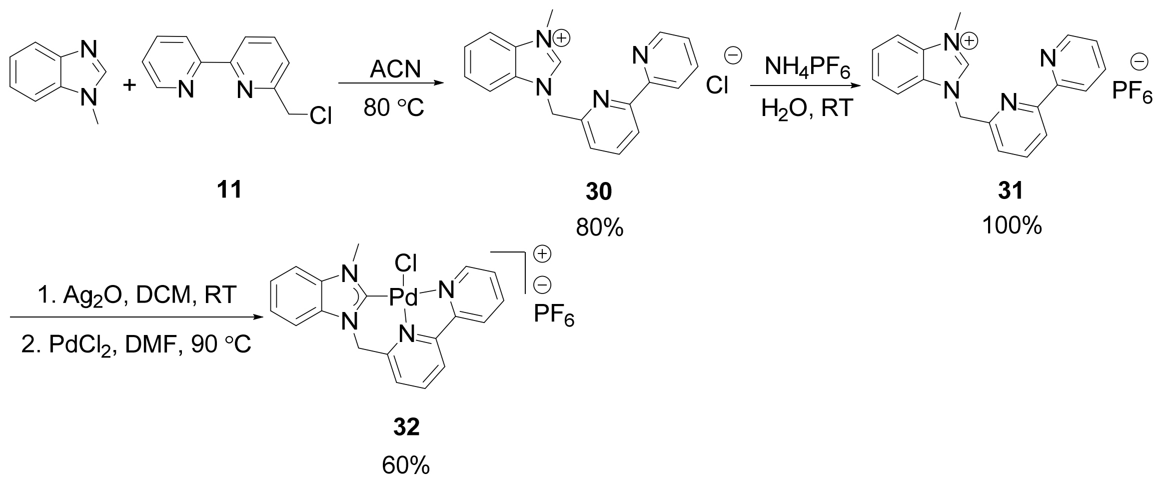

Scheme 18: Synthesis of complex **32**.

Table 2. Further evaluation of bifunctional catalysts **17** under optimal conditions.

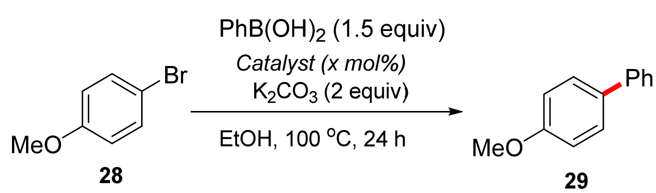

Entry	Cat.	Cat. Loading (mol %)	Yield[a] (%)
1	–	–	<5
2	**32**	0.20	67
3	**17**	0.1	89

[a] NMR yield determined using 1,3,5-trimethoxybenzene as internal standard.

With the optimal conditions in our hand, a variety of biaryl compounds with different FGs were synthesized to evaluate the generality of the protocol with **17** as catalyst (**19** was not developed at that time). The method realized good to excellent yields for substrates with either EWGs or EDGs, as well as heterocycles and aliphatic coupling partner (**Figure 14**). Most notably, as Buchwald-Hartwig coupling did not occur under the condition, a free primary aniline-containing substrate **41** was found to be compatible with the optimal condition and afforded high yield of the product, showing the complementary character of these catalysts compared to well-established Buchwald ligand scaffolds. The installation of vinyl groups by cross-coupling is known to be a challenging process, which typically requires specialized reagents. However, vinylboronic acid pinacol ester served as a viable partner to deliver styrene derivative **42** in this study although 1 mol% of **17** was needed.

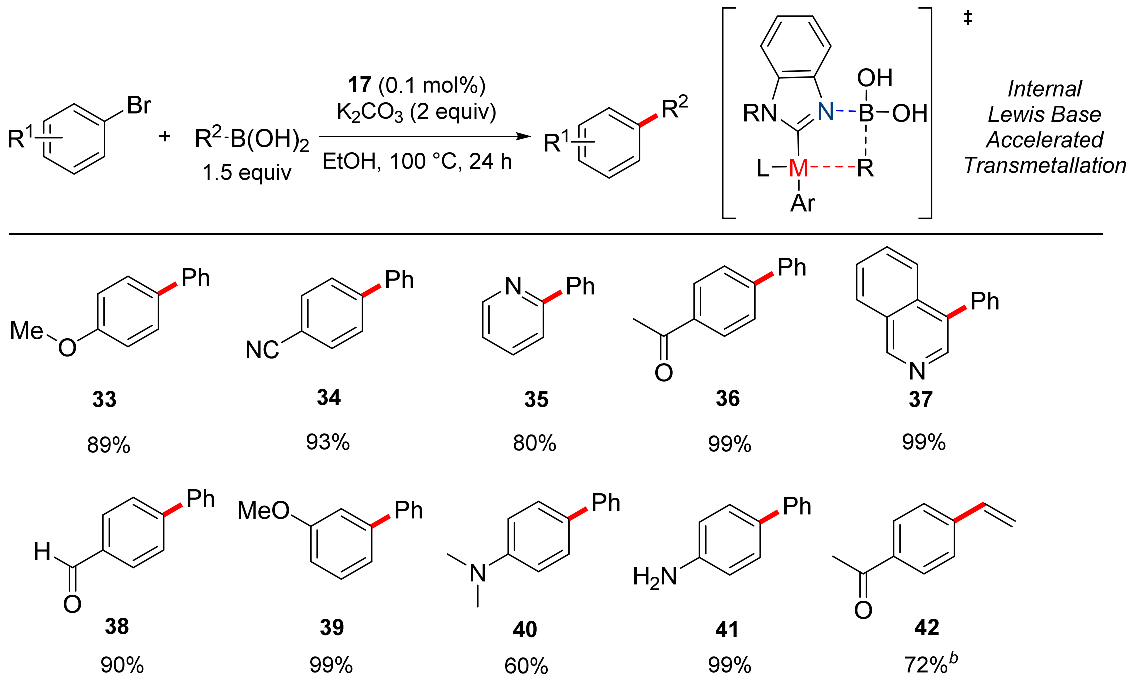

[a]Isolated yields
[b]1 mol % of catalyst 17 was used with vinylboronic acid pinacol ester as coupling partner.

Figure 14: Benzimidazolyl-Pd **17** catalyzed Suzuki-Miyaura reaction;[a] the formed bonds and proposed bifunational mode are highlighted.

4.2.2. Optimization of Sonogashira-Hagihara Reaction

Since the free N on imidazolyl-metal complexes is also known to be a Brønsted base to form *p*NHC-metal species (**Scheme 4** and **Figure 14**), the bifunctional catalysts could potentially be used in catalyzing the copper-free Sonogashira reactions, where the lone pair of N would accelerate metalation of the terminal alkyne coupling partner. The quantitative yield was obtained when complex **17** was used as catalyst, K_2CO_3 as base and EtOH as solvent, even when the catalyst loading was as low as 0.5 mol% (entry 2, **Table 3**). The control reactions with $Pd(OAc)_2$ and no catalyst afforded much lower yields (entry 3 and 4). The yield dropped dramatically when the catalyst loading was further decreased to 0.10% (entry 5). By adding TBAI (entry 6) and elevating the reaction temperature to 120 °C (entry 7), the reaction took place with quantitative yields. Entry 7 was identified as the optimal condition. Sonogashira couplings demonstrated selectivities for different aryl halogens that iodo- and bromo-arenes reacted with phenylacetylene in excellent yields, but chloroaryl resulted in low yield (entry 8 and 9). Notice that the reaction was compatible with aqueous media when 1:1 mixture of water and ethanol was employed as co-solvent in the presence of TBAI additive (entry 10 and 11). Ethanol was selected to exploring the substrate scope at this point since it is considered as eco-friendly solvent.

The difference in catalysis was evaluated by the control reactions using **2** and **18** as catalysts (entry 12 and 13). These two complexes delivered inferior results and confirmed that **17** was the optimal catalyst under the sustainable condition. When the FGs on the bromoarene changed from EWG to EDG, optimal condition still performed well after a small amount of condition screening and quantitative yield was obtained (entry 14-17). Aqueous solvent was compatible with *p*-bromoanisole that the solvent of 1:1 water and ethanol did not lower the yield (entry 18). Evaluating the reaction on *p*-bromoanisole in optimal conditions with classic NHC catalyst **32** gave only 13% yield, which was a significant drop compared with the optimal catalyst **17** (entry 19), highlighting the importance of the bifunctionality of our catalyst design.

Table 3. Optimization of Sonogashira-Hagihara reaction.

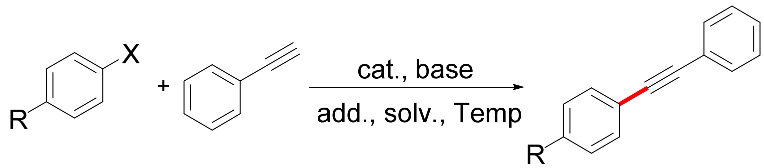

Entry[a]	**Cat.**	**Cat. loading (mol %)**	**Base**	**Add.**	**Solv. (1:1 if mixed)**	**Temp. (°C)**	**Sub.**	**Yield**[b] (%)
1	**2**	5.0	Cs_2CO_3	NA	DMF	100	*p*-ketone-Br	99
2	**17**	0.50	K_2CO_3	NA	EtOH	100	*p*-ketone-Br	>99
3	$Pd(OAc)_2$	1.0	K_2CO_3	NA	EtOH	100	*p*-ketone-Br	23
4	–	–	K_2CO_3	NA	EtOH	100	*p*-ketone-Br	9
5	**17**	0.10	K_2CO_3	NA	EtOH	100	*p*-ketone-Br	34
6	**17**	0.10	K_2CO_3	TBAI	EtOH	100	*p*-ketone-Br	66
7	**17**	0.10	K_2CO_3	TBAI	EtOH	120	*p*-ketone-Br	>99
8	**17**	0.10	K_2CO_3	TBAI	EtOH	120	*p*-ketone-Cl	22
9	**17**	0.10	K_2CO_3	TBAI	EtOH	120	*p*-ketone-I	80
10	**17**	0.10	K_2CO_3	NA	$EtOH/H_2O$	100	*p*-ketone-Br	36
11	**17**	0.10	K_2CO_3	TBAI	$EtOH/H_2O$	100	*p*-ketone-Br	>99
12	**18**	0.10	K_2CO_3	TBAI	EtOH	120	*p*-ketone-Br	71
13	**2**	0.10	K_2CO_3	TBAI	EtOH	120	*p*-ketone-Br	87
14	**17**	1.0	K_2CO_3	NA	EtOH	100	*p*-methoxy-Br	47
15	**17**	1.0	K_2CO_3	TBAI	EtOH	100	*p*-methoxy-Br	>99
16	**17**	0.10	K_2CO_3	TBAI	EtOH	100	*p*-methoxy-Br	52
17	**17**	0.10	K_2CO_3	TBAI	EtOH	120	*p*-methoxy-Br	98
18	**17**	0.10	K_2CO_3	TBAI	$EtOH/H_2O$	120	*p*-methoxy-Br	98
19	**32**	0.20	K_2CO_3	TBAI	EtOH	120	*p*-methoxy-Br	13

[a] All reactions have phenylacetylene (1.5 equiv), base (2.0 equiv) and additive (1.5 equiv) to aryl halogen, conc. = 0.12 M unless otherwise noted.

[b] NMR yield determined using 1,3,5-trimethoxybenzene as internal standard.

With the optimal condition in our hand, a variety of internal alkynes were prepared by the sustainable Sonogashira couplings catalyzed by **17**. The method realized good to excellent yields for substrates with both EWGs and EDGs, as well as heterocycles and aliphatic coupling partners (**Figure 15**).

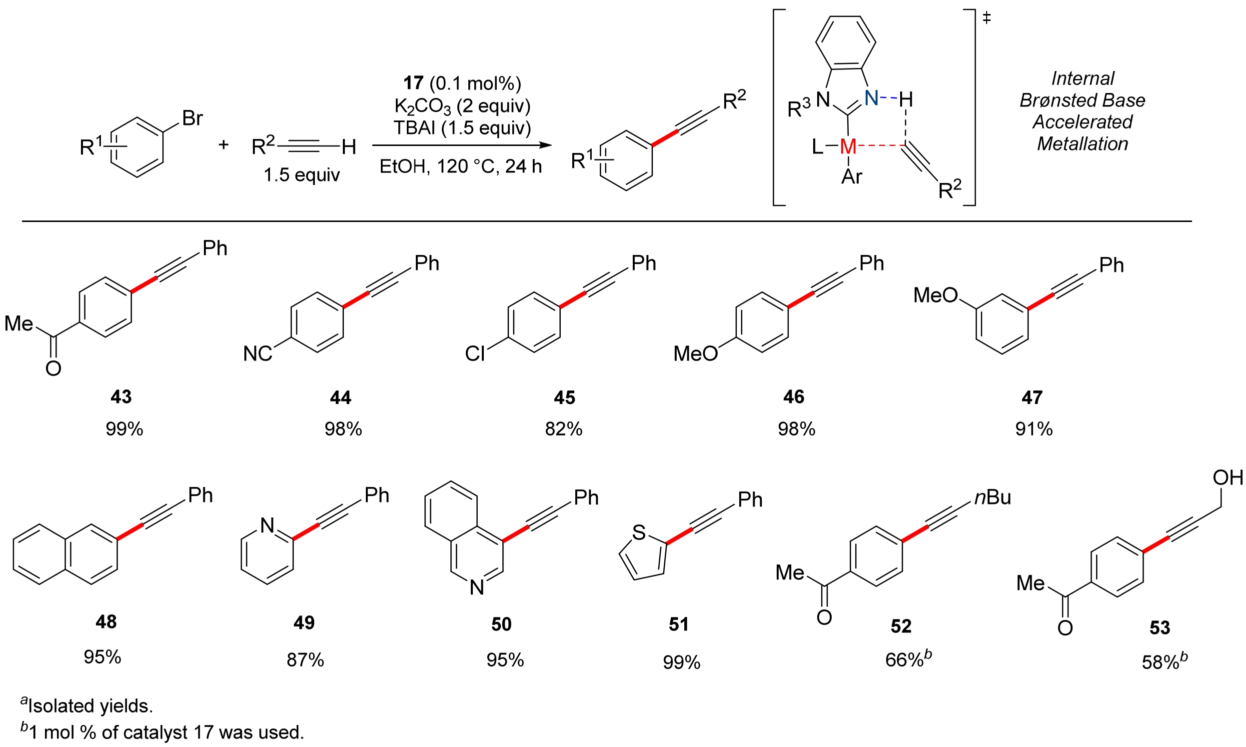

Figure 15: Internal alkynes prepared by *p*NHC-Pd catalyzed Sonogashira-Hagihara reaction;[a] the formed bonds and proposed bifunational mode are highlighted.

4.2.3. Optimization of Heck-Mizoroki Reaction

More condition screenings were performed to mapping out the optimal condition for Heck reaction than Suzuki and Sonogashira. There was no difference in terms of yield when non-green conditions were used, no matter using complex **2** or **17** (entry 2-5, **Table 4**). However, when EtOH was used as solvent, the use of catalyst **17** (1.0 mol%) afforded much lower yield (entry 6-18). The combination of using Na_2CO_3 as base and high temperature seemed to be positive to deliver higher yields (entry 19 and 20). When 1:1 mixture of water and EtOH was employed as solvent, reaction with Na_2CO_3 as base still performed better than the other kinds of common bases (entry 21-31). Nonetheless, the yield dropped dramatically when the catalyst loading was decreased to 0.1 mol% (entry 24). After mapping through different levels for the factor of solvent (e.g. *n*-propanol, *i*-propanol and the 1:1 mixture with water), temperature and additive (entry 32-39), the use of *n*-BuOH as solvent, Na_2CO_3 as base, TBAI as an additive and 140 °C as reaction temperature with just 0.1 mol% catalyst **17** was identified as one applicable condition (entry 35). The condition was further explored by lowering the reaction temperature to 120 °C (entry 39) and identified as the optimal condition. The condition was applied on other alcoholic media and complexes **2** and **18** but no comparable results were obtained (entries 42, 45-47). Once again, **17** demonstrated its superiority in catalysis for Heck reaction over **2** and **18**. Also, complex **17** performed well not only for arenes with EWGs but also EDGs, such as *p*-methoxy, under the optimal condition (entry 49). But using the classic NHC-Pd **32** with N blocked by methyl or no catalyst gave no yield under the optimal condition (entry 48, 50 and 51), highlighting the importance of the free N of the monomer form of our catalysts.

Table 4. Optimization of Heck-Mizoroki reaction.

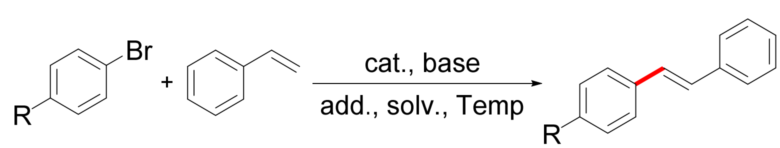

Entry[a]	Cat.	Cat. Loading (mol %)	Base	Add.	Solv. (1:1 if mixed)	Temp. (°C)	Sub.	yield[b] (%)
1	**2**	2.5	K_2CO_3	TBAB	DMF	140	*p*-ketone	65
2	**2**	2.5	K_2CO_3	TBAB	DMSO	140	*p*-ketone	69
3	**17**	2.5	K_2CO_3	TBAB	DMSO	140	*p*-ketone	72
4	**2**	1.0	K_2CO_3	TBAB	DMSO	140	*p*-ketone	68

Table 4. (continued).

5	**17**	**1.0**	**K_2CO_3**	**TBAB**	**DMSO**	**140**	***p*-ketone**	**22**
6	**17**	1.0	K_2CO_3	TBAI	EtOH	100	*p*-ketone	24
7	**17**	1.0	Na_2CO_3	NA	EtOH	100	*p*-ketone	63
8	**17**	1.0	Li_2CO_3	NA	EtOH	100	*p*-ketone	27
9	**17**	1.0	Li_2CO_3	TBAI	EtOH	100	*p*-ketone	24
10	**17**	1.0	Li_2CO_3	NA	EtOH	120	*p*-ketone	21
11	**17**	1.0	K_2CO_3	NA	EtOH	120	*p*-ketone	47
12	**17**	1.0	Na_2CO_3	NA	EtOH	120	*p*-ketone	86
13	**17**	1.0	NaOH	NA	EtOH	120	*p*-ketone	<5
14	**17**	1.0	NaOtBu	NA	EtOH	120	*p*-ketone	<5
15	**17**	1.0	Na_3PO_4	NA	EtOH	120	*p*-ketone	54
16	**17**	1.0	Na_2CO_3	TBAI	EtOH	120	*p*-ketone	10
17	**17**	1.0	Na_2CO_3	TBAB	EtOH	120	*p*-ketone	28
18	**17**	1.0	Na_3PO_4	TBAI	EtOH	120	*p*-ketone	26
19	**17**	0.50	Na_2CO_3	NA	EtOH	120	*p*-ketone	>99
20	**17**	0.10	Na_2CO_3	NA	EtOH	120	*p*-ketone	35
21	**17**	1.0	Na_2CO_3	NA	EtOH/H_2O	100	*p*-ketone	>99
22	**17**	0.50	Na_2CO_3	NA	EtOH/H_2O	100	*p*-ketone	>99
23	**17**	0.50	Na_2CO_3	NA	EtOH/H_2O	100	*p*-ketone	>99
24	**17**	0.10	Na_2CO_3	TBAI	EtOH/H_2O	100	*p*-ketone	48
25	**17**	0.10	Li_2CO_3	TBAI	EtOH/H_2O	100	*p*-ketone	20
26	**17**	0.10	Na_2CO_3	TBAI	EtOH/H_2O	120	*p*-ketone	58
27	**17**	0.10	K_2CO_3	TBAI	EtOH/H_2O	100	*p*-ketone	39
28	**17**	0.10	K_3PO_4	TBAI	EtOH/H_2O	100	*p*-ketone	21
29	**17**	0.10	Cs_2CO_3	TBAI	EtOH/H_2O	100	*p*-ketone	38
30	**17**	0.10	DIPEA	TBAI	EtOH/H_2O	100	*p*-ketone	39
31	**17**	0.10	NaOAc	TBAI	EtOH/H_2O	100	*p*-ketone	13
32	**17**	0.10	Na_2CO_3	TBAI	*n*BuOH/H_2O	120	*p*-ketone	50
33	**17**	0.10	Na_2CO_3	TBAI	*n*Propanol/H_2O	120	*p*-ketone	70
34	**17**	0.10	Na_2CO_3	TBAI	*n*Propanol/H_2O	140	*p*-ketone	51
35	**17**	0.10	Na_2CO_3	TBAI	*n*BuOH	140	*p*-ketone	>99
36	**17**	0.10	Na_2CO_3	TBAI	*n*Propanol	140	*p*-ketone	14
37	**17**	1.0	Na_2CO_3	NA	*n*BuOH	120	*p*-ketone	>99
38	**17**	1.0	Na_2CO_3	NA	*n*BuOH	140	*p*-ketone	>99
39	**17**	0.10	Na_2CO_3	TBAI	*n*BuOH	120	*p*-ketone	>99
40	**17**	0.10	Na_2CO_3	TBAI	*n*BuOH	110	*p*-ketone	34
41	**17**	0.10	Na_2CO_3	TBAI	*n*BuOH	100	*p*-ketone	9
42	**17**	0.10	Na_2CO_3	TBAI	*i*Propanol	120	*p*-ketone	40
43	**17**	0.10	Na_2CO_3	TBAI	*n*BuOH	120	*p*-ketone	72[c]
44	**17**	0.10	Na_2CO_3	TBAI	*n*BuOH	120	*p*-ketone	29[c]
45	**17**	0.10	Na_2CO_3	TBAI	EtOH	120	*p*-ketone	18

Table 4. (continued).

46	**18**	**0.10**	**Na_2CO_3**	**TBAI**	***n*BuOH**	**120**	***p*-ketone**	**81**
47	**2**	0.10	Na_2CO_3	TBAI	*n*BuOH	120	*p*-ketone	13
48	–	–	Na_2CO_3	TBAI	*n*BuOH	120	*p*-ketone	<5
49	**17**	0.10	Na_2CO_3	TBAI	*n*BuOH	120	*p*-methoxy	81
50	**32**	0.20	Na_2CO_3	TBAI	*n*BuOH	120	*p*-methoxy	<5
51	–	–	Na_2CO_3	TBAI	*n*BuOH	120	*p*-methoxy	<5

[a] All reactions have phenylacetylene (1.5 equiv), base (2.0 equiv) and additive (1.5 equiv) to aryl halogen, conc. = 0.12 M unless otherwise noted.

[b] NMR yield determined using 1,3,5-trimethoxybenzene as internal standard.

[c] less base was used.

With the optimal condition in our hand, a variety of internal alkenes were prepared by the sustainable Heck coupling catalyzed by **17**. The method realized good to excellent yields for substrates with both EWGs and EDGs, as well as heterocycles and Michael acceptor (coupling partner), although 1 mol% of **17** was used (**Figure 16**). The substrates that could potentially undergo Buchwald-Hartwig couplings (**60** and **61**) were specifically cross-coupled with styrene to give single Heck product, showing the selectivity of the optimal condition.

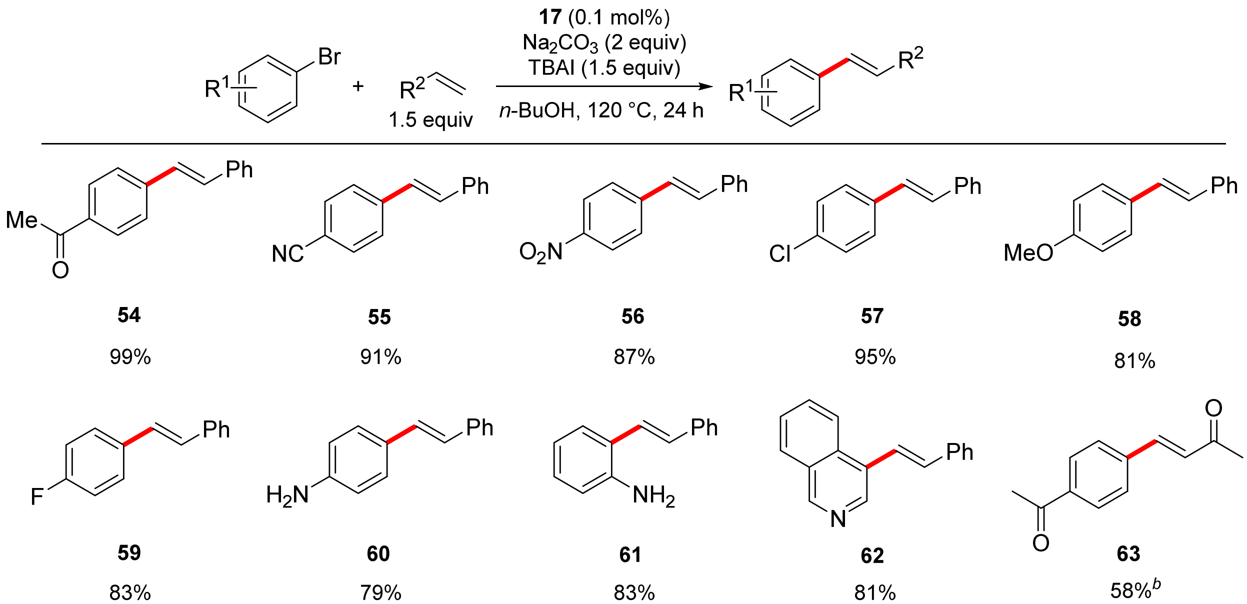

[a]Isolated yield.
[b]1 mol % of catalyst 17 was used.

Figure 16: Internal alkenes prepared by *p*NHC-Pd **17** catalyzed Heck-Mizoroki reaction;[a] the formed bonds are highlighted.

CHAPTER 5

Approaches to Light-Mediated Fluoroethylation of (Hetero)Arenes

5.1. Introduction to Light-Mediated Fluorination of (Hetero)Arenes

About 20% of the top 200 pharmaceutical products by retail sales contained at least one fluorine atom in 2016. A lot of methods for the introduction of fluorine into small molecules have been developed.[49] However, the general and sustainable transformations, especially the direct C–H fluorination, are still highly needed in both academia and industry. In order to apply it in late-stage functionalization of pharmaceuticals, researchers have investigated the mild, light-mediated and highly efficient fluorination for substrates with common FGs in drug molecules, such as carboxylic acid, esters and C–H bonds. Paquin and co-workers reported a photofluorodecarboxylation of aryloxy carboxylic acids using a ruthenium-based catalyst, visible-light irradiation and Selectflour® to give the fluorinated ethers in good yields (**Scheme 19**).[50] Chen and co-workers reported a visible light-mediated benzylic fluorination using Selectfluor® as the fluorine source and 9-fluorenone as the radical-initiating catalyst (**Scheme 20**).[51] Methods that introduce different fluoroalkyls, e.g. di- and trifluoromethyl, into bioactive molecules have been reported to evaluate the antimetabolite property, lipophilicity and acidity for drug candidates. For example, Akita et al. used the difluoromethylative reagent with sulfoximine EWG to afford the oxy-/difluoromethylative bifuctionalization of alkenes using fac-[Ir(ppy)$_3$] (see **Figure 5**) as photocatalyst. The scope is significantly broad with moderate to high yields (**Figure 17**).[52] However, no study of monofluoroethylation has been revealed to the best of our knowledge.

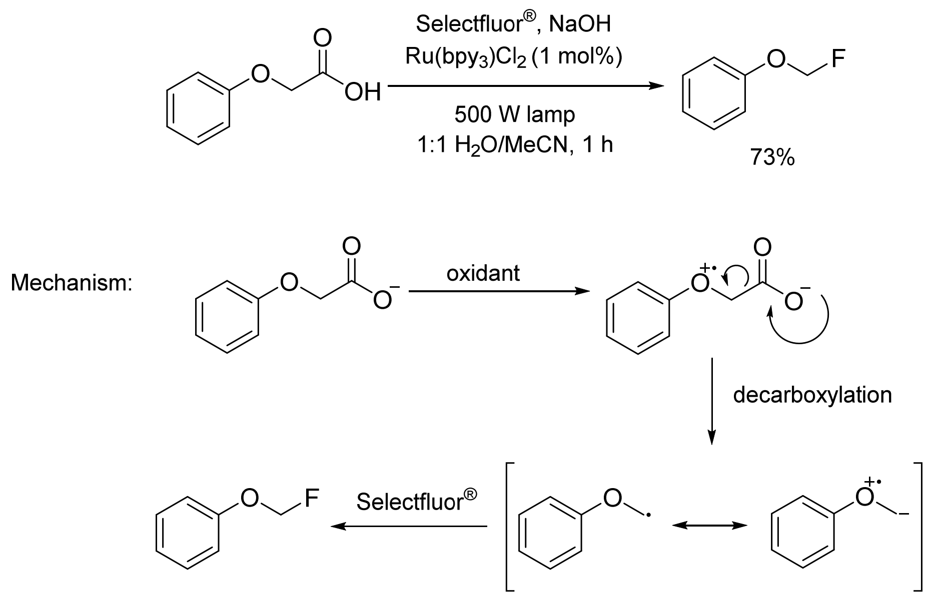

Scheme 19: Fluorinated ethers generated by light-mediated, photodecarboxylative fluorination.

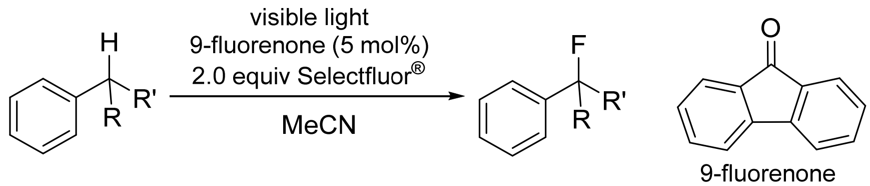

Scheme 20: Benzylic fluorination by visible light-promoted metal-free C–H activation.

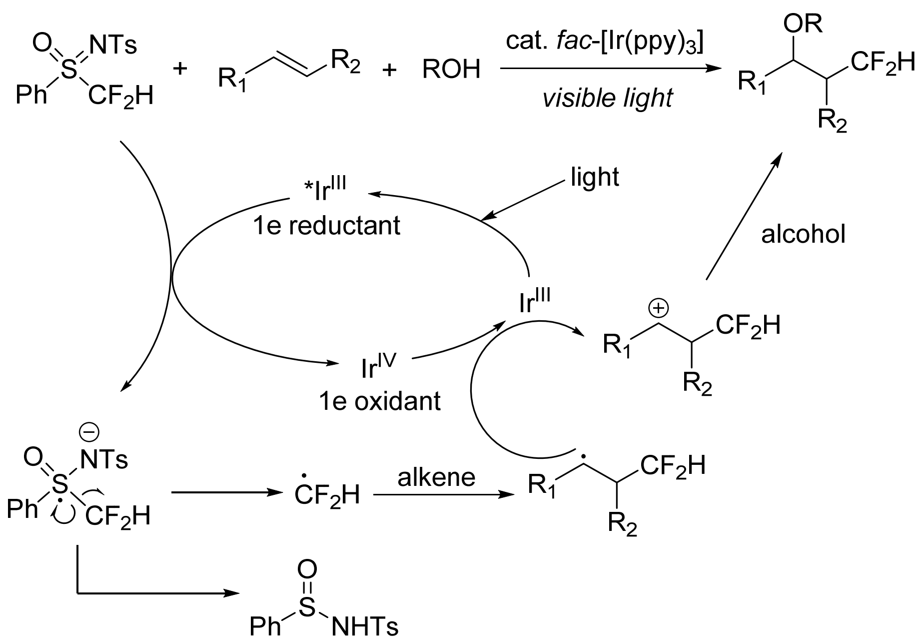

Figure 17: Oxydifluoromethylation of alkenes and the plausible mechanism.

5.2. Radical Ring-Opening Reaction of Cyclopropanone Precursor and *in situ* Photofluoroethylation of (Hetero)Arenes

Cyclopropanone is a promising moiety in organic chemistry for the synthetic potential of ring-opening and ring-expansion reactions. However, these highly strained ketones are known to prone to polymerization when nucleophile is presented and they are also highly volatile, which make the preparation and storage very challenging. Thus, cyclopropanone precursors that can generate cyclopropanone under equilibrium *in situ* are favored by synthetic chemists instead of the strained ketones in most cases. Because the classic precursors, cyclopropanone hydrate and hemiketal, are disadvantaged in the high reactivity and volatility,[53] investigations on new precursors are desired. Chen and co-workers reported a new type of precursor, 1-(phenylsulfonyl)cyclopropanol (**64c**, **Scheme 21**), with several steps of isolation and moderate overall yield in 2008.[54] The Lindsay research group optimized the reaction condition exhaustively to realize the one-pot and gram-scale synthesis with no column isolation or recrystallization needed.

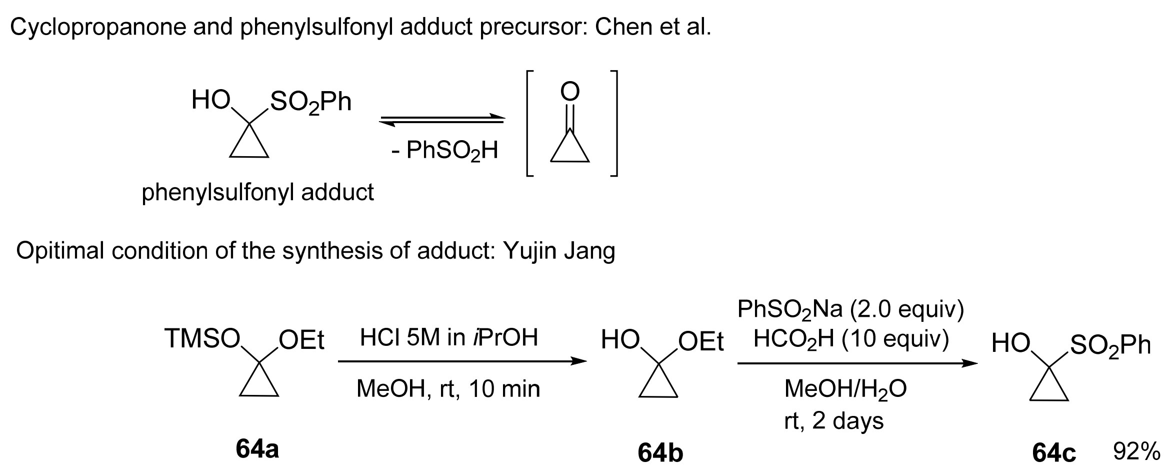

Scheme 21: Equilibrium of cyclopropanone and its precursor phenylsulfonyl adduct. Optimal condition of the synthesis of adduct investigated by the Lindsay group.

The Lindsay group studies various organic transformations related to cyclopropanone precursors and one of them is the radical ring-opening reaction to prepare fluoropropionic acid and the follow-up Minisci-type decarboxylative fluoroethylation. The Selectfluor®-initiated, radical ring-opening reaction of cyclopropanone sulfinic acid adduct was observed after exhaustive screening of conditions. By reacting Selectfluor® with the homemade (**Scheme 22 a**, **b** and **c**) or commercially available (**64a**, **d**) cyclopropanone precursors in the presence of Ag(I) (**a**) or at 60 °C (**b**, **c** and **d**) in aqueous media, fluoropropionic acid (**65**) was prepared with good and identical yields, demonstrating the general accessibility of the product. The mechanism is proposed in **Scheme 23**. Radical initiated by Ag(I) and Selectfluor® on OH of the methylsulfonyl adduct can open the cyclopropane ring and generate the primary radical on the terminal carbon. The primary radical could be quenched by the highly reactive Ag(II)-F species, form the C–F bond and regenerate Ag(I) for the next catalytic cycle. Finally, the fluorocarboxylic acid **65** could be obtained in the aqueous phase after hydrolysis of the acylsulfinate intermediate.

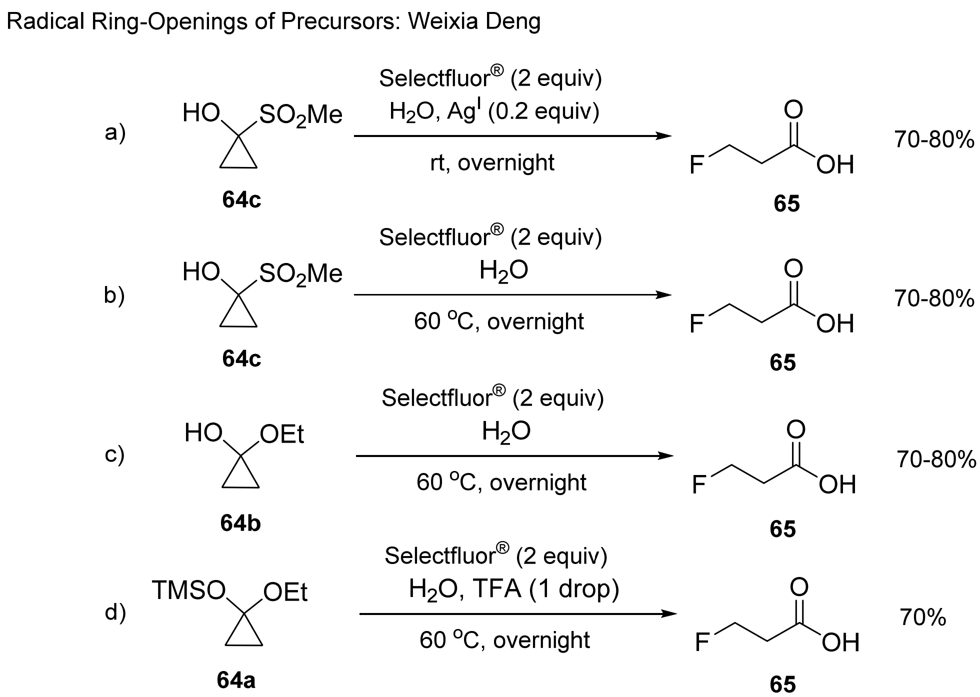

Scheme 22: Four Distinct Conditions for Fluoropropionic Acid **65** Generated by Radical Ring-Opening Reactions of Cyclopropanone Precursors (work of Weixia Deng in our group).

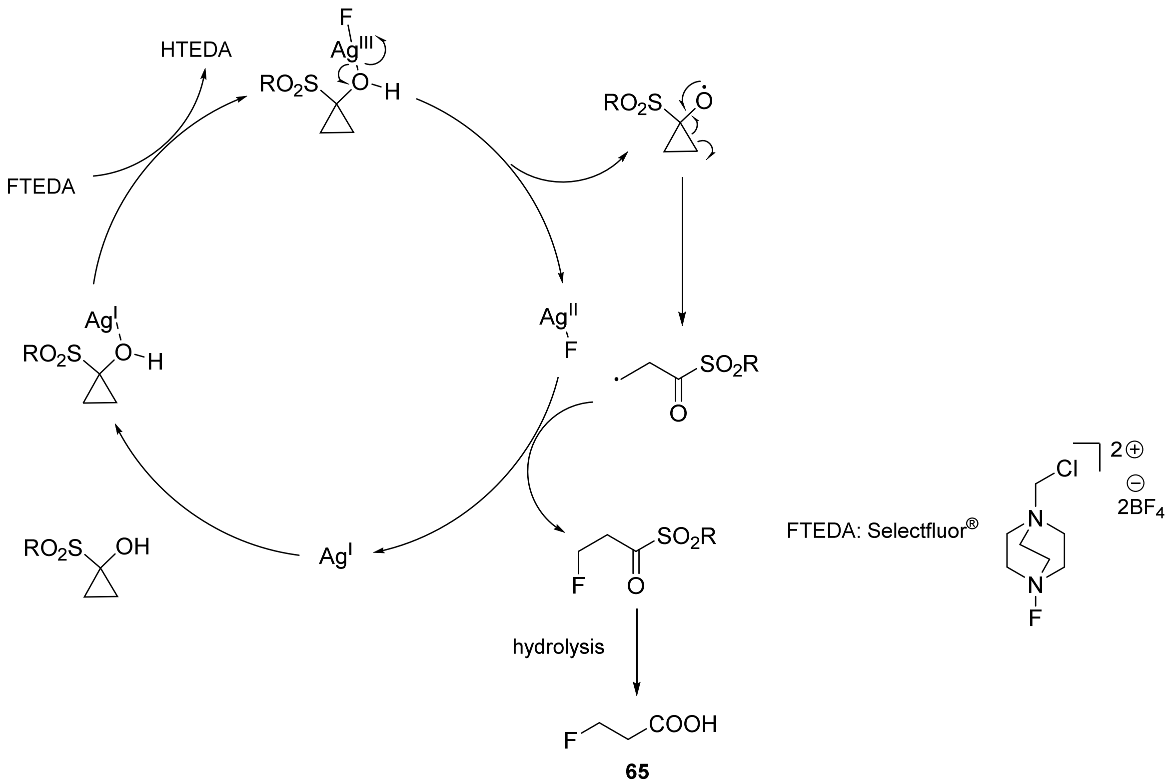

Scheme 23: Proposed Mechanism of Fluoropropionic Acid **65** Formation.

We then focused on the application of **65** to introduce fluoroethyl into small molecules through a general and mild synthetic method. While most modern literatures about decarboxylative Minisci-type C–H functionalization use *N*-hydroxyphthalimide esters (NHP-esters),[55] rather than the acid itself, and expensive Ir(III) or organic dye photocatalysts (see **Figure 5**), we were delighted to find the method reported by Jin and co-workers in 2019, where the light-mediated, decarboxylative, Minisci-type C–H alkylation used carboxylic acid as coupling partner and Fe(II) as photocatalyst.[56] Inspired by their work, butyric acid was selected as the model substrate for our first strategy to use fluoropropionic acid. However, the yield reported in the literature (78%) could hardly be repeated even after we tried to control several marginal factors carefully (**Table 5**).

Table 5. Iron catalyzed decarboxylative alkylation of lepidine reported by Jin et al. and in-lab repeating reactions with marginal factors carefully controlled.

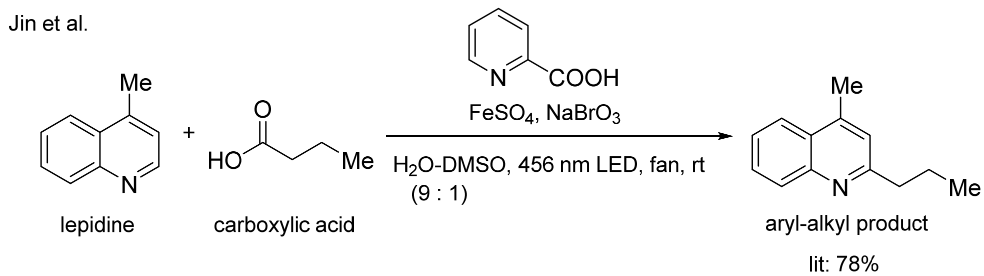

Entry	Cat. (%)	Additive	Degass	Fan	Distance of LED to vial	H_2O/DMSO	Yield[a] (%)
1	5	$NaBrO_3$	Y	N	NA	9:1	28
2	5	$NaBrO_3$	Y	Y	8.0 cm	9:1	40
3	5	$NaBrO_3$	N	Y	8.0 cm	9:1	29
4	5	$NaBrO_3$	Y	Y	8.0 cm	7:3	11
5	5	$NaBrO_3$	Y	Y	8.0 cm	7 (pH 3):3	30
6	5	$NaBrO_3$	Y	Y	8.0 cm	9 (pH 3):1	12
7	10	$NaBrO_3$	Y	Y	8.0 cm	9 (pH 3):1	31
8	10	$NaBrO_3$	Y	Y	8.0 cm	9:1	34
9	10	$NaBrO_3$	Y	Y	8.0 cm	9:1	35[b]
10	10	$NaClO_3$	Y	Y	8.0 cm	9:1	33

[a] NMR yield determined using 1,3,5-trimethoxybenzene as internal standard.

[b] 4 ml reaction vial was used instead of microwave vial.

When fluoropropionic acid was used for the C–H functionalization of lepidine with the conditions of Entry 2 (**Table 5**), no matter it was prepared and isolated from the reaction of 1-(methylsulfonyl)cyclopropanol and Selectfluor® or directly used *in situ* without isolation, no desired product was observed even after exhaustive screening of reaction conditions. We also tried to couple fluoropropionic acid with alkenes through radical process but no desired product was observed (**Scheme 24**).

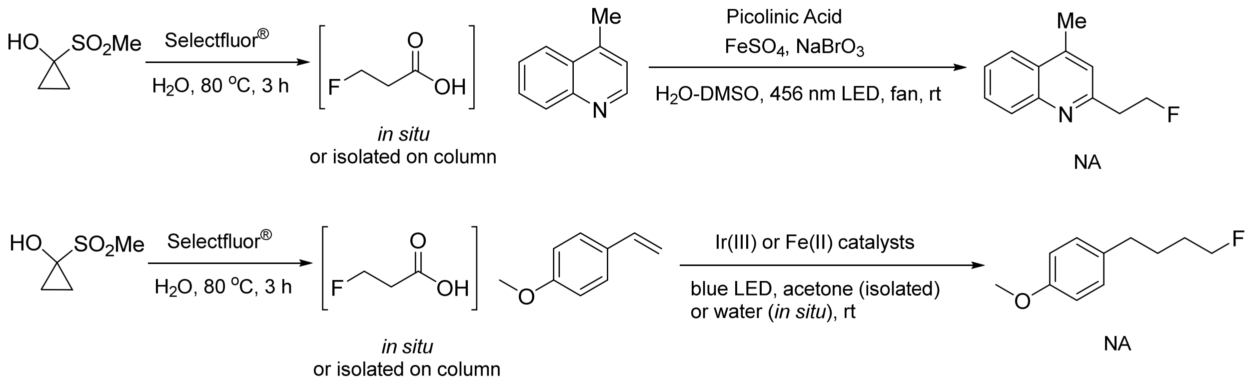

Scheme 24: Approaches to couple fluoroethyl onto lepidine and vinylbenzene.

By combining the reaction condition of preparing fluoropropionic acid in the presence of excess Selectfluor® in aqueous media with no light at rt (**Scheme 22 a**) with the follow up Minisci-type C–H functionalization, Weixia Deng in our group realized the fluoroethylation of 4-*tert*-butylpyridine in one pot (**Scheme 25 a**). After the carboxylic acid was generated *in situ*, heteroarene, oxidant (ammonium persulfate) and H_2SO_4 (10%) were added and the mixture was heated to 75 °C. Light was strictly avoided through the whole process and the yields of the fluoroethylated product were kept at low level (15-20%). The further optimization of the one-pot Minisci-type fluoroethylation of 4-*tert*-butylpyridine is undergoing in the Lindsay laboratory.

With the aforementioned results in our hand, we finally decided to prepare and use the NHP-ester of fluoropropionic acid after isolating the acid on column (SiO_2, 3% MeOH/DCM). Recently, Weixia Deng in our laboratory observed that Ni-bipyridine complex catalyzed the cross-electrophile coupling reaction of NHP ester with *p*-iodoacetophenone in excellent yield via the radical mechanism (**Scheme 25 b**).[57] Investigations on more sustainable approach with less catalyst loading, greener solvent and broad substrate scope are currently underway in our laboratory.

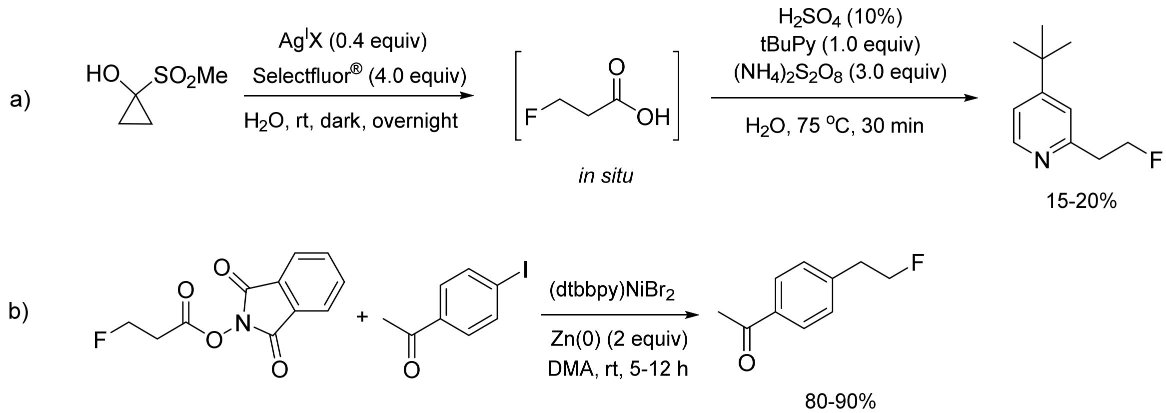

Scheme 25: Decarboxylative cross-electrophile coupling of NHP-ester with aryl iodide.

CHAPTER 6

Rational Design and Syntheses of Classic NHC-Ir Complexes for Hyperpolarization Processes

6.1. Introduction to Hyperpolarization Processes and the Relation with NHC-Ir Structures

Hyperpolarization processes can significantly increase the signal strength of nuclear magnetic resonance (NMR) and magnetic resonance imaging (MRI) of target molecules, which makes the *in vivo* observation of molecular metabolism a clinical reality.[38] It derives the associated non-Boltzmann distribution of spin energies from *para* hydrogen (*p*-H_2) via its reversible binding to a metal catalyst (NHC-Ir(I) complexes in most cases of SABRE). The process starts from Ir binding with *p*-H_2. Polarization is then transferred through the resulting scalar coupling network to a ligated substrate. The ligated substrate and H_2 dissociate from the complex to complete the catalytic cycle (**Figure 7**). Ligand dissociation delivers the free substrate where its modified magnetic properties improve detection without changing chemical identity. Previous studies have shown that aromatic NHC ligands are more effective mediators of the SABRE process than alkyl NHCs. Further study of the correlation between NHC chemical properties with SABRE activity was conducted by Duckett et al.[38] They designed and synthesized a large family of classic NHC-Ir complexes with various FGs on the phenyl substitution of NHC-N-wingtip or on the backbone of NHC. Several key factors, including electronics, steric effects, binding and dissociating rate of H_2 and substrate and deuterated NHC isotopologues were investigated for these NHC-Ir complexes to check the influence on SABRE activity. The most important feature of efficient complexes was the electron deficiency of NHC ligands and the bond length of Ir-C_1 was used as the key parameter to correlate electron deficiency with SABRE effect. Complexes with relatively stable EWGs on the backbone of NHC performed better in the hyperpolarization process compared with regular or e-rich NHCs as shown in the literature reported by Duckett et al.[38]

6.2. Design and Syntheses of Novel NHC-Ir Complexes

Since 1,3-bis(mesityl)imidazolium iridium complex had been well studied, the synthesis of 1,3-bis(mesityl)benzimidazole ligand and Ir complex was promising as the electronic property on the NHC ligand would be changed. After exhaustive screening of the synthetic routes for the aryl diamine (**66**, **Scheme 26**), the special Bulchwald-Hartwig reaction using tri-*tert*-butylphosphonium tetrafluoroborate as ligand and degassed solvent was identified as the optimal method for the sterically hindered aryl diamine synthesis.[58] Refluxing **66** in triethyl orthoformate at 135 °C and adding TMSCl by the end resulted the benzimidazolium chloride salt **67**. By following the typical procedure to prepare bis(mesityl)imidazole-Ir complex reported by Duckett et al., where KO*t*Bu was used to deprotonate C(1)-H and $[Ir(COD)Cl]_2$ was added to get the desired complex, the new bis(mesityl)benzimidazole-Ir complex **68** was synthesized in good yield. Crystals of **68** was grown from THF/2-propanol by the layering technique (**Figure 18**).

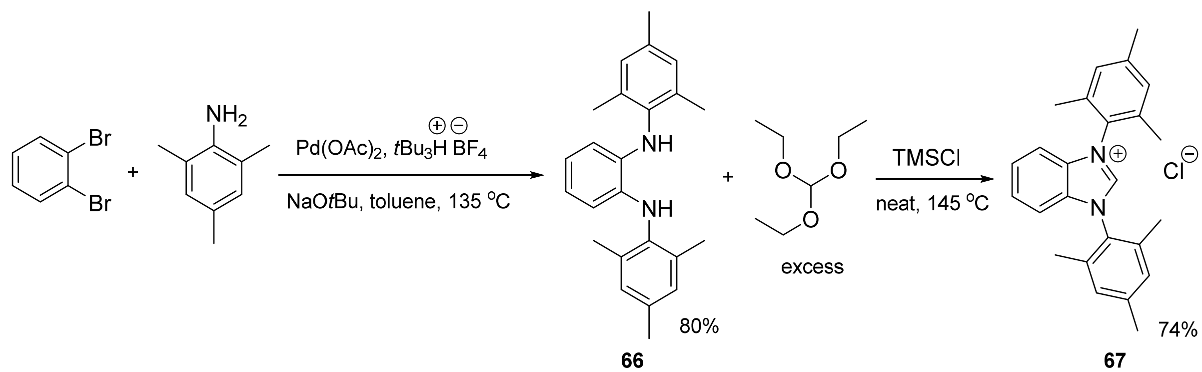

Scheme 26: Synthesis of 1,3-bis(mesityl)benimidazolium chloride ligand **67**.

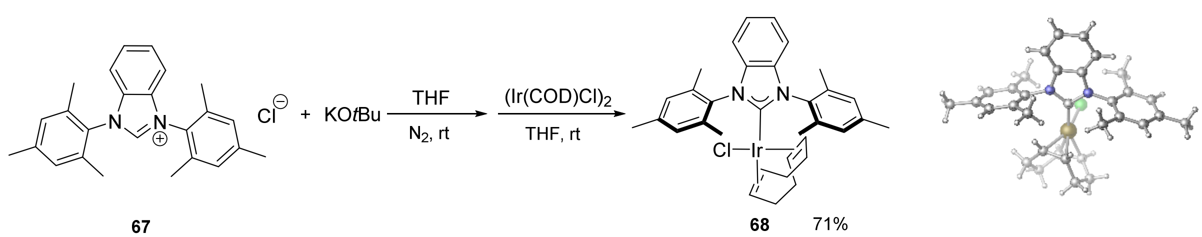

Figure 18: Synthesis of bis(mesityl)benzimidazole-Ir complex **68** and the corresponding X-Ray structure (omitting solvents; Ir = yellow, N = blue, Cl = green, C = grey, large, H = grey, small).

Inspired by the bipyridine side-arm design of our *p*NHC ligands, a NHC-Ir complexes with one mesityl replaced by pyridine side-arm was designed and synthesized (**70**, **Scheme 27**). The structure was supposed to have significant differences in steric and electronic effects compared with the classic bis(mesityl)imidazolium **68** and would influence the binding and dissociating of substrates on the Ir center thus affect the hyperpolarization effect. For the synthesis of complex **70**, 1-mesityl-1*H*-imidazole was refluxed in MeCN with 2-(Bromomethyl)pyridine hydrobromide for

2 days to yield the pyridine-modified bidentate *N*-mesitylimidazolium bromide **69** in 60% yield. Complex **70** was synthesized similarly as **68** by using the typical procedure reported by Duckett et al. The purifications were performed on column chromatography (SiO_2). However, lots of attempts on crystallizing the complex turned out to be just precipitate or microcrystals (DCM/Hexanes, Acetone/Hexanes, etc.). Notice that **70** was prone to decomposition thus further attempts of recrystallization were stopped, although the crystal structure had been reported in the literature.[59]

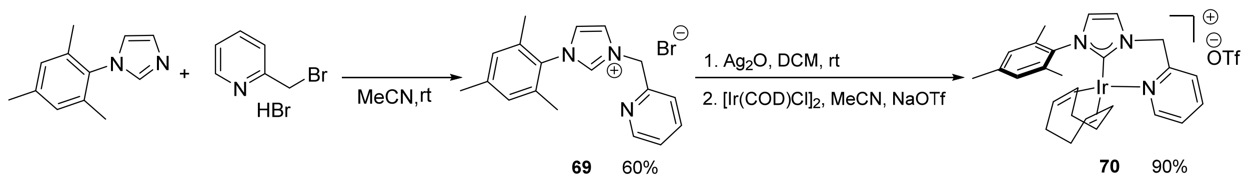

Scheme 27: Synthesis of (bi)pyrdine-modified monomesitylimidazolium chloride ligand (**69**) and Ir complexe (**70**).

In the meantime, Roger Machín-Rivera in our laboratory synthesized another electron-deficient NHC-Ir complex **71** (**Scheme 28**). Reaction of *N*,*N'*-dimesitylformamidine with oxalyl chloride afforded the neutral five-membered oxalamide as an off-white solid. Treatment of the carbene precursor with NaHMDS (NaHMDS = $NaN(SiMe_3)_2$) in THF at -80 °C leads to the unisolatable neutral diamidocarbene and the Ir complex was obtained with 40% yield after treating the carbene with $[Ir(COD)Cl]_2$, isolated on deactivated SiO_2 column.[60]

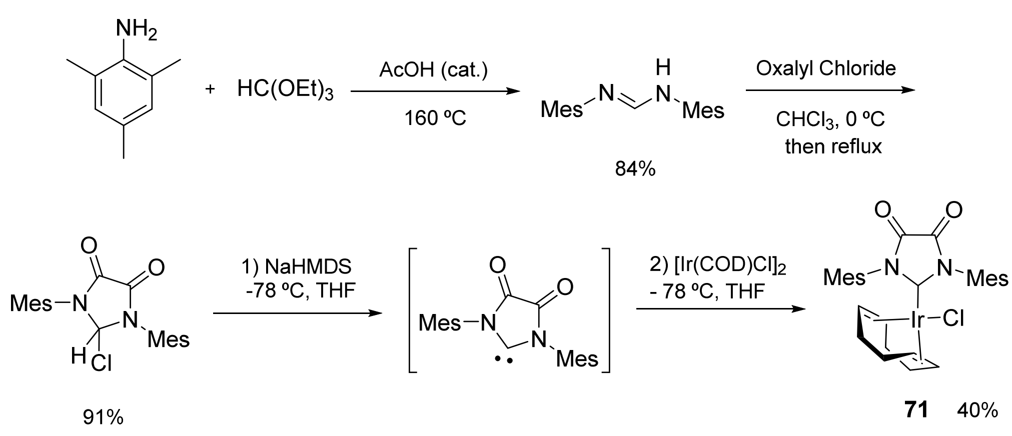

Scheme 28: Synthesis of oxalamide-based NHC-Ir complex **71**.

The Lindsay group has investigated various classic NHC-Ir complexes in collaboration with the Theis group at North Carolina State University. Besides the aforementioned **68**, **70**, and **71**, we are investigating more derivatives. The evaluation of hyperpolarization effect of these candidates are currently underway in our laboratory and Theis group, respectively.

Conclusion

In summary, a family of benzimidazolyl palladium complexes were readily prepared and evaluated as bifunctional catalysts. They existed in dinuclear benzimidazolyl form instead of the monomer *p*NHC form. All of the complexes could be isolated and three crystals were obtained and analyzed by X-Ray crystallography to further confirm the structures. The electronic effect could be altered on the backbone of the bipyridine side-arm via the similar synthetic route. More efforts are investigated in this direction so far.

These complexes were applied in C–H activation and one of the key intermediate, the acylated NHC-Pd-bipyridine complex, was crystallized out. So far, no positive result about the final C–H activated product was able to achieve and further exploration is underway in our laboratory.

Three cross-coupling reactions, Suzuki-Miyaura, Sonogashira-Hagihara and Heck-Mizoroki were found to be catalyzed by the new catalysts under sustainable conditions with excellent to quantitative yields and broad substrate scope. The lone pair of N wingtip accelerated the transmetalation step thus delivered quantitative yields. The family of imidazolyl metal complexes are anticipated to function for other organic transformations in the future.

Fluoropropionic acid can be generated by the Selectfluor®-initiated, radical ring-opening reaction of 1-sulfonylcyclopropanol. Based on the previous observation in our group, investigations on coupling the fluorocarboxylic acid with small molecules were conducted. Although the light-mediated, Minisci-type reaction was not as successful as expected, the cross-electrophile coupling of the NHP-ester with aryl iodide could be the alternative way to do fluoroethylation on bioactive drug molecules.

A family of classic NHC-Ir complexes were readily prepared for the use in hyperpolarization processes in the future. The crystal of bis(mesityl)benzimidazole-Ir was obtained and a NHC-Ir complex with a pyridine side-arm inspired by our benzimidazolyl-Pd design was synthesized and isolated on column. Further understanding about the correlation of NHC-Ir structure with hyperpolarization effect will be obtained by collaborating with the Theis group.

Experimental

General Experimental Conditions

General: Unless stated otherwise, all non-aqueous reactions were performed in oven-dried glassware sealed with microwave caps or rubber septa under a nitrogen atmosphere, and were stirred with Teflon-coated magnetic stir bars.[61] Liquid reagents and solvents were transferred by syringe using standard Schlenk techniques. Tetrahydrofuran (THF), diethyl ether (Et_2O), dichloromethane (CH_2Cl_2), toluene (PhMe), acetonitrile (MeCN), and methanol (MeOH) were dried by passage over a column of activated alumina (JC Meyers Solvent System). Anhydrous dimethyl sulfoxide (DMSO) and *N*,*N*-dimethylformamide (DMF) were obtained in Sure Seal bottles from Aldrich and used as received. All other solvents and reagents were used as received unless otherwise noted. Thin layer chromatography was performed using Silicycle silica gel 60 F-254 precoated plates (0.25 mm) and visualised by UV irradiation and anisaldehyde, CAM, potassium permanganate, or iodine stain. Sorbent silica gel (particle size 40-63 µm) was used for flash chromatography of the indicated solvent system according to standard techniques.[62] Flash chromatography was performed on a Biotage Isolera One. Nuclear magnetic resonance (NMR) spectra (^1H, ^{13}C) were recorded on Varian or Bruker spectrometers operating at either 300, 400, 500, 600 or 700 MHz for 1H and 100 or 150 MHz for ^{13}C experiments. Chemical shifts (δ) for ^1H NMR spectra are recorded in parts per million from tetramethylsilane with the solvent resonance as the internal standard (chloroform, δ 7.26 ppm or DMSO, δ 2.50 ppm). Data are reported as follows: chemical shift, multiplicity (s = singlet, d = doublet, t = triplet, q = quartet, qn = quintet, m = multiplet and br = broad), coupling constant in Hz, and integration. Chemical shifts for ^{13}C NMR spectra are recorded in parts per million from tetramethylsilane using the central peak of deuterochloroform (δ 77.16 ppm) or DMSO (δ 39.52 ppm) as the internal standard. All spectra were obtained with complete proton decoupling. Only select ^1H and ^{13}C spectra are reported. Infrared (IR) spectra were collected on a Thermo Scientific Nicolet iS5 FTIR instrument using attenuated total reflectance (ATR) mode and signals are reported in reciprocal centimeters (cm^{-1}). Only selected IR frequencies are reported. High-resolution mass spectral data were obtained from the NC State University Mass Spectrum Facility, using a Thermo Fisher Scientific Exactive Plus for ESI.

Reagents: methyl lithium (MeLi), *n*-butyl lithium (*n*BuLi), lithium diisopropylamide (LDA), tris(dibenzylideneacetone)dipalladium ($Pd_2(dba)_3$), palladium acetate ($Pd(OAc)_2$) and palladium chloride ($PdCl_2$) were purchased from commercial sources and used without further purification.

Experimental Procedures and Characterization Data

Syntheses of ligands and complexes

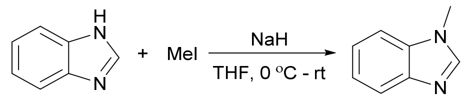

1-methyl-1*H*-benzo[*d*]imidazole.[63] An oven-dried microwave vial equipped with a magnetic stirbar was charged with benzimidazole (591 mg, 5.0 mmol, 1.0 equiv) and dry THF (10 mL), and NaH (60% in mineral oil, 309 mg, 7.7 mmol, 1.54 equiv) was added in 3 portions at 0 °C over a period of 50 minutes. MeI (0.34 mL, 5.49 mmol, 1.1 equiv) was then added to the reaction in one portion at the same temperature. The resulting mixture was allowed to slowly warm to room temperature over a period of 5 hours, before the reaction was quenched by addition of aq. sat. $NaHCO_3$. CH_2Cl_2 was added, the layers were separated, and the aqueous layer was further extracted three times with CH_2Cl_2. The combined organic layers were washed with brine, dried over Na_2SO_4, filtered and concentrated *in vacuo*. The crude product was purified by flash chromatography (0-5% MeOH/CH_2Cl_2 elution gradient) to afford the target molecule (594 mg, 90% yield) as a white solid. All analyses were consistent with previously reported data.[63]

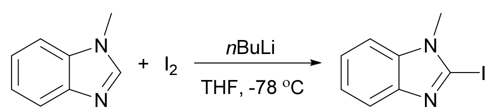

1

2-iodo-1-methyl-1*H*-benzo[*d*]imidazole (1).[64] An oven-dried microwave vial equipped with a magnetic stirbar was charged with 1-methyl-1*H*-benzo[*d*]imidazole (80 mg, 0.61 mmol, 1.0 equiv) and dry THF (0.60 mL), the solution was cooled to –78 °C and *n*-BuLi (2.5 M in hexane, 0.29 mL, 0.73 mmol, 1.2 equiv) was added dropwise. After stirring for 15 minutes, a solution of I_2 (230 mg, 0.91 mmol, 1.5 equiv) in 1.2 mL dry THF was added and then the mixture was allowed to warm to room temperature. The resulting black solution was left stirring at room temperature for another 15 minutes, before aq. sat. NH_4Cl was added at –78 °C. The resulting mixture was extracted three times with Et_2O and the combined organic layers were washed with brine, dried over $MgSO_4$, filtered and concentrated *in vacuo*. The crude product was purified by flash chromatography (30% EtOAc/Hexanes) to afford 90.3 mg (57%) of **1** as a white solid. All analyses were consistent with previously reported data.[64]

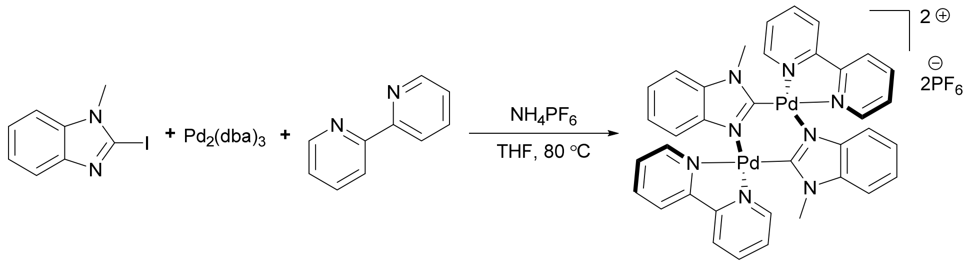

1 2

Palladium complex 2. In an inert atmosphere glove-box, an oven-dried microwave vial equipped with a magnetic stirbar was charged with **1** (200 mg, 0.78 mmol, 2.0 equiv), $Pd_2(dba)_3$ (354.8 mg, 0.39 mmol, 1.0 equiv) and 2,2'-bipyridine (121.1 mg, 0.78 mmol, 2.0 equiv). The vial was capped, taken out of the glove-box, and dry THF (15 mL) was added. The reaction was heated at 80 °C for 24 h to yield a green/grey suspension. The mixture was allowed to cool to rt and NH_4PF_6 (138.9 mg, 0.85 mmol, 2.2 equiv) was added in one portion. The reaction was heated at 80 °C for 12 h, allowed to cool to rt and passed through a pad of celite, eluting with THF. After removal of solvents under reduced pressure, the resulting orange oil was isolated by flash chromatography on basic Al_2O_3 (0-5% MeOH/CH_2Cl_2 elution gradient) to yield the pure complex **2** (75-208 mg, 18-50%) as a yellow powder. It should be noted that the yield was up to 50% when $Pd_2(dba)_3$ was used as received, and dropped dramatically after storing in the glovebox for months, an effect which has been observed and discussed previously.[65] Pale yellow crystals suitable for X-ray crystallography were obtained by slow vapor diffusion of hexanes into a concentrated solution of **2** in acetone, affording a **2**•acetone complex. **mp** 281 °C (decomposition). **^{1}H NMR** (400 MHz, DMSO-d_6) δ 8.84-8.77 (m, 4H), 8.55 (d, J = 5.6 Hz, 2H), 8.48-8.40 (m, 4H), 8.19 (d, J = 5.5 Hz, 2H), 7.75-7.66 (m, 4H), 7.64-7.57 (m, 4H), 7.34-7.25 (m, 4H), 4.02 (s, 6H), 2.07 (s, 6H, acetone). **^{13}C NMR** (100 MHz, DMSO-d_6) δ 168.3, 156.7, 155.1, 153.8, 149.9, 141.8, 141.6, 140.9, 135.8, 128.3, 127.2, 124.4, 123.9, 122.5, 122.1, 114.5, 111.1, 33.3, 30.7 (acetone). **IR** (neat, cm^{-1}) 1704, 1605, 1569, 1499, 1473, 1448, 1387, 1317, 1288, 1233, 1160, 1091, 1066, 1038, 1010, 826, 740, 728, 666, 649, 554, 417. **HRMS** (HESI) calcd for $[C_{36}H_{30}N_8Pd_2]^{2+}$: m/z 393.03261, found 393.03264.

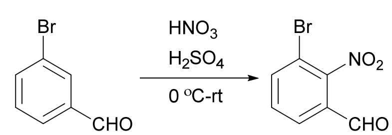

6

3-bromo-2-nitrobenzaldehyde (6).[66] An oven-dried microwave vial equipped with a magnetic stirbar was charged with fuming nitric acid (100 μL) and concentrated sulfuric acid (1.4 mL) at

0 °C, followed by 3-bromobenzaldehyde (315 µL, 2.7 mmol) added over a period of 20 min. The reaction was allowed to warm to rt, heated at 40 °C for 12 h and then poured into crushed ice. 1M aq. NaOH was added slowly until pH 7 was reached, and the aqueous phase was extracted three times with CH_2Cl_2. The combined organic layers were washed with brine, dried over Na_2SO_4, filtered and concentrated *in vacuo*. The crude product was purified by flash chromatography (10-20% EtOAc/Hexanes elution gradient) to afford the pure **6** (126.7 mg, 20%) as a white solid. All analyses were consistent with previously reported data.[66]

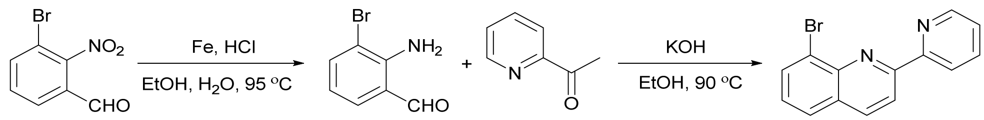

6 7

8-bromo-2-(pyridin-2-yl)quinoline (7).[67] A microwave vial equipped with a magnetic stirbar was charged with **6** (189 mg, 0.82 mmol, 1.0 equiv), iron powder (220 mg, 3.93 mmol, 4.8 equiv), absolute EtOH (2.9 mL), concentrated HCl (1 drop) and water (0.4 mL). The resulting black suspension was heated at 95 °C for 2 h and then allowed to cool to rt. EtOAc and aq. sat. $NaHCO_3$ were added and the layers separated. The aqueous layer was further extracted three times with EtOAc, and the combined organic layers were washed with brine, dried over $MgSO_4$, filtered and concentrated *in vacuo* to yield the crude aniline intermediate as a yellow oil. Absolute EtOH (5.3 mL), 2-acetylpyridine (122 µL, 1.09 mmol, 1.33 equiv) and KOH (23 mg, 0.41 mmol, 0.5 equiv) were added to an oven-dried microwave vial containing the crude aniline intermediate and then heated at 90 °C for 2 days. The reaction was allowed to cool to rt and CH_2Cl_2 and H_2O were added. The layers were separated, the aqueous layer was further extracted with CH_2Cl_2, and the combined organic layers were washed with brine, dried over Na_2SO_4, filtered and concentrated *in vacuo*. The resulting crude product was purified by flash chromatography (15-25% EtOAc/Hexanes elution gradient) to afford the pure **7** (186.4 mg, 80% over 2 steps) as a white solid. All analyses were consistent with previously reported data.[67]

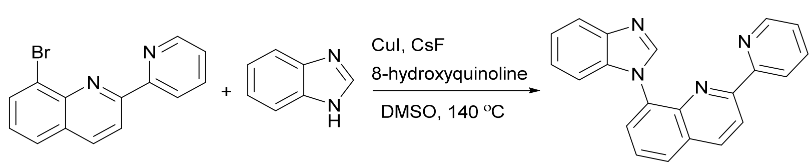

7 8

8-(1*H*-benzo[*d*]imidazol-1-yl)-2-(pyridin-2-yl)quinoline (8). In an inert atmosphere glove-box, an oven-dried microwave vial equipped with a magnetic stirbar was charged with **7** (100 mg, 0.35

mmol, 1.0 equiv), benzimidazole (50 mg, 0.42 mmol, 1.2 equiv), CuI (3.4 mg, 0.018 mmol, 0.05 equiv), 8-hydroxyquinoline (5.1 mg, 0.035 mmol, 0.10 equiv) and CsF (133.3 mg, 0.88 mmol, 2.5 equiv). The vial was capped, taken out of the glove-box and dry DMSO (6 mL) was added. The reaction was heated at 140 °C for 24 h to yield a black suspension which was allowed to cool to room temperature. EtOAc and H_2O were added, the layers were separated and the aqueous layer was further extracted three times with EtOAc. The combined organic layers were washed with brine, dried over Na_2SO_4, filtered and concentrated *in vacuo*. The crude product was purified by flash chromatography (0-4% MeOH/CH_2Cl_2 elution gradient) to afford pure **S5** (93 mg, 82%) as a yellow powder. **mp** 207-209 °C. **^{1}H NMR** (600 MHz, DMSO-d_6) δ 8.75 (s, 1H), 8.73-8.67 (m, 3H), 8.24-8.20 (m, 1H), 8.12 (dd, J = 7.4, 1.3 Hz, 1H), 8.05 (d, J = 7.9 Hz, 1H), 7.90-7.83 (m, 3H), 7.49-7.44 (m, 1H), 7.43 (d, J = 8.0 Hz, 1H), 7.35-7.30 (m, 1H), 7.30-7.26 (m, 1H). **^{13}C NMR** (150 MHz, DMSO-d_6) δ 155.7, 154.7, 149.3, 145.8, 143.3, 141.6, 137.9, 137.4, 134.8, 132.9, 129.1, 128.3, 127.1, 126.7, 124.9, 123.1, 122.2, 121.1, 119.7, 119.3, 111.0. **IR** (neat, cm^{-1}) 3145, 3053, 2918, 1874, 1710, 1594, 1563, 1494, 1462, 1423, 1278, 1242, 1189, 993, 950, 856, 787, 726, 678, 626, 556, 457. **HRMS** (HESI) calcd for $[C_{21}H_{14}N_4+H]^+$: *m/z* 323.12912, found 323.12936.

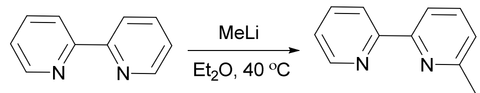

9

6-methyl-2,2'-bipyridine (9).[68] An oven-dried 100 mL round-bottom flask equipped with a magnetic stirbar was charged with 2,2’-bipyridine (1.0 g, 6.4 mmol, 1.0 equiv) and dry Et_2O (40 mL) and the resulting solution was cooled to 0 °C. A solution of MeLi (4.0 mL, 1.6 M in Et_2O, 6.4 mmol, 1.0 equiv) was added dropwise, and the resulting black solution was heated to 40 °C for 3 h. The reaction was allowed to cool to room temperature and H_2O was added. The layers were separated and the aqueous layer was extracted three times with Et_2O. The combined organic layers were washed with brine, dried over Na_2SO_4, filtered and concentrated *in vacuo* to afford the crude **9** an orange oil. A saturated solution of $KMnO_4$ in acetone (100 mL) was added, stirred for a few seconds and the mixture was filtered on Celite eluting with acetone to remove the MnO_2 precipitate. Solvents were evaporated *in vacuo* and the crude product was purified by flash chromatography (10% EtOAc/hexanes) to afford pure **9** (503 mg, 46%) as a pale yellow oil. All analyses were consistent with previously reported data.[68]

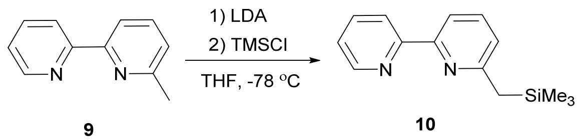

6-((trimethylsilyl)methyl)-2,2'-bipyridine (10).[69] An oven-dried microwave vial equipped with a magnetic stirbar was charged with **9** (503 mg, 2.96 mmol, 1.0 equiv) and dry THF (11 mL) and the resulting solution was cooled to –78 °C. A solution of lithium diisopropylamide (1.48 mL, 2.0 M in THF/heptane/ethylbenzene, 2.96 mmol, 1.0 equiv) was added dropwise, and the resulting black mixture was stirred at the same temperature for 1 hour. TMSCl (412 µL, 3.25 mmol, 1.1 equiv) was then added rapidly, and the mixture was stirred vigorously for 20 seconds. The reaction was quenched by rapid addition of absolute EtOH (0.6 mL), and the cold mixture was poured into a separatory funnel containing aq. sat. $NaHCO_3$ and allowed to warm to room temperature. The solution was extracted three times with CH_2Cl_2, and the combined organic layers were washed with brine, dried over Na_2SO_4, filtered and concentrated *in vacuo*. The crude product was purified by flash chromatography (10% EtOAc/1% Et_3N/hexanes) to afford pure **10** (590 mg, 82%) as a colorless oil. All analyses were consistent with previously reported data.[69]

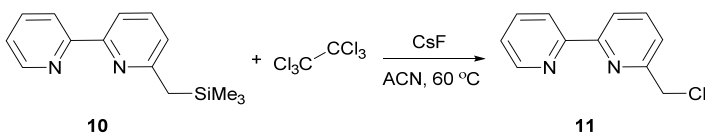

6-(chloromethyl)-2,2'-bipyridine (11).[69] An oven-dried microwave vial equipped with a magnetic stirbar was charged with **S7** (590 mg, 2.43 mmol, 1.0 equiv), hexachloroethane (2.31 g, 9.76 mmol, 4.0 equiv), CsF (1.48 g, 9.74 mmol, 4.0 equiv) and dry MeCN (22 mL). The resulting heterogeneous mixture was heated at 60 °C for 4 hours, allowed to cool to room temperature and then EtOAc and H_2O were added. The layers were separated and the aqueous layer was extracted three times with EtOAc. The combined organic layers were washed with brine, dried over Na_2SO_4, filtered and concentrated *in vacuo*. The crude product was purified by flash chromatography (30% EtOAc/hexanes) to afford **11** (472 mg, 95%) as a colorless oil. All analyses were consistent with previously reported data.[69]

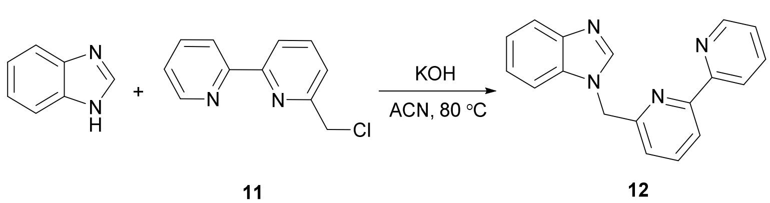

1-([2,2'-bipyridin]-6-ylmethyl)-1*H*-benzo[*d*]imidazole (12). An oven-dried microwave vial equipped with a magnetic stirbar was charged with **11** (472 mg, 2.31 mmol, 1.0 equiv), benzimidazole (272.4 mg, 2.31 mmol, 1.0 equiv), KOH (154.8 mg, 2.76 mmol, 1.2 equiv) and dry MeCN (22 mL). The resulting white heterogeneous mixture was heated at 80 °C for 24 h. The resulting pale red solution was allowed to cool to room temperature and then CH_2Cl_2 and aq. sat. $NaHCO_3$ were added. The layers were separated and the aqueous layer was extracted three times with CH_2Cl_2. The combined organic layers were washed with brine, dried over Na_2SO_4, filtered and concentrated *in vacuo*. The crude product was purified by flash chromatography (0-5% MeOH/1% Et_3N/CH_2Cl_2 elution gradient) to afford **12** (625.6 mg, 95%) as a white solid. **mp** 125-126 °C. **^{1}H NMR** (600 MHz, $CDCl_3$) δ 8.58 (dd, *J* = 4.9, 1.7 Hz, 1H), 8.25 (dd, *J* = 10.7, 7.9 Hz, 2H), 8.04 (s, 1H), 7.80 (d, *J* = 7.9 Hz, 1H), 7.68 (td, *J* = 7.7, 1.8 Hz, 1H), 7.58 (t, *J* = 7.8 Hz, 1H), 7.31-7.27 (m, 1H), 7.23-7.15 (m, 3H), 6.86 (d, *J* = 7.7 Hz, 1H), 5.39 (s, 2H). **^{13}C NMR** (150 MHz, $CDCl_3$) δ 156.1, 155.4, 154.7, 149.1, 143.9, 143.7, 138.0, 136.9, 133.9, 124.0, 123.1, 122.3, 121.1, 121.0, 120.4, 120.2, 110.1, 50.4. **IR** (neat, cm^{-1}) 3085, 3062, 2915, 1616, 1579, 1563, 1496, 1452, 1425, 1373, 1335, 1288, 1271, 1177, 1092, 990, 880, 779, 765, 753, 653, 619, 583, 424. **HRMS** (HESI) calcd for $[C_{18}H_{14}N_4+H]^+$: *m/z* 287.12912, found 287.12932.

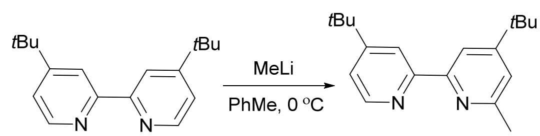

13

4,4'-di-*tert*-butyl-6-methyl-2,2'-bipyridine (13).[70] An oven-dried 50 mL round-bottom flask equipped with a magnetic stirbar was charged with 4,4'-di-*tert*-butyl-2,2'-bipyridine (500 mg, 1.9 mmol, 1.0 equiv) and dry toluene (8 mL) and the resulting solution was cooled to 0 °C. A solution of MeLi (1.3 mL, 3.1 M in Et_2O, 4.1 mmol, 2.2 equiv) was added dropwise, and the resulting black solution was allowed to stir at rt for 14 h. The reaction was allowed to cool to 0 °C and H_2O was added. The layers were separated and the aqueous layer was extracted three times with Et_2O. The combined organic layers were washed with brine, dried over $MgSO_4$, filtered and concentrated *in vacuo* to afford the crude **13** an orange oil. A suspension of MnO_2 in CH_2Cl_2 (4 equiv) was added, stirred for 1 h and the mixture was filtered on Celite eluting with acetone to remove the MnO_2 precipitate. Solvents were evaporated *in vacuo* and the crude product was purified by flash chromatography (10% EtOAc/hexanes) to afford pure **13** (253 mg, 48%) as a white solid. All analyses were consistent with previously reported data.[70]

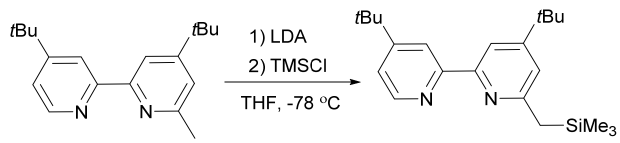

13 **14**

4,4'-di-*tert*-butyl-6-((trimethylsilyl)methyl)-2,2'-bipyridine (14).[69] An oven-dried microwave vial equipped with a magnetic stirbar was charged with **13** (253 mg, 0.90 mmol, 1.0 equiv) and dry THF (4 mL) and the resulting solution was cooled to –78 °C. A solution of lithium diisopropylamide (0.45 mL, 2.0 M in THF/heptane/ethylbenzene, 0.90 mmol, 1.0 equiv) was added dropwise, and the resulting black mixture was stirred at the same temperature for 1 hour. TMSCl (125 µL, 0.99 mmol, 1.1 equiv) was then added rapidly, and the mixture was stirred vigorously for 20 seconds. The reaction was quenched by rapid addition of absolute EtOH (0.15 mL), and the cold mixture was poured into a separatory funnel containing aq. sat. $NaHCO_3$ and allowed to warm to room temperature. The solution was extracted three times with CH_2Cl_2, and the combined organic layers were washed with brine, dried over Na_2SO_4, filtered and concentrated *in vacuo*. The crude product was purified by flash chromatography (10% EtOAc/1% Et_3N/hexanes) to afford pure **14** (209 mg, 65%) as a yellow oil. **^{1}H NMR** (500 MHz, $CDCl_3$) δ 8.56 (d, *J* = 5.2 Hz, 1H), 8.49 (d, *J* = 1.9 Hz, 1H), 8.13 (d, *J* = 1.8 Hz, 1H), 7.22 (dd, *J* = 5.2, 2.0 Hz, 1H), 6.97 (d, *J* = 1.8 Hz, 1H), 2.39 (s, 2H), 1.34 (s, 9H), 1.33 (s, 9H), 0.08 (s, 9H).

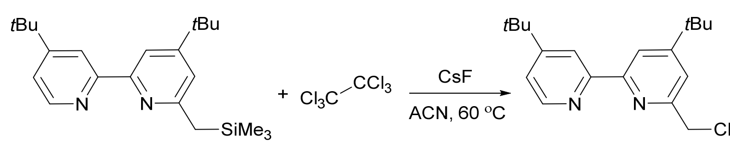

14 **15**

4,4'-di-*tert*-butyl-6-(chloromethyl)-2,2'-bipyridine (15).[69] An oven-dried microwave vial equipped with a magnetic stirbar was charged with **14** (556.50 mg, 1.57 mmol, 1.0 equiv), hexachloroethane (1.49 g, 6.28 mmol, 4.0 equiv), CsF (953.90 g, 6.28 mmol, 4.0 equiv) and dry MeCN (22 mL). The resulting heterogeneous mixture was heated at 60 °C for 4 hours, allowed to cool to room temperature and then EtOAc and H_2O were added. The layers were separated and the aqueous layer was extracted three times with EtOAc. The combined organic layers were washed with brine, dried over Na_2SO_4, filtered and concentrated *in vacuo*. The crude product was purified by flash chromatography (30% EtOAc/hexanes) to afford **15** (412 mg, 83%) as a colorless oil. **^{1}H NMR** (500 MHz, $CDCl_3$) δ 8.47 (d, *J* = 5.2 Hz, 1H), 8.34 (d, *J* = 2.0 Hz, 1H), 8.27 (d, *J* = 1.8 Hz, 1H), 7.16 (dd, *J* = 5.2, 2.0 Hz, 1H), 4.66 (s, 2H), 1.27 (s, 9H), 1.26 (s, 9H).

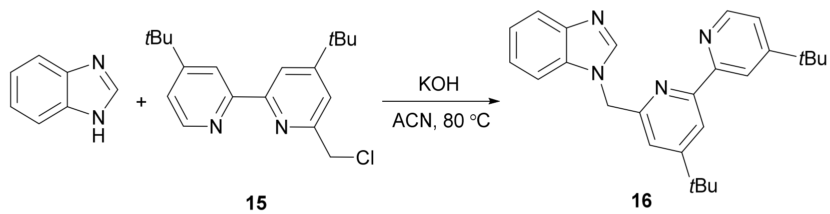

15 16

1-((4,4'-di-*tert*-butyl-[2,2'-bipyridin]-6-yl)methyl)-1H-benzo[*d*]imidazole (16). An oven-dried microwave vial equipped with a magnetic stirbar was charged with **15** (356.5 mg, 1.13 mmol, 1.0 equiv), benzimidazole (132.9 mg, 1.13 mmol, 1.0 equiv), KOH (76.0 mg, 1.35 mmol, 1.2 equiv) and dry MeCN (11 mL). The resulting white heterogeneous mixture was heated at 80 °C for 24 h. The resulting white suspension was allowed to cool to room temperature and then CH_2Cl_2 and aq. sat. $NaHCO_3$ were added. The layers were separated and the aqueous layer was extracted three times with CH_2Cl_2. The combined organic layers were washed with brine, dried over Na_2SO_4, filtered and concentrated *in vacuo*. The crude product was purified by flash chromatography (0-5% MeOH/1% Et_3N/CH_2Cl_2 elution gradient) to afford **16** (402.8 mg, 90%) as a white solid. **mp** 137-138 °C. **^{1}H NMR** (500 MHz, $CDCl_3$) δ 8.57 (d, J = 5.2 Hz, 1H), 8.36 (d, J = 1.7 Hz, 1H), 8.28 (d, J = 2.0 Hz, 1H), 8.13 (s, 1H), 7.90-7.82 (m, 1H), 7.33-7.25 (m, 2H), 7.11 (d, J = 1.7 Hz, 1H), 5.54 (s, 2H), 1.35 (s, 9H), 1.30 (s, 9H). **^{13}C NMR** (125 MHz, $CDCl_3$) δ 162.6, 161.1, 156.6, 155.9, 154.4, 149.1, 144.0, 143.7, 134.4, 123.1, 122.3, 121.1, 120.5, 118.6, 118.3, 117.6, 110.4, 50.8, 35.2, 35.1, 30.7, 30.6. **IR** (neat, cm^{-1}) 3051, 2962, 2903, 2866, 1590, 1549, 1493, 1464, 1422, 1381, 1362, 1340, 1269, 1203, 1180, 1121, 1009, 993, 965, 900, 846, 793, 724, 683, 654, 619, 594, 535.

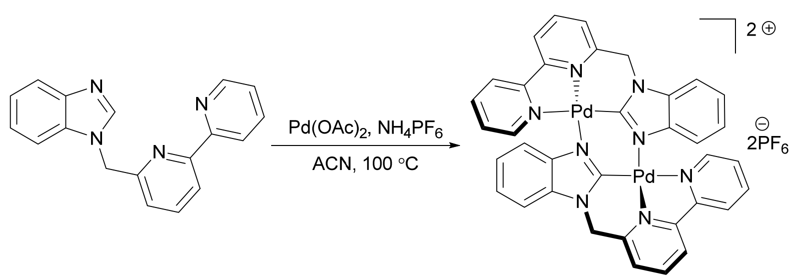

12 17

Palladium complex 17. In an inert atmosphere glove-box, an oven-dried microwave vial equipped with a magnetic stirbar was charged with **12** (400.6 mg, 1.40 mmol, 1.0 equiv), $Pd(OAc)_2$ (314.1 mg, 1.40 mmol, 1.0 equiv) and NH_4PF_6 (250.8 mg, 1.54 mmol, 1.1 equiv). The vial was capped and taken out of the glove-box, dry MeCN (14 mL) was added and the reaction was heated at 100 °C for 24 hours to yield a green/black mixture. The reaction was allowed to cool to room temperature and then passed through a pad of celite, eluting with MeCN. After evaporation of the solvent under reduced pressure, the resulting solid was dissolved in CH_2Cl_2, filtered on a pad of basic Al_2O_3 and evaporated under reduced pressure. Crystals suitable for X-ray crystallography were obtained by slow vapor diffusion of hexanes into a concentrated solution of **17** in MeCN, affording a **17**•MeCN complex (417.8 mg, 56%) as yellow crystals. **mp** 273 °C (decomposition). **^{1}H NMR** (600 MHz, DMSO-d_6) δ 8.80 (d, J = 8.1 Hz, 2H), 8.77 (d, J = 8.1 Hz, 2H), 8.59 (t, J = 7.9 Hz, 2H), 8.35 (td, J = 7.9, 1.6 Hz, 2H), 8.22 (d, J = 7.9 Hz, 2H), 8.02 (d, J = 8.3 Hz, 2H), 7.87 (d, J = 8.1 Hz, 2H), 7.82 (dd, J = 5.7, 1.5 Hz, 2H), 7.59-7.55 (m, 2H), 7.48 (t, J = 7.7 Hz, 2H), 7.34 (t, J = 7.7 Hz, 2H), 6.49 (d, J = 16.9 Hz, 2H), 5.84 (d, J = 16.8 Hz, 2H), 2.1 (s, 3H, MeCN). **^{13}C NMR** (150 MHz, DMSO-d_6) δ 161.8, 157.5, 154.7, 153.9, 149.9, 142.4, 141.5, 139.6, 133.9, 127.4, 126.8, 124.2, 123.6, 123.1, 122.7, 117.9 (MeCN), 115.9, 111.0, 49.8, 1.0 (MeCN). **IR** (neat, cm^{-1}) 3091, 1604, 1571, 1443, 1397, 1321, 1287, 1256, 1162, 1039, 1025, 824, 768, 738, 648, 554, 422. **HRMS** (HESI) calcd for $[C_{36}H_{26}N_8Pd_2]^{2+}$: m/z 391.01696, found 391.01698.

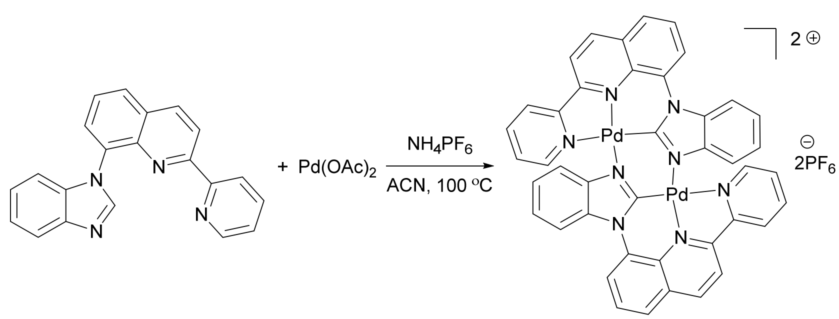

8

18

Palladium complex 18. In an inert atmosphere glove-box, an oven-dried microwave vial equipped with a magnetic stirbar was charged with **8** (60.4 mg, 0.19 mmol, 1.0 equiv), $Pd(OAc)_2$ (42.1 mg, 0.19 mmol, 1.0 equiv) and NH_4PF_6 (36.6 mg, 0.22 mmol, 1.2 equiv). The vial was capped and taken out of the glove-box, dry MeCN (6 mL) was added and the reaction was heated at 100 °C for 24 hours to yield a dark yellow solution. The reaction was allowed to cool to room temperature and then passed through a pad of celite, eluting with MeCN. After evaporation of the solvent under reduced pressure, the resulting glassy yellow solid was purified by flash chromatography on basic Al_2O_3 (0-5% MeOH/CH_2Cl_2 elution gradient) to yield pure **18** (65.5 mg, 61%) as a yellow powder. **mp** 294 °C (decomposition). **^{1}H NMR** (500 MHz, DMSO-d_6) δ 9.31 (d, J = 8.6 Hz, 2H), 8.91 (dd, J = 18.2, 8.4 Hz, 4H), 8.81 (d, J = 7.6 Hz, 2H), 8.43-8.37 (m, 4H), 8.27-8.17 (m, 4H), 7.96 (d, J = 8.1 Hz, 2H), 7.59-7.53 (m, 4H), 7.46 (t, J = 7.8 Hz, 2H), 7.27 (t, J = 7.7 Hz, 2H). **^{13}C NMR** (150 MHz, DMSO-d_6) δ 162.1, 159.8, 155.7, 150.4, 143.0, 141.9, 141.6, 136.2, 133.0, 132.7, 130.6, 129.5, 128.3, 128.0, 125.9, 125.7, 124.6, 123.9, 121.9, 117.2, 113.1. **IR** (neat, cm^{-1}) 3087, 1600, 1565, 1524, 1464, 1412, 1364, 1340, 1280, 1236, 1208, 1153, 1053, 1025, 1007, 990, 824, 738, 686, 653, 622. **HRMS** (HESI) calcd for $[C_{42}H_{26}N_8Pd_2]^{2+}$: *m/z* 427.01696, found 427.01841.

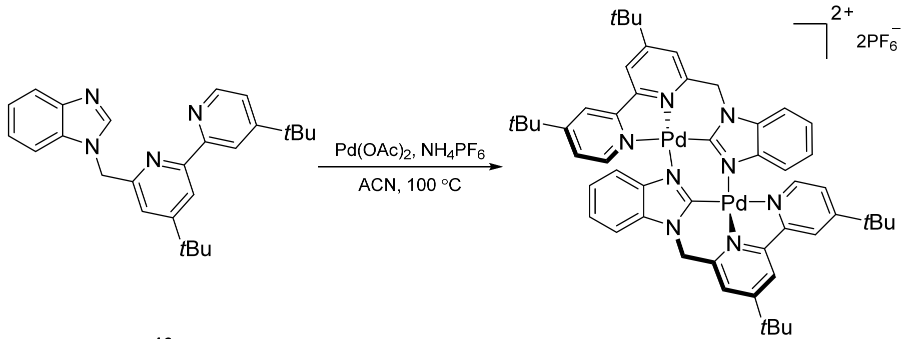

16 19

Palladium complex 19. In an inert atmosphere glove-box, an oven-dried microwave vial equipped with a magnetic stirbar was charged with **16** (121.8 mg, 0.31 mmol, 1.0 equiv), $Pd(OAc)_2$ (69.0 mg, 0.31 mmol, 1.0 equiv) and NH_4PF_6 (55.4 mg, 0.34 mmol, 1.1 equiv). The vial was capped and taken out of the glove-box, dry MeCN (4 mL) was added and the reaction was heated at 100 °C for 24 hours to yield a yellow mixture. The reaction was allowed to cool to room temperature and then passed through a pad of celite, eluting with MeCN and concentrated *in vacuo*. The crude product was purified by flash chromatography (0-1% MeOH/CH_2Cl_2 elution gradient) to afford **19** (178.1 mg, 89%) as a yellow powder. Crystals suitable for X-ray crystallography were obtained by slow vapor diffusion of hexanes into a concentrated solution of **19** in CH_2Cl_2, affording a **19**•CH_2Cl_2 complex as yellow crystals. **mp** 270 °C (decomposition). **^{1}H NMR** (700 MHz, DMSO-*d*$_6$) δ 8.76 (dd, *J* = 17.7, 2.0 Hz, 4H), 8.28 (d, *J* = 4.4 Hz, 4H), 7.96 (d, *J* = 8.3 Hz, 2H), 7.87 (d, *J* = 8.1 Hz, 2H), 7.71 (d, *J* = 6.1 Hz, 2H), 7.54 (dd, *J* = 6.0, 1.9 Hz, 2H), 7.48 (t, *J* = 7.7 Hz, 2H), 7.35 (t, *J* = 7.6 Hz, 2H), 6.45 (d, *J* = 16.8 Hz, 2H), 5.80 (d, *J* = 16.7 Hz, 2H), 1.53 (s, 18H), 1.35 (s, 18H). **^{13}C NMR** (126 MHz, DMSO-*d*$_6$) δ 166.7, 165.9, 162.6, 157.3, 154.8, 153.8, 149.7, 139.7, 134.0, 124.1, 123.7, 123.1, 122.9, 121.6, 121.2, 115.9, 111.0, 54.9 (CH_2Cl_2), 50.0, 36.2, 35.9, 29.9, 29.8. **IR** (neat, cm^{-1}) 2962, 1612, 1552, 1468, 1392, 1368, 1321, 1259, 1232, 1204, 1163, 1126, 1043, 1025, 738, 607, 555.

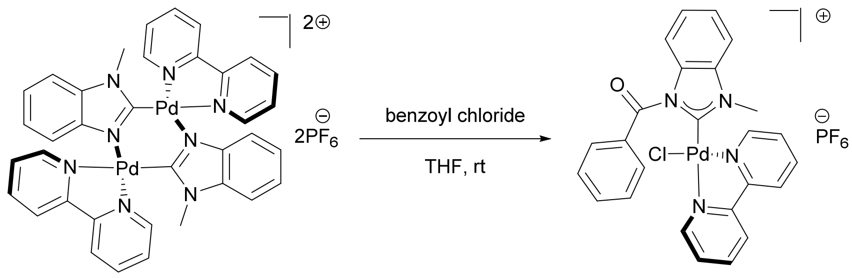

2 **22**

Palladium complex 22. An oven-dried microwave vial equipped with a magnetic stirbar was charged with complex **2** (20.2 mg, 0.019 mmol, 1.0 equiv) and dry THF (3.0 mL). Benzoyl chloride (4.4 µL, 0.038 mmol, 2.0 equiv) was added at room temperature and the reaction was stirred for 12 h. The resulting heterogeneous mixture was decanted, the liquid phase was evaporated *in vacuo*, and the resulting solid was washed with Et_2O, the solvent was removed with a pipet and the solid was dried to afford **22** (7.1 mg, 28%) of as a yellow solid with 80% purity by ^{1}H NMR. Colorless crystals suitable for X-ray crystallography were obtained by slow vapor diffusion of hexanes into a concentrated solution of **22** in CH_2Cl_2. It should be noted that **22** could not be purified by flash chromatography (basic Al2O3 or SiO2) as it was found to be highly sensitive to hydrolysis. **^{1}H NMR** (700 MHz, DMSO-*d*$_6$) δ 8.70 (dd, *J* = 5.4, 1.6 Hz, 1H), 8.67-8.62 (m, 1H), 8.60 (d, *J* = 8.1 Hz, 1H), 8.47 (dd, *J* = 5.7, 1.4 Hz, 1H), 8.43 (td, *J* = 7.8, 1.4 Hz, 1H), 8.38 (td, *J* = 7.9, 1.6 Hz, 1H), 8.06 (d, *J* = 8.0 Hz, 1H), 8.02 (d, *J* = 8.1 Hz, 1H), 7.87-7.79 (m, 3H), 7.73-7.60 (m, 3H), 7.26 (t, *J* = 7.5 Hz, 1H), 7.07 (s, 2H), 4.43 (s, 3H). **^{13}C NMR** (150 MHz, DMSO-*d6*) δ 169.5, 169.5, 155.4, 154.6, 153.4, 148.2, 141.8, 141.6, 135.0, 133.7, 133.1, 133.1, 130.7, 129.2, 128.7, 128.6, 127.9, 127.4, 126.0, 125.9, 124.1, 123.5, 114.8, 112.5, 36.1. **IR** (neat, cm^{-1}) 2922, 1711, 1603, 1499, 1448, 1395, 1357, 1312, 1248, 1217, 1176, 1110, 1022, 830, 761, 717, 663, 650, 591, 555. **HRMS** (HESI) calcd for $[C_{25}H_{20}ClN_4OPd]^+$: *m/z* 533.03550, found 533.03533.

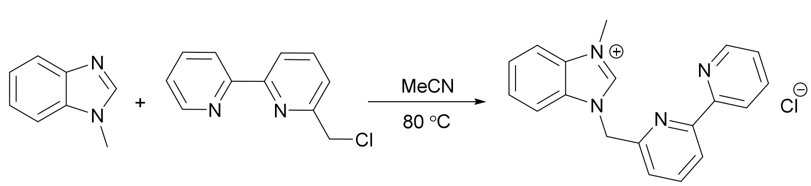

11 **30**

1-([2,2'-bipyridin]-6-ylmethyl)-3-methyl-1*H*-benzo[*d*]imidazol-3-ium chloride (30).[71] An oven-dried microwave vial equipped with a magnetic stirbar was charged with 1-methyl-1*H*-benzo[*d*]imidazole (93.5 mg, 0.71 mmol, 1.35 equiv), **11** (107.2 mg, 0.52 mmol, 1.0 equiv) and dry MeCN (3.5 mL). The reaction was heated at 80 °C for 48 hours, affording a white heterogeneous mixture that was allowed to cool to room temperature and filtered. The filtrate was discarded and the solid residue was washed with cold MeCN, THF and Et_2O sequentially and dried *in vacuo* to afford **S10** (166.6 mg, 95%) as a white powder. **mp** 183-184 °C. **^{1}H NMR** (500 MHz, $CDCl_3$) δ 11.74 (s, 1H), 8.59-8.55 (m, 1H), 8.29 (d, *J* = 7.7 Hz, 1H), 8.10 (d, *J* = 7.9 Hz, 1H), 7.96-7.92 (m, 1H), 7.84-7.75 (m, 2H), 7.72 (td, *J* = 7.7, 1.8 Hz, 1H), 7.69-7.66 (m, 1H), 7.56 (dtd, *J* = 13.9, 7.4, 3.7 Hz, 2H), 7.23 (ddd, *J* = 7.4, 4.7, 1.1 Hz, 1H), 6.09 (s, 2H), 4.25 (s, 3H). **^{13}C NMR** (150 MHz, $CDCl_3$) δ 156.1, 155.2, 152.0, 149.2, 144.2, 138.7, 137.1, 132.0, 131.7, 127.2, 127.1, 124.1, 123.7, 121.2, 121.1, 114.6, 112.6, 52.5, 33.8. **IR** (neat, cm^{-1}) 3169, 1583, 1574, 1452, 1432, 1355, 1281, 1220, 1169, 1149, 1098, 1080, 994, 829, 776, 759, 744, 695, 642, 620, 569, 555, 469, 426. **HRMS** (HESI) calcd for $[C19H17N4]^+$: *m/z* 301.14477, found 301.14519.

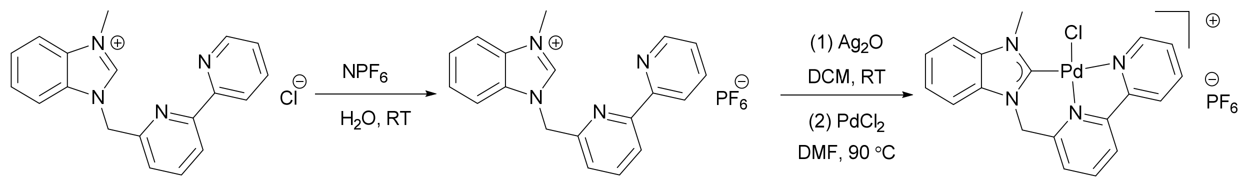

Palladium complex 32.[72,73] A microwave vial equipped with a magnetic stirbar was charged with **30** (242.5 mg, 0.72 mmol, 1.0 equiv) and H_2O (1.3 mL). NH_4PF_6 (1.17 g, 7.2 mmol, 10.0 equiv) was added to the resulting solution in several small portions, and the precipitate that formed immediately was filtered, washed with H_2O, cold EtOH and Et_2O sequentially and dried *in vacuo* to afford the crude benzimidazolium hexafluorophosphate salt intermediate (335.6 mg, >99%) as a white powder, which was used directly in the next step without further purification. An oven-dried microwave vial equipped with a magnetic stirbar was charged with the crude benzimidazolium hexafluorophosphate salt intermediate (335.6 mg, 1.0 equiv) and dry CH_2Cl_2 (15 mL), Ag_2O (87.1 mg, 0.38 mmol, 0.5 equiv) was added and the reaction was stirred in the dark at room temperature for 16 hours. All volatiles were removed *in vacuo*, dry DMF (15 mL) and $PdCl_2$ (132.9 mg, 0.75 mmol, 1.0 equiv) were added and the resulting solution was stirred at 90 °C for 16 hours. The mixture was allowed to cool to room temperature, passed through a pad of celite eluting with dry DMF and concentrated *in vacuo* to afford the crude complex **32** a yellow solid which was purified by flash chromatography on basic Al_2O_3 (0-10% MeCN/DCM elution gradient, followed by 1-5% MeOH/DCM elution gradient) to yield the pure complex **32** (261.6 mg, 62% over 2 steps) as a yellow powder. **mp** 243 °C. **^{1}H NMR** (600 MHz, DMSO-*d_6*) δ 9.13 (d, *J* = 5.5 Hz, 1H), 8.72 (dd, *J* = 13.9, 8.0 Hz, 2H), 8.53-8.43 (m, 2H), 8.13 (dd, *J* = 11.6, 7.9 Hz, 2H), 8.00-

7.94 (m, 1H), 7.84 (d, J = 8.1 Hz, 1H), 7.62-7.56 (m, 1H), 7.57-7.52 (m, 1H), 6.10 (s, 2H), 4.28 (s, 3H). **^{13}C NMR** (150 MHz, DMSO-d_6) δ 159.5, 157.6, 155.2, 152.9, 148.8, 142.6, 142.0, 134.4, 132.6, 127.6, 126.7, 124.7, 124.6, 124.1, 123.7, 112.1, 111.7, 50.2, 35.9. **IR** (neat, cm^{-1}) 3392, 3113, 1602, 1575, 1483, 1452, 1401, 1348, 1326, 1297, 1276, 1245, 1109, 1091, 1056, 1027, 823, 777, 743, 687, 650, 586, 554, 433. **HRMS** (HESI) calcd for $[C_{19}H_{16}ClN_4Pd]^+$: m/z 441.00928, found 441.00967.

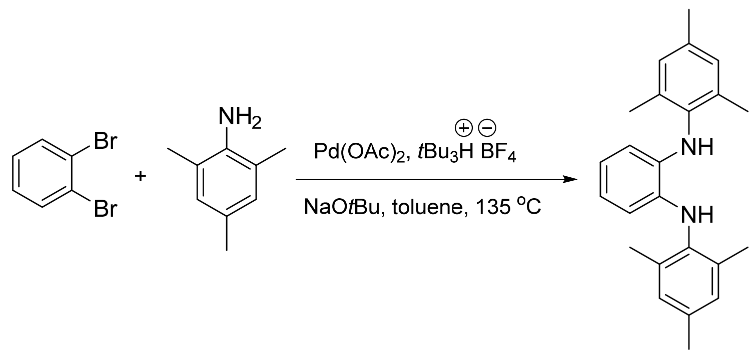

66

***N*^{1},*N*^{2}-dimesitylbenzene-1,2-diamine (66).**[58] In an inert atmosphere glove-box, an oven-dried microwave vial equipped with a magnetic stirbar was charged with $Pd(OAc)_2$ (9.5 mg, 0.042 mmol, 0.10 equiv), tri-*tert*-butylphosphonium tetrafluoroborate (12.3 mg, 0.042 mmol, 0.10 equiv) and NaO*t*Bu (122.2 mg, 1.27 mmol, 3.0 equiv). The vial was capped, taken out of the glove-box and dry toluene (1 mL) was added. The reaction was degassed/backfilled with Argon three times and heated at 60 °C for 15 min. Then 1,2-dibromobenzene (100 mg, 0.42 mmol, 1.0 equiv) and 2,4,6-trimethylaniline (120 mg, 0.89 mmol, 2.1 equiv) were added and heated at 135 °C for 24 h to yield a black suspension which was allowed to cool to room temperature. Et_2OAc and aq. sat. NH_4Cl were added, the layers were separated and the aqueous layer was further extracted three times with Et_2O. The combined organic layers were dried over Mg_2SO_4, filtered and concentrated *in vacuo*. The crude product was purified by flash chromatography (10% CH_2Cl_2/hexanes elution gradient) to afford pure **66** (116 mg, 80%) as a white powder. All analyses were consistent with previously reported data.[58]

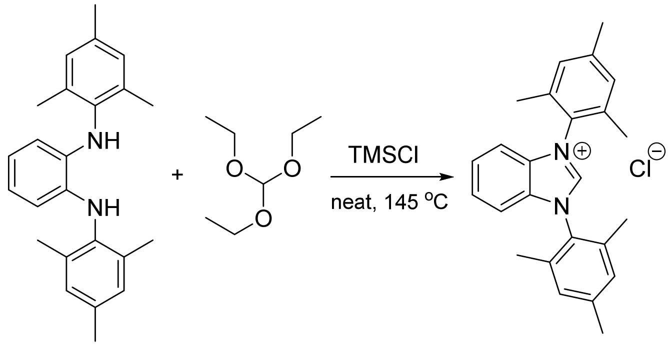

66 **67**

1,3-bis(2,4,6-trimethylphenyl)-1*H*-benzo[*d*]imidazol-3-ium chloride (67).[74] In a 100 mL two neck round-bottomed flask was weighed **66** (389 mg, 1.13 mmol) and triethyl orthoformate (40 mL) was added and a fractional distillation apparatus equipped with a Vigreux column and a thermometer on the head of the latter was connected with the central neck of the flask. The green solution was stirred at 145 °C until the color switched to orange (15 min) and then a small flux of nitrogen was passed through the solution until 20 mL of a mixture of EtOH and $HC(OEt)_3$ distilled out (1 hour). Then the temperature was lowered to 90 °C and trimethylsilyl chloride (6.5 mL) was added at once. Then the solution was cooled down to room temperature and the precipitate was filtered off and washed with Et_2O (15 mL, three times) then concentrated *in vacuo* to afford pure **67** (328 mg, 74%) as a grey powder. All analyses were consistent with previously reported data.[74]

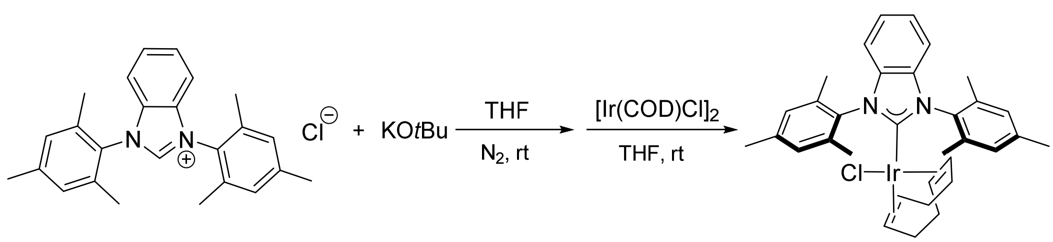

67 **68**

Iridium complex 68.[75] An oven-dried microwave vial equipped with a magnetic stirbar was charged with **67** (51.2 mg, 0.13 mmol, 2.2 equiv), KO*t*Bu (16.0 mg, 0.14 mmol, 2.4 equiv) and dry THF (1 mL) and the resulting suspension was stirred at rt for 30 min. A solution of $[Ir(COD)Cl]_2$ (40 mg, 0.06 mmol, 1.0 equiv) in THF (1 mL) was added, and the resulting orange solution was allowed to stir at rt for 2 h. The suspension was passed through a short pad of celite and the solvent was removed under reduced pressure to afford the crude **68** an orange powder. The crude product was purified by flash chromatography (CH_2Cl_2) followed by crystallization from 6:7 THF/*i*PrOH to afford pure **68** (64.2 mg, 71%) as an orange crystal. **^{1}H NMR** (600 MHz, $CDCl_3$) δ 7.18-7.15 (m, 2H), 7.09 (s, 2H), 7.05 (s, 2H), 6.88-6.85 (m, 2H), 4.28 (dt, *J* = 5.0, 1.9 Hz, 2H), 3.14 (dd, J = 5.3, 2.2 Hz, 2H), 2.41 (s, 6H), 2.27 (s, 6H), 2.04 (s, 6H), 1.81-1.68 (m, 4H), 1.46-1.39 (m, 2H), 1.37-1.29 (m, 2H). **^{13}C NMR** (150 MHz, $CDCl_3$) δ 191.8, 139.0, 138.2, 135.6, 135.3, 133.1, 130.0, 128.5, 123.3, 110.7, 85.1, 77.4, 77.2, 77.0, 52.0, 33.7, 29.0, 21.4, 19.7, 18.3.

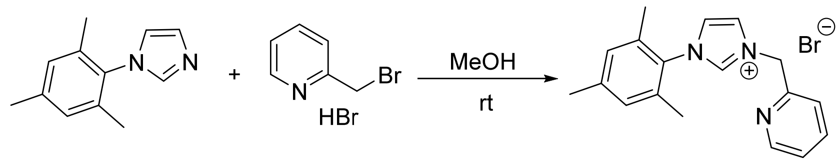

69

1-mesityl-3-(pyridin-2-ylmethyl)-1*H*-imidazol-3-ium bromide (69).[59] 2-picolyl bromide was pretreated by suspending its hydrobromide salt (205 mg, 0.81 mmol, 1.0 equiv) in 5 mL of sat. aq. K_2CO_3. Et_2O was added and the organic phase was transferred in a microwave vial equipped with a magnetic stirbar containing 1-(2,4,6-trimethylphenyl)-imidazole (150 mg, 0.81 mmol, 1.0 equiv). The Et_2O was extracted under reduced pressure and MeOH (5 mL) was added under N_2 protection. The resulting solution was heated with stirring at 110 °C for 3 days during which the desired product crystallised out of the reaction mixture. The precipitates were collected by filtration and washed with MeCN to afford pure **69** (174.3 mg, 60%) as a yellow powder. All analyses were consistent with previously reported data.[59]

69 70

Iridium complex 70.[59] An oven-dried microwave vial equipped with a magnetic stirbar was charged with **69** (50 mg, 0.14 mmol, 1.0 equiv), Ag_2O (24.3 mg, 0.11 mmol, 0.75 equiv) and dry CH_2Cl_2 (6 mL) and the resulting suspension was stirred overnight at rt. The product was recovered after filtration over celite as an off-white solid. The silver complex was transferred to a microwave vial equipped with a magnetic stirbar using MeCN (3 mL). A solution of $[Ir(COD)Cl]_2$ (42.2 mg, 0.06 mmol, 0.5 equiv) in MeCN (1 mL) was added. After 30 minutes, sodium trifluoromethanesulfonate (21.7 mg, 0.13 mmol, 1.0 equiv) was added to the suspension. After stirring for another 30 minutes, the solution was filtered through a dry pad of celite to remove the sodium chloride byproduct. The solvent was evaporated under reduced pressure to yield a red glassy solid. This red solid was dissolved in 5 mL dry dichloromethane and 10 mL dry hexanes was added to the solution to afford a precipitate **70** (91 mg, 90%). All analyses were consistent with previously reported data.[59]

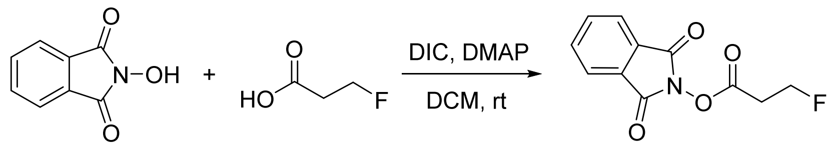

1,3-dioxoisoindolin-2-yl 3-fluoropropanoate.[76] An oven-dried microwave vial equipped with a magnetic stirbar was charged with 3-fluoropropanoic acid (50 mg, 0.54 mmol, 1.0 equiv), N-hydroxyphthalimide (88.1 mg, 0.54 mmol, 1.0 equiv) 4-Dimethylaminopyridine (6.6 mg, 0.054 mmol, 0.1 equiv) and dry CH_2Cl_2 (3 mL). *N*, *N*'-Diisopropylcarbodiimide (75 mg, 0.59 mmol, 1.1 equiv) was added dropwise and the resulting suspension was stirred overnight at rt. The resulting solution was passed through a pad of celite and rinsed with additional CH_2Cl_2. The combined organic layers were concentrated *in vacuo*. The crude product was purified by flash chromatography (10% CH_2Cl_2/hexanes elution gradient) to afford pure ester product (121.5 mg, 95%) as a white powder. **mp** 163 °C. **^{1}H NMR** (500 MHz, $CDCl_3$) δ 7.90 (dd, *J* = 5.4, 3.1 Hz, 2H), 7.80 (dd, *J* = 5.5, 3.1 Hz, 2H), 4.83 (dt, *J* = 46.1, 5.9 Hz, 2H), 3.11 (dt, *J* = 23.2, 5.9 Hz, 2H). **^{13}C NMR** (150 MHz, $CDCl_3$) δ 166.5, 166.4, 161.6, 134.9, 128.8, 124.1, 78.6, 77.5, 32.7, 32.5.

General procedure A: Suzuki-Miyaura cross-coupling catalyzed by palladium complex 17

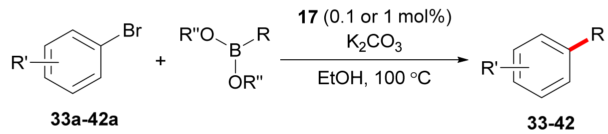

A microwave vial equipped with a magnetic stirbar was charged with the aryl bromide **33a-42a** (1.0 equiv), K_2CO_3 (2.0 equiv), the boronic acid (1.5 equiv), catalyst **17** (0.10 mol%, in stock solution in absolute EtOH), and absolute EtOH [0.12M]. The vial was capped under ambient air and stirred at 100 °C for 24 hours. The reaction was allowed to cool to room temperature, Et_2O and H_2O were added and the layers were separated. The aqueous layer was extracted three times with Et_2O, the combined organic layers were washed with brine, dried over $MgSO_4$, filtered and concentrated *in vacuo* to afford the crude product **33-42**, which was purified by flash chromatography (see specific procedures for individual purification conditions).

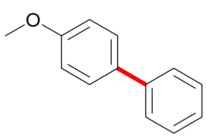

4-methoxy-1,1'-biphenyl (33). General procedure A was followed, using 4-bromo-anisole (**33a**) (38 mg, 0.21 mmol, 1.0 equiv), **17** (0.22 mg, 2.1×10^{-4} mmol, 0.1 mol-%), K_2CO_3 (57 mg, 0.41 mmol, 2.0 equiv), phenylboronic acid (37.5 mg, 0.31 mmol, 1.5 equiv) and EtOH (1.7 mL), resulting 33.6 mg (89%) of biaryl **33** as a white powder after isolation by flash chromatography (SiO_2, 0-5% EtOAc/Hexanes). All analyses were consistent with the reported data.[77b,d,e,f]

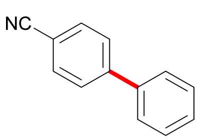

[1,1'-biphenyl]-4-carbonitrile (34). General procedure A was followed, using 4-bromobenzonitrile (**34a**) (37.3 mg, 0.21 mmol, 1.0 equiv), **17** (0.22 mg, 2.1×10^{-4} mmol, 0.1 mol-%), K_2CO_3 (56.7 mg, 0.41 mmol, 2.0 equiv), phenylboronic acid (37.8 mg, 0.31 mmol, 1.5 equiv) and EtOH (1.7 mL), resulting 32 mg (93%) of biaryl **34** as a white powder after isolation by flash chromatography (SiO_2, 0-5% EtOAc/Hexanes). All analyses were consistent with the reported data.[77b]

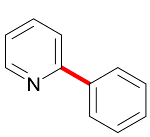

2-phenylpyridine (35). General procedure A was followed, using 2-bromopyridine (**35a**) (33.2 mg, 0.21 mmol, 1.0 equiv), **17** (0.23 mg, 2.1×10^{-4} mmol, 0.1 mol-%), K_2CO_3 (58 mg, 0.41 mmol, 2.0 equiv), phenylboronic acid (39 mg, 0.31 mmol, 1.5

equiv) and EtOH (1.7 mL), resulting 26 mg (80%) of biaryl **35** as a colorless oil after isolation by flash chromatography (SiO_2, 10-20% EtOAc/Hexanes). All analyses were consistent with the reported data.[77a,b]

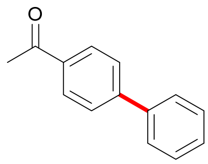

1-([1,1'-biphenyl]-4-yl)ethan-1-one (36). General procedure A was followed, using 4'- bromoacetophenone (**36a**) (41.8 mg, 0.21 mmol, 1.0 equiv), **17** (0.22 mg, 2.1×10^{-4} mmol, 0.1 mol-%), K_2CO_3 (57 mg, 0.41 mmol, 2.0 equiv), phenylboronic acid (37.5 mg, 0.31 mmol, 1.5 equiv) and EtOH (1.7 mL), resulting 41 mg (99%) of biaryl **36** as a white powder after isolation by flash chromatography (SiO_2, 10-20% EtOAc/Hexanes). All analyses were consistent with the reported data.[77a,e,f]

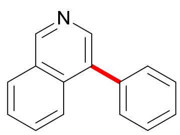

4-phenylisoquinoline (37). General procedure A was followed, using 4-bromoisoquinoline (**37a**) (43 mg, 0.21 mmol, 1.0 equiv), **17** (0.22 mg, 2.1×10^{-4} mmol, 0.1 mol-%), K_2CO_3 (56.8 mg, 0.41 mmol, 2.0 equiv), phenylboronic acid (37.6 mg, 0.31 mmol, 1.5 equiv) and EtOH (1.6 mL), resulting 43 mg (99%) of biaryl **37** as a white powder after isolation by flash chromatography (SiO_2, 10% EtOAc/Hexanes). All analyses were consistent with the reported data.[77b]

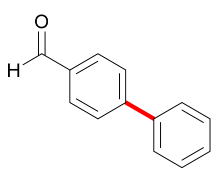

[1,1'-biphenyl]-4-carbaldehyde (38). General procedure A was followed, using 4-bromobenzaldehyde (**38a**) (37.9 mg, 0.21 mmol, 1.0 equiv), **17** (0.22 mg, 2.1×10^{-4} mmol, 0.1 mol-%), K_2CO_3 (56 mg, 0.41 mmol, 2.0 equiv), phenylboronic acid (37.5 mg, 0.31 mmol, 1.5 equiv) and EtOH (1.7 mL), resulting 34 mg (90%) of biaryl **38** as a white powder after isolation by flash chromatography (SiO_2, 0-5% EtOAc/Hexanes). All analyses were consistent with the reported data.[77f]

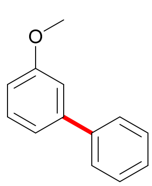

3-methoxy-1,1'-biphenyl (39). General procedure A was followed, using 1-bromo-3-methoxybenzene (**39a**) (38.2 mg, 0.21 mmol, 1.0 equiv), **17** (0.22 mg, 2.1×10^{-4} mmol, 0.1 mol-%), K_2CO_3 (56.8 mg, 0.41 mmol, 2.0 equiv), phenylboronic acid (37.4 mg, 0.31 mmol, 1.5 equiv) and EtOH (1.8 mL), resulting 38 mg (99%) of biaryl **39** as a white solid after isolation by flash chromatography (SiO_2, 0-2% EtOAc/Hexanes). All analyses were consistent with the reported data.[77e]

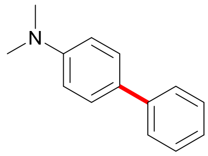

2-(N,N-dimethyl-[1,1'-biphenyl]-4-amine (40). General procedure A was followed, using 2-bromonaphthalene (**40a**) (41 mg, 0.21 mmol, 1.0 equiv), **17** (0.22 mg, 2.1 × 10^{-4} mmol, 0.1 mol-%), K_2CO_3 (56.8 mg, 0.41 mmol, 2.0 equiv), phenylboronic acid (37 mg, 0.31 mmol, 1.5 equiv) and EtOH (1.7 mL), resulting 24 mg (60%) of biaryl **40** as a white solid after isolation by flash chromatography (SiO_2, 5% EtOAc/Hexanes). All analyses were consistent with the reported data.[77d]

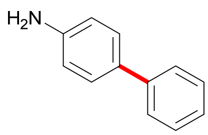

[1,1'-biphenyl]-4-amine (41). General procedure A was followed, using 4-bromoaniline (**41a**) (35.3 mg, 0.21 mmol, 1.0 equiv), **17** (0.22 mg, 2.1 × 10^{-4} mmol, 0.1 mol-%), K_2CO_3 (56.7 mg, 0.41 mmol, 2.0 equiv), phenylboronic acid (37.4 mg, 0.31 mmol, 1.5 equiv) and EtOH (1.7 mL), resulting 49 mg (99%) of biaryl **41** as a pale yellow solid after isolation by flash chromatography (SiO_2, 10-20% EtOAc/Hexanes). All analyses were consistent with the reported data.[77e]

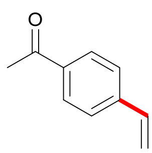

1-(4-vinylphenyl)ethan-1-one (42). General procedure A was followed, using 4'-bromoacetophenone (**42a**) (40.8 mg, 0.21 mmol, 1.0 equiv), **17** (2.2 mg, 2.1 × 10^{-3} mmol, 1 mol-%), K_2CO_3 (56.7 mg, 0.41 mmol, 2.0 equiv), vinylboronic acid pinacol ester (47 mg, 0.31 mmol, 1.5 equiv) and EtOH (1.7 mL), resulting 21.6 mg (72%) of **42** as a colorless oil after isolation by flash chromatography (SiO_2, 1-3% EtOAc/Hexanes). All analyses were consistent with the reported data.[77c]

General procedure B: Sonogashira-Hagihara coupling catalyzed by palladium complex 17

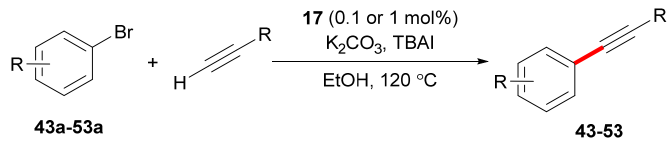

A microwave vial equipped with a magnetic stirbar was charged with the aryl bromide **43a-53a** (1.0 equiv), K_2CO_3 (2.0 equiv), TBAI (1.5 equiv), the terminal alkyne (1.5 equiv), catalyst **17** (0.10 mol%, in stock solution in absolute EtOH), and absolute EtOH [0.12M]. The vial was capped under ambient air and stirred at 120 °C for 24 hours. The reaction was allowed to cool to room temperature, Et_2O and H_2O were added and the layers were separated. The aqueous layer was extracted three times with Et_2O, the combined organic layers were washed with brine, dried over $MgSO_4$, filtered and concentrated *in vacuo* to yield the crude product **43-53**, which was purified by flash chromatography (see specific procedures for individual purification conditions).

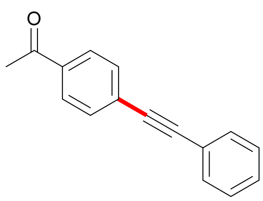

1-(4-(phenylethynyl)phenyl)ethan-1-one (43). General procedure B was followed, using 4'-bromoacetophenone (**43a**) (41 mg, 0.21 mmol, 1.0 equiv), **17** (0.22 mg, 2.1×10^{-4} mmol, 0.1 mol-%), K_2CO_3 (57 mg, 0.41 mmol, 2.0 equiv), TBAI (114 mg, 0.31 mmol, 1.5 equiv), phenylacetylene (31.4 mg, 0.31 mmol, 1.5 equiv) and EtOH (1.6 mL), resulting 46.2 mg (99%) of internal alkyne **43** as a white solid after isolation by flash chromatography (SiO_2, 5-10% EtOAc/Hexanes). The reaction carried out in the media of EtOH (0.8 mL)/H_2O (0.8 mL) without changing the amount of all the other chemicals delivered the same yield. All analyses were consistent with the reported data.[78e]

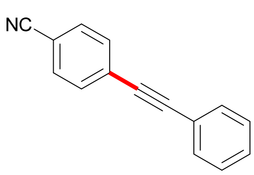

4-(phenylethynyl)benzonitrile (44). General procedure B was followed, using 4-bromobenzonitrile (**44a**) (34 mg, 0.19 mmol, 1.0 equiv), **17** (0.2 mg, 1.9×10^{-4} mmol, 0.1 mol-%), K_2CO_3 (51.4 mg, 0.37 mmol, 2.0 equiv), TBAI (103.1 mg, 0.28 mmol, 1.5 equiv), phenylacetylene (28.5 mg, 0.28 mmol, 1.5 equiv) and EtOH (1.7 mL), resulting 37 mg (98%) of internal alkyne **44** as a white powder after isolation by flash chromatography (SiO_2, 0-2% EtOAc/Hexanes). All analyses were consistent with the reported data.[78e]

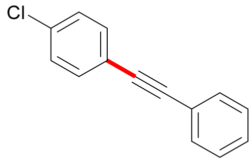

1-chloro-4-(phenylethynyl)benzene (45). General procedure B was followed, using 1-bromo-4-chlorobenzene (**45a**) (39.2 mg, 0.21 mmol, 1.0 equiv), **17** (0.22 mg, 2.1 × 10^{-4} mmol, 0.1 mol-%), K_2CO_3 (56.8 mg, 0.41 mmol, 2.0 equiv), TBAI (113.8 mg, 0.31 mmol, 1.5 equiv), phenylacetylene (31.4 mg, 0.31 mmol, 1.5 equiv) and EtOH (1.6 mL), resulting 35.8 mg (82%) of internal alkyne **45** as a white solid after isolation by flash chromatography (SiO_2, 1% EtOAc/Hexanes). All analyses were consistent with the reported data.[78d]

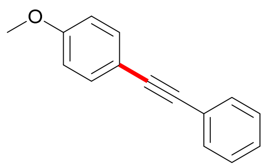

1-methoxy-4-(phenylethynyl)benzene (46). General procedure B was followed, using 4-bromo-anisole (**46a**) (41 mg, 0.21 mmol, 1.0 equiv), **17** (0.22 mg, 2.1 × 10^{-4} mmol, 0.1 mol-%), K_2CO_3 (57 mg, 0.41 mmol, 2.0 equiv), TBAI (114 mg, 0.31 mmol, 1.5 equiv), phenylacetylene (31.4 mg, 0.31 mmol, 1.5 equiv) and EtOH (1.7 mL), resulting 42 mg (98%) of internal alkyne **46** as a white solid after isolation by flash chromatography (SiO_2, 0-1% EtOAc/Hexanes). The reaction carried out in the media of EtOH (0.8 mL)/H_2O (0.8 mL) without changing the amount of all the other chemicals delivered the same yield. All analyses were consistent with the reported data.[78c,e]

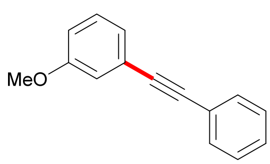

1-methoxy-3-(phenylethynyl)benzene (47). General procedure B was followed, using 1-bromo-3-methoxybenzene (**47a**) (40.8 mg, 0.21 mmol, 1.0 equiv), **17** (0.22 mg, 2.1 × 10^{-4} mmol, 0.1 mol-%), K_2CO_3 (56.7 mg, 0.41 mmol, 2.0 equiv), TBAI (113.8 mg, 0.31 mmol, 1.5 equiv), phenylacetylene (31.4 mg, 0.31 mmol, 1.5 equiv) and EtOH (1.6 mL), resulting 39 mg (91%) of internal alkyne **47** as a yellow oil after isolation by flash chromatography (SiO_2, 1-2% EtOAc/Hexanes). All analyses were consistent with the reported data.[78e]

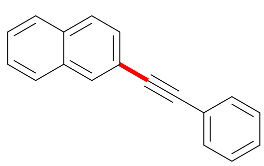

2-(phenylethynyl)naphthalene (48). General procedure B was followed, using 2-bromonaphthalene (**48a**) (42.5 mg, 0.21 mmol, 1.0 equiv), **17** (0.22 mg, 2.1 × 10^{-4} mmol, 0.1 mol-%), K_2CO_3 (56.8 mg, 0.41 mmol, 2.0 equiv), TBAI (113.8 mg, 0.31 mmol, 1.5 equiv), phenylacetylene (31.4 mg, 0.31 mmol, 1.5 equiv) and EtOH (1.6 mL), resulting 44.5 mg (95%) of internal alkyne **48** as a white solid after isolation by flash chromatography (SiO_2, 1% EtOAc/Hexanes). All analyses were consistent with the reported data.[78c]

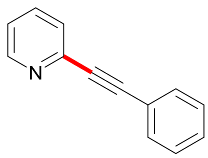

2-(phenylethynyl)pyridine (49). General procedure B was followed, using 2-bromopyridine (**49a**) (32.4 mg, 0.21 mmol, 1.0 equiv), **17** (0.22 mg, 2.1×10^{-4} mmol, 0.1 mol-%), K_2CO_3 (57 mg, 0.41 mmol, 2.0 equiv), TBAI (114 mg, 0.31 mmol, 1.5 equiv), phenylacetylene (31.4 mg, 0.31 mmol, 1.5 equiv) and EtOH (1.7 mL), resulting 32.3 mg (87%) of internal alkyne **49** as a dark green oil after isolation by flash chromatography (SiO_2, 10-20% EtOAc/Hexanes). All analyses were consistent with the reported data.[78a,e,f]

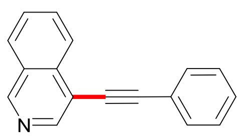

4-(phenylethynyl)isoquinoline (50). General procedure B was followed, using 4-bromoisoquinoline (**50a**) (38.7 mg, 0.19 mmol, 1.0 equiv), **17** (0.2 mg, 1.9×10^{-4} mmol, 0.1 mol-%), K_2CO_3 (51.4 mg, 0.37 mmol, 2.0 equiv), TBAI (103.1 mg, 0.28 mmol, 1.5 equiv), phenylacetylene (28.5 mg, 0.28 mmol, 1.5 equiv) and EtOH (1.6 mL), resulting 40 mg (95%) of internal alkyne **50** as a yellow oil after isolation by flash chromatography (SiO_2, 15-30% EtOAc/Hexanes). All analyses were consistent with the reported data.[78f]

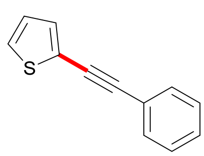

2-(phenylethynyl)thiophene (51). General procedure B was followed, using 2-bromothiophene (**51a**) (33.4 mg, 0.21 mmol, 1.0 equiv), **17** (0.22 mg, 2.1×10^{-4} mmol, 0.1 mol-%), K_2CO_3 (56.8 mg, 0.41 mmol, 2.0 equiv), TBAI (113.8 mg, 0.31 mmol, 1.5 equiv), phenylacetylene (31.5 mg, 0.31 mmol, 1.5 equiv) and EtOH (1.6 mL), resulting 37.8 mg (99%) of internal alkyne **51** as a yellow powder after isolation by flash chromatography (SiO_2, Hexanes). All analyses were consistent with the reported data.[78a,e,f]

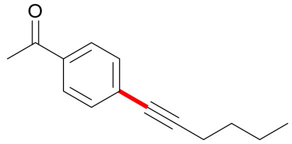

1-(4-(hex-1-yn-1-yl)phenyl)ethan-1-one (52). General procedure B was followed, using 4'-bromoacetophenone (**52a**) (40.8 mg, 0.21 mmol, 1.0 equiv), **17** (2.2 mg, 2.1 × 10-3 mmol, 1 mol-%), K_2CO_3 (56.8 mg, 0.41 mmol, 2.0 equiv), TBAI (113.8 mg, 0.31 mmol, 1.5 equiv), 1-hexyne (25.2 mg, 0.31 mmol, 1.5 equiv) and EtOH (1.6 mL), resulting 27.1 mg (66%) of internal alkyne **52** as a yellow oil after isolation by flash chromatography (SiO2, 0-5% EtOAc/Hexanes). All analyses were consistent with the reported data.[78b]

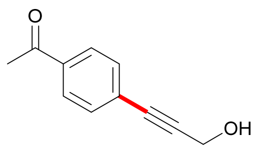

1-(4-(3-hydroxyprop-1-yn-1-yl)phenyl)ethan-1-one (53). General procedure B was followed, using 4'-bromoacetophenone (**53a**) (40.8 mg, 0.21 mmol, 1.0 equiv), **17** (2.2 mg, 2.1 × 10^{-3} mmol, 1 mol-%), K_2CO_3 (56.8 mg, 0.41 mmol, 2.0 equiv), TBAI (113.8 mg, 0.31 mmol, 1.5 equiv), propargyl alcohol (17.2 mg, 0.31 mmol, 1.5 equiv) and EtOH (1.5 mL), resulting 20.7 mg (58%) of internal alkyne **53** as a colorless oil after isolation by flash chromatography (SiO_2, 20-30% EtOAc/Hexanes). All analyses were consistent with the reported data.[78g]

General procedure C: Heck-Mizoroki coupling catalyzed by palladium complex 17

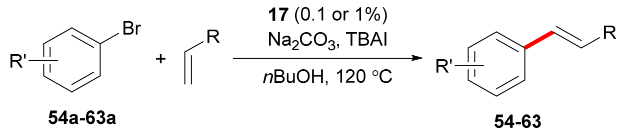

A microwave vial equipped with a magnetic stirbar was charged with the aryl bromide **54a-63a** (1.0 equiv), K_2CO_3 (2.0 equiv), TBAI (1.5 equiv), the terminal alkyne (1.5 equiv), catalyst **17** (0.10 mol%, in stock solution in absolute EtOH), and absolute EtOH [0.12M]. The vial was capped under ambient air and stirred at 120 °C for 24 hours. The reaction was allowed to cool to room temperature, Et_2O and H_2O were added and the layers were separated. The aqueous layer was extracted three times with Et_2O, the combined organic layers were washed with brine, dried over $MgSO_4$, filtered and concentrated *in vacuo* to yield the crude product **54-63**, which was purified by flash chromatography (see specific procedures for individual purification conditions).

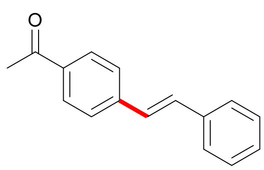

(E)-1-(4-styrylphenyl)ethan-1-one (54). General procedure C was followed, using 4'-bromoacetophenone (**54a**) (36 mg, 0.18 mmol, 1.0 equiv), **17** (0.19 mg, 1.8 × 10^{-4} mmol, 0.1 mol-%), Na_2CO_3 (38.2 mg, 0.36 mmol, 2.0 equiv), TBAI (100 mg, 0.27 mmol, 1.5 equiv), styrene (28.1 mg, 0.28 mmol, 1.5 equiv) and *n*BuOH (1.5 mL), resulting 42 mg (99%) of internal alkene **54** as a white powder after isolation by flash chromatography (SiO_2, 10-20% EtOAc/Hexanes). All analyses were consistent with the reported data.[79h]

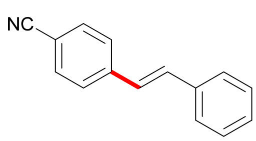

(E)-4-styrylbenzonitrile (55). General procedure C was followed, using 4-bromobenzonitrile (**55a**) (32.8 mg, 0.18 mmol, 1.0 equiv), **17** (0.19 mg, 1.8 × 10^{-4} mmol, 0.1 mol-%), Na_2CO_3 (38.2 mg, 0.36 mmol, 2.0 equiv), TBAI (100 mg, 0.27 mmol, 1.5 equiv), styrene (28.1 mg, 0.27 mmol, 1.5 equiv) and *n*BuOH (1.5 mL), resulting 34 mg (91%) of internal alkene **55** as a white solid after isolation by flash chromatography (SiO_2, 5-8% EtOAc/Hexanes). All analyses were consistent with the reported data.[79d]

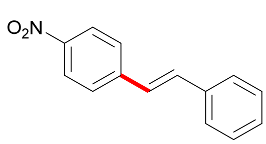

(E)-1-nitro-4-styrylbenzene (56). General procedure C was followed, using 1-bromo-4-nitrobenzene (**56a**) (35.7 mg, 0.18 mmol, 1.0 equiv), **17** (0.19 mg, 1.8 × 10^{-4} mmol, 0.1 mol-%), Na_2CO_3 (38.2 mg, 0.36 mmol, 2.0

equiv), TBAI (100 mg, 0.27 mmol, 1.5 equiv), styrene (28.1 mg, 0.27 mmol, 1.5 equiv) and *n*BuOH (1.5 mL), resulting 35.2 mg (87%) of internal alkene **56** as a yellow powder after isolation by flash chromatography (SiO_2, 5% EtOAc/Hexanes). All analyses were consistent with the reported data.[79i]

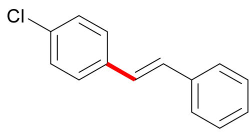

(E)-1-chloro-4-styrylbenzene (57). General procedure C was followed, using 1-bromo-4-chlorobenzene (**57a**) (178 mg, 0.93 mmol, 1.0 equiv), **17** (1 mg, 9.3×10^{-4} mmol, 0.1 mol-%), Na_2CO_3 (197 mg, 1.86 mmol, 2.0 equiv), TBAI (500 mg, 1.4 mmol, 1.5 equiv), styrene (145.4 mg, 1.4 mmol, 1.5 equiv) and *n*BuOH (6 mL), resulting 190 mg (95%) of internal alkene **57** as a white powder after isolation by flash chromatography (SiO_2, 0-1% EtOAc/Hexanes). All analyses were consistent with the reported data.[79g]

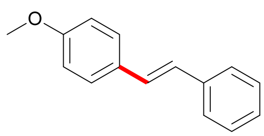

(E)-1-methoxy-4-styrylbenzene (58). General procedure C was followed, using 4-bromo-anisole (**58a**) (33.7 mg, 0.18 mmol, 1.0 equiv), **17** (0.19 mg, 1.8×10^{-4} mmol, 0.1 mol-%), Na_2CO_3 (38.2 mg, 0.36 mmol, 2.0 equiv), TBAI (100 mg, 0.27 mmol, 1.5 equiv), styrene (28.1 mg, 0.28 mmol, 1.5 equiv) and *n*BuOH (1.5 mL), resulting 30.7 mg (81%) of internal alkene **58** as a white powder after isolation by flash chromatography (SiO_2, 1-3% EtOAc/Hexanes). All analyses were consistent with the reported data[49] except the limited peaks of un-isolatable impurities.[79d,f,h]

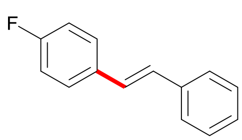

(E)-1-fluoro-4-styrylbenzene (59). General procedure C was followed, using 1-bromo-4-fluorobenzene (**59a**) (32 mg, 0.18 mmol, 1.0 equiv), **17** (0.2 mg, 1.8×10^{-4} mmol, 0.1 mol-%), Na_2CO_3 (39 mg, 0.36 mmol, 2.0 equiv), TBAI (100 mg, 0.27 mmol, 1.5 equiv), styrene (28.1 mg, 0.27 mmol, 1.5 equiv) and *n*BuOH (1.5 mL), resulting 30 mg (83%) of internal alkene **59** as a white powder after isolation by flash chromatography (SiO_2, 0-1% EtOAc/Hexanes). All analyses were consistent with the reported data.[79f]

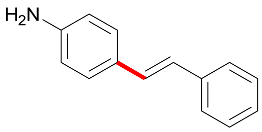

(E)-4-styrylaniline (60). General procedure C was followed, using 4-bromoaniline (**60a**) (64 mg, 0.37 mmol, 1.0 equiv), **17** (0.4 mg, 3.7×10^{-4} mmol, 0.1 mol-%), Na_2CO_3 (79 mg, 0.74 mmol, 2.0 equiv), TBAI (206 mg, 0.56 mmol, 1.5 equiv), styrene (58.1 mg, 0.56 mmol, 1.5 equiv) and *n*BuOH (3 mL), resulting 57.4 mg (79%) of internal alkene **60** as a yellow powder after isolation by flash chromatography (SiO_2, 10-20% EtOAc/Hexanes). All analyses were consistent with the reported data.[79e]

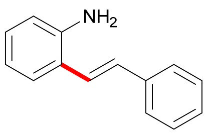

(E)-2-styrylaniline (61). General procedure C was followed, using 2-bromoaniline (**61a**) (64 mg, 0.37 mmol, 1.0 equiv), **17** (0.4 mg, 3.7×10^{-4} mmol, 0.1 mol-%), Na_2CO_3 (79 mg, 0.74 mmol, 2.0 equiv), TBAI (206 mg, 0.56 mmol, 1.5 equiv), styrene (58.1 mg, 0.56 mmol, 1.5 equiv) and *n*BuOH (3 mL), resulting 60.3 mg (83%) of internal alkene **61** as a white powder after isolation by flash chromatography (SiO_2, 0-10% EtOAc/Hexanes). All analyses were consistent with the reported data.[79c]

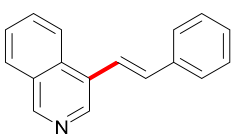

4-phenylisoquinoline (62). General procedure C was followed, using 4-bromoisoquinoline (**62a**) (77.5 mg, 0.37 mmol, 1.0 equiv), **17** (0.4 mg, 3.7×10^{-4} mmol, 0.1 mol-%), Na_2CO_3 (79 mg, 0.74 mmol, 2.0 equiv), TBAI (206 mg, 0.56 mmol, 1.5 equiv), styrene (58.1 mg, 0.56 mmol, 1.5 equiv) and *n*BuOH (3 mL), resulting 70 mg (81%) of internal alkene **62** as a white oil after isolation by flash chromatography (SiO_2, 15% EtOAc/Hexanes). All analyses were consistent with the reported data.[79a]

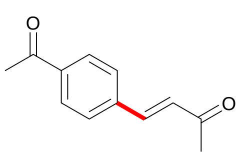

(E)-4-(4-acetylphenyl)but-3-en-2-one (63). General procedure C was followed, using 4'-bromoacetophenone (**63a**) (40.8 mg, 0.2 mmol, 1.0 equiv), **17** (2.2 mg, 2.1×10^{-3} mmol, 1 mol-%), Na_2CO_3 (43.5 mg, 0.41 mmol, 2.0 equiv), TBAI (113.8 mg, 0.31 mmol, 1.5 equiv), methyl vinyl ketone (21.5 mg, 0.31 mmol, 1.5 equiv) and *n*BuOH (1.7 mL), resulting 22.4 mg (48%) of internal alkene **63** as a yellow powder after isolation by flash chromatography (SiO_2, 20-25% EtOAc/Hexanes). All analyses were consistent with the reported data.[79b]

References

1. Beletskaya, I. P.; Cheprakov, A. V., The heck reaction as a sharpening stone of palladium catalysis. *Chem. Rev.* **2000,** *100*, 3009-3066. (b) Dounay, A. B.; Overman, L. E., The asymmetric intramolecular Heck reaction in natural product total synthesis. *Chem. Rev.* **2003,** *103*, 2945-2963. (c) Chinchilla, R.; Najera, C., The sonogashira reaction: A booming methodology in synthetic organic chemistry. *Chem. Rev.* **2007,** *107*, 874-922. (d) Martin, R.; Buchwald, S. L., Palladium-Catalyzed Suzuki-Miyaura Cross-Coupling Reactions Employing Dialkylbiaryl Phosphine Ligands. *Accounts. Chem. Res.* **2008,** *41*, 1461-1473. (e) Zhu, J. C.; Enamorado, M. F.; Comins, D. L., Synthesis of C-4 Substituted Amido Nicotine Derivatives via Copper(I)- and (II)-Catalyzed Cross-Coupling Reactions. *J. Org. Chem.* **2016,** *81*, 11529-11534. (f) Torborg, C.; Beller, M., Recent Applications of Palladium-Catalyzed Coupling Reactions in the Pharmaceutical, Agrochemical, and Fine Chemical Industries. *Adv. Synth. Catal.* **2009,** *351*, 3027-3043.
2. Miyaura, N.; Yamada, K.; Suzuki, A., New Stereospecific Cross-Coupling by the Palladium-Catalyzed Reaction of 1-Alkenylboranes with 1-Alkenyl or 1-Alkynyl Halides. *Tetrahedron Lett.* **1979,** *20*, 3437-3440.
3. (a) Nicolaou, K. C.; Sorensen, E. J.; Snyder, S. A., *Classics in total synthesis*. VCH: Weinheim, 1996. (b) Diederich, F.; Stang, P. J., *Metal-catalyzed cross-coupling reactions*. John Wiley & Sons: 2008.
4. (a) Brow, D. G.; Bostrom, J., Analysis of Past and Present Synthetic Methodologies on Medicinal Chemistry: Where Have All the New Reactions Gone? *J. Med. Chem.* **2016,** *59*, 4443-4458. (b) Blakemore, D. C.; Castro, L.; Churcher, I.; Rees, D. C.; Thomas, A. W.; Wilson, D. M.; Wood, A., Organic synthesis provides opportunities to transform drug discovery. *Nat. Chem.* **2018,** *10*, 383-394.
5. Heck, R. F.; Nolley, J. P., Palladium-Catalyzed Vinylic Hydrogen Substitution Reactions with Aryl, Benzyl, and Styryl Halides. *J. Org. Chem.* **1972,** *37*, 2320-&.
6. Sonogashira, K.; Tohda, Y.; Hagihara, N., Convenient Synthesis of Acetylenes - Catalytic Substitutions of Acetylenic Hydrogen with Bromoalkenes, Iodoarenes, and Bromopyridines. *Tetrahedron Lett.* **1975,** *50*, 4467-4470.
7. (a) Larsen, R. D.; King, A. O.; Chen, C. Y.; Corley, E. G.; Foster, B. S.; Roberts, F. E.; Yang, C. H.; Lieberman, D. R.; Reamer, R. A.; Tschaen, D. M.; Verhoeven, T. R.; Reider, P. J., Efficient Synthesis of Losartan, a Nonpeptide Angiotensin-Ii Receptor Antagonist. *J. Org. Chem.* **1994,** *59*, 6391-6394. (b) Link, J. O.; Taylor, J. G.; Xu, L. H.; Mitchell, M.; Guo, H. Y.; Liu, H. T.; Kato, D.; Kirschberg, T.; Sun, J. Y.; Squires, N.; Parrish, J.; Keller, T.; Yang, Z. Y.; Yang, C.; Matles,

M.; Wang, Y. J.; Wang, K.; Cheng, G. F.; Tian, Y.; Mogalian, E.; Mondou, E.; Cornpropst, M.; Perry, J.; Desai, M. C., Discovery of Ledipasvir (GS-5885): A Potent, Once-Daily Oral NS5A Inhibitor for the Treatment of Hepatitis C Virus Infection. *J. Med. Chem.* **2014,** *57*, 2033-2046.

8. Varkonyi, O.; Hoppe, C.; Muresan, S. IBEX-access and exploit SAR data from patents and journals. Presented at ChemAxon EUGM, Budapest, Hungary, June 7−8, 2008; http://www.chemaxon.com/forum/viewpost16936.html#16936.

9. Anastas, P.; Eghbali, N., Green Chemistry: Principles and Practice. *Chem. Soc. Rev.* **2010,** *39*, 301-312.

10. Larsson, D. G. J., Pollution from drug manufacturing: review and perspectives. *Philos. T. R. Soc. B* **2014,** *369* (1656).

11. Li, C. J.; Trost, B. M., Green chemistry for chemical synthesis. *P. Natl. Acad. Sci. U.S.A.* **2008,** *105*, 13197-13202.

12. (a) Santoro, S.; Ferlin, F.; Luciani, L.; Ackermann, L.; Vaccaro, L., Biomass-derived solvents as effective media for cross-coupling reactions and C–H functionalization processes. *Green. Chem.* **2017,** *19*, 1601-1612. (b) Hoffmann, I.; Blumenroder, B.; Thumann, S. O. N.; Dommer, S.; Schatz, J., Suzuki cross-coupling in aqueous media. *Green. Chem.* **2015,** *17*, 3844-3857.

13. Lipshutz, B. H.; Gallou, F.; Handa, S., Evolution of Solvents in Organic Chemistry. *Acs. Sustain. Chem. Eng.* **2016,** *4*, 5838-5849.

14. Mudraboyina, B. P.; Fu, D.; Jessop, P. G., Supercritical fluid rectification of lignin microwave-pyrolysis oil. *Green. Chem.* **2015,** *17*, 169-172.

15. Yamaguchi, J.; Yamaguchi, A. D.; Itami, K., C–H Bond Functionalization: Emerging Synthetic Tools for Natural Products and Pharmaceuticals. *Angew. Chem. Int. Edit.* **2012,** *51*, 8960-9009.

16. Bedford, R. B.; Betham, M., N-H carbazole synthesis from 2-chloroanilines via consecutive amination and C–H activation. *J. Org. Chem.* **2006,** *71*, 9403-9410.

17. Gutekunst, W. R.; Baran, P. S., Total Synthesis and Structural Revision of the Piperarborenines via Sequential Cyclobutane C–H Arylation. *J. Am. Chem. Soc.* **2011,** *133*, 19076-19079.

18. (a) Ito, E.; Fukushima, T.; Kawakami, T.; Murakami, K.; Itami, K., Catalytic Dehydrogenative C–H Imidation of Arenes Enabled by Photo-generated Hole Donation to Sulfonimide. *Chem.* **2017,** *2*, 383-392. (b) Engle, K. M.; Mei, T. S.; Wasa, M.; Yu, J. Q., Weak Coordination as a Powerful Means for Developing Broadly Useful C–H Functionalization Reactions. *Accounts. Chem. Res.* **2012,** *45*, 788-802.

19. Chu, L.; Shang, M.; Tanaka, K.; Chen, Q. H.; Pissarnitski, N.; Streckfuss, E.; Yu, J. Q., Remote Meta-C–H Activation Using a Pyridine-Based Template: Achieving Site-Selectivity via the Recognition of Distance and Geometry. *ACS Cent. Sci.* **2015,** *1*, 394-399.

20. Gandeepan, P.; Ackermann, L., Transient Directing Groups for Transformative C–H Activation by Synergistic Metal Catalysis. *Chem.* **2018,** *4*, 199-222.

21. (a) Hopkinson, M. N.; Richter, C.; Schedler, M.; Glorius, F., An overview of N-heterocyclic carbenes. *Nature* **2014,** *510*, 485-496. (b) Nelson, D. J.; Nolan, S. P., Quantifying and understanding the electronic properties of N-heterocyclic carbenes. *Chem. Soc. Rev.* **2013,** *42*, 6723-6753.

22. Kuwata, S.; Hahn, F. E., Complexes Bearing *Protic* N-Heterocyclic Carbene Ligands. *Chem. Rev.* **2018,** *118*, 9642-9677.

23. Gurbuz, N.; Karaca, E. O.; Ozdemir, I.; Cetinkaya, B., Cross coupling reactions catalyzed by (NHC)Pd(II) complexes. *Turk. J. Chem.* **2015,** *39*, 1115-1157.

24. Dobereiner, G. E.; Chamberlin, C. A.; Schley, N. D.; Crabtree, R. H., Acyl Protection Strategy for Synthesis of a *Protic* NHC Complex via N-Acyl Methanolysis. *Organometallics* **2010,** *29*, 5728-5731.

25. Das, R.; Hepp, A.; Daniliuc, C. G.; Hahn, F. E., Synthesis of Complexes with *Protic* NH,NH-NHC Ligands via Oxidative Addition of 2-Halogenoazoles to Zero-Valent Transition Metals. *Organometallics* **2014,** *33*, 6975-6987.

26. Godula, K.; Sames, D., C–H bond functionalization in complex organic synthesis. *Science* **2006,** *312*, 67-72.

27. Xie, J.; Jin, H. M.; Xu, P.; Zhu, C. J., When C–H bond functionalization meets visible-light photoredox catalysis. *Tetrahedron Lett.* **2014,** *55*, 36-48.

28. Nicewicz, D. A.; MacMillan, D. W. C., Merging photoredox catalysis with organocatalysis: The direct asymmetric alkylation of aldehydes. *Science* **2008,** *322*, 77-80.

29. Ischay, M. A.; Anzovino, M. E.; Du, J.; Yoon, T. P., Efficient visible light photocatalysis of [2+2] enone cycloadditions. *J. Am. Chem. Soc.* **2008,** *130*, 12886-12887.

30. Hagmann, W. K., The many roles for fluorine in medicinal chemistry. *J. Med. Chem.* **2008,** *51*, 4359-4369.

31. Gillis, E. P.; Eastman, K. J.; Hill, M. D.; Donnelly, D. J.; Meanwell, N. A., Applications of Fluorine in Medicinal Chemistry. *J. Med. Chem.* **2015,** *58*, 8315-8359.

32. Zafrani, Y.; Sod-Moriah, G.; Yeffet, D.; Berliner, A.; Amir, D.; Marciano, D.; Elias, S.; Katalan, S.; Ashkenazi, N.; Madmon, M.; Gershonov, E.; Saphier, S., CF_2H, a Functional Group-Dependent

Hydrogen-Bond Donor: Is It a More or Less Lipophilic Bioisostere of OH, SH, and CH_3? *J. Med. Chem.* **2019,** *62*, 5628-5637.

33. Chen, X. Y.; Sorensen, E. J., Pd-Catalyzed, *ortho* C–H Methylation and Fluorination of Benzaldehydes Using Orthanilic Acids as Transient Directing Groups. *J. Am. Chem. Soc.* **2018,** *140*, 2789-2792.

34. Chen, W.; Huang, Z.; Tay, N. E. S.; Giglio, B.; Wang, M. Z.; Wang, H.; Wu, Z. H.; Nicewicz, D. A.; Li, Z. B., Direct arene C–H fluorination with $^{18}F^{-}$ via organic photoredox catalysis. *Science* **2019,** *364*, 1170-1174.

35. Chen, W. C.; Teo, X. Q.; Lee, M. Y.; Radda, G. K.; Lee, P., Robust hyperpolarized C-13 metabolic imaging with selective non-excitation of pyruvate (SNEP). *NMR Biomed.* **2015,** *28*, 1021-1030.

36. Adams, R. W.; Aguilar, J. A.; Atkinson, K. D.; Cowley, M. J.; Elliott, P. I. P.; Duckett, S. B.; Green, G. G. R.; Khazal, I. G.; Lopez-Serrano, J.; Williamson, D. C., Reversible Interactions with para-Hydrogen Enhance NMR Sensitivity by Polarization Transfer. *Science* **2009,** *323*, 1708-1711.

37. Rayner, P. J.; Duckett, S. B., Signal Amplification by Reversible Exchange (SABRE): From Discovery to Diagnosis. *Angew. Chem. Int. Edit.* **2018,** *57*, 6742-6753.

38. Rayner, P. J.; Norcott, P.; Appleby, K. M.; Iali, W.; John, R. O.; Hart, S. J.; Whitwood, A. C.; Duckett, S. B., Fine-tuning the efficiency of *para*-hydrogen-induced hyperpolarization by rational N-heterocyclic carbene design. *Nat. Commun.* **2018,** *9*, 4251.

39. Sini, G.; Eisenstein, O.; Crabtree, R. H., Preferential C-binding versus N-binding in imidazole depends on the metal fragment involved. *Inorg. Chem.* **2002,** *41*, 602-604.

40. Meier, N.; Hahn, F. E.; Pape, T.; Siering, C.; Waldvogel, S. R., Molecular recognition utilizing complexes with NH,NR-stabilized carbene ligands. *Eur. J. Inorg. Chem.* **2007,** *9*, 1210-1214.

41. Wang, X. J.; Chen, H. Y.; Li, X. W., Ir(III)-induced C-bound to N-bound tautomerization of a N-heterocyclic carbene. *Organometallics* **2007,** *26*, 4684-4687.

42. (a) Ruiz, J.; Perandones, B. F., Base-promoted tautomerization of imidazole ligands to N-heterocyclic carbenes and subsequent transmetalation reaction. *J. Am. Chem. Soc.* **2007,** *129*, 9298-9299. (b) Ito, Y.; Hirao, T.; Tsubata, K.; Saegusa, T. A New Preparation of Imidazolidinylidene Palladium(II) Complexes. *Tetrahedron Lett.* **1978**, *19*, 1535−1538. (c) Tan, T. T. Y.; Hahn, F. E., Synthesis of Iridium(III) and Rhodium(III) Complexes Bearing C8-Metalated Theophylline Ligands by Directed C–H Activation. *Organometallics* **2019,** *38*, 2250-2258.

43. Chernyshev, V. M.; Khazipov, O. V.; Shevchenko, M. A.; Chernenko, A. Y.; Astakhov, A. V.; Eremin, D. B.; Pasyukov, D. V.; Kashin, A. S.; Ananikov, V. P., Revealing the unusual role of bases

in activation/deactivation of catalytic systems: O-NHC coupling in M/NHC catalysis. *Chem. Sci.* **2018,** *9*, 5564-5577.

44. Polynski, M. V.; Ananikov, V. P., Modeling Key Pathways Proposed for the Formation and Evolution of "Cocktail"-Type Systems in Pd-Catalyzed Reactions Involving ArX Reagents. *ACS Catal.* **2019,** *9*, 3991-4005.

45. He, F.; Danopoulos, A. A.; Braunstein, P., Trifunctional *p*NHC, Imine, Pyridine Pincer-Type Iridium(III) Complexes: Synthetic, Structural, and Reactivity Studies. *Organometallics* **2016,** *35*, 198-206.

46. Rubio-Perez, L.; Iglesias, M.; Munarriz, J.; Polo, V.; Passarelli, V.; Perez-Torrente, J. J.; Oro, L. A., A well-defined NHC-Ir(III) catalyst for the silylation of aromatic C–H bonds: substrate survey and mechanistic insights. *Chem. Sci.* **2017,** *8*, 4811-4822.

47. Mo, F. Y.; Dong, G. B., Regioselective ketone-alkylation with simple olefins via dual activation. *Science* **2014,** *345*, 68-72.

48. Malapit, C. A.; Bour, J. R.; Brigham, C. E.; Sanford, M. S., Base-free nickel-catalysed decarbonylative Suzuki-Miyaura coupling of acid fluorides. *Nature* **2018,** *563*, 100-104.

49. McGrath, N. A.; Brichacek, M.; Njardarson, J. T., A Graphical Journey of Innovative Organic Architectures That Have Improved Our Lives. *J. Chem. Educ.* **2010,** *87*, 1348-1349.

50. Rueda-Becerril, M.; Mahe, O.; Drouin, M.; Majewski, M. B.; West, J. G.; Wolf, M. O.; Sammis, G. M.; Paquin, J. F., Direct C–F Bond Formation Using Photoredox Catalysis. *J. Am. Chem. Soc.* **2014,** *136*, 2637-2641.

51. Xia, J. B.; Zhu, C.; Chen, C., Visible Light-Promoted Metal-Free C–H Activation: Diarylketone-Catalyzed Selective Benzylic Mono- and Difluorination. *J. Am. Chem. Soc.* **2013,** *135*, 17494-17500.

52. Arai, Y.; Tomita, R.; Ando, G.; Koike, T.; Akita, M., Oxydifluoromethylation of Alkenes by Photoredox Catalysis: Simple Synthesis of CF_2H-Containing Alcohols. *Chem. Eur. J.* **2016,** *22*, 1262-1265.

53. Salaun, J., 1-Ethynylcyclopropyl Tosylate Solvolysis .2. Para-Aryl Substituent Effect Upon Rate and Product Distribution. *J. Org. Chem.* **1977,** *42*, 28-32.

54. Liu, J.; An, Y.; Jiang, H. Y.; Chen, Z. L., 1-(Arylsulfonyl)cyclopropanol, a new cyclopropanone equivalent and its application to prepare 1-alkynyl cyclopropylamine. *Tetrahedron Lett.* **2008,** *49*, 490-494.

55. Kammer, L. M.; Rahman, A.; Opatz, T., A Visible Light-Driven Minisci-Type Reaction with N-Hydroxyphthalimide Esters. *Molecules* **2018,** *23*, 764.

56. Li, Z. L.; Wang, X. F.; Xia, S. Q.; Jin, J., Ligand-Accelerated Iron Photocatalysis Enabling Decarboxylative Alkylation of Heteroarenes. *Org. Lett.* **2019,** *21*, 4259-4265.

57. Huihui, K. M. M.; Caputo, J. A.; Melchor, Z.; Olivares, A. M.; Spiewak, A. M.; Johnson, K. A.; DiBenedetto, T. A.; Kim, S.; Ackerman, L. K. G.; Weix, D. J., Decarboxylative Cross-Electrophile Coupling of N-Hydroxyphthalimide Esters with Aryl Iodides. *J. Am. Chem. Soc.* **2016,** *138*, 5016-5019.

58. Dickschat, J. V.; Urban, S.; Pape, T.; Glorius, F.; Hahn, F. E., Sterically demanding and chiral N,N'- disubstituted N-heterocyclic germylenes and stannylenes. *Dalton Trans.* **2010,** *39*, 11519-11521.

59. Lu, Z. Y.; Demianets, I.; Hamze, R.; Terrile, N. J.; Williams, T. J., A Prolific Catalyst for Selective Conversion of Neat Glycerol to Lactic Acid. *ACS Catal.* **2016,** *6*, 2014-2017.

60. Braun, M.; Frank, W.; Reiss, G. J.; Ganter, C., An N-Heterocyclic Carbene Ligand with an Oxalamide Backbone. *Organometallics* **2010,** *29* , 4418-4420.

61. Shriver, D. F.; Drezdzon, M. A. *The manipulation of air-sensitive compounds*. Wiley: New York; Chichester, 1986.

62. Still, W. C.; Kahn, M.; Mitra, A., Rapid Chromatographic Technique for Preparative Separations with Moderate Resolution. *J. Org. Chem.* **1978,** *43*, 2923-2925.

63. Nakatake, D.; Yokote, Y.; Matsushima, Y.; Yazaki, R.; Ohshima, T., *Green Chem.* **2016,** *18*, 1524-1530.

64. Boga, C.; Del Vecchio, E.; Forlani, L.; Todesco, P. E., *J. Organomet. Chem.* **2000,** *601*, 233-236.

65. (a) Bruno, N. C.; Tudge, M. T.; Buchwald, S. L., *Chem. Sci.* **2013,** *4*, 916-920. (b) Zalesskiy, S. S.; Ananikov, V. P., *Organometallics* **2012,** *31*, 2302-2309.

66. Butini, S.; Gabellieri, E.; Brindisi, M.; Giovani, S.; Maramai, S.; Kshirsagar, G.; Guarino, E.; Brogi, S.; La Pietra, V.; Giustiniano, M.; Marinelli, L.; Novellino, E.; Campiani, G.; Cappelli, A.; Gemma, S., *Eur. J. Med. Chem.* **2013,** *70*, 233-247.

67. Tong, L. P.; Zong, R. F.; Thummel, R. P., *J. Am. Chem. Soc.* **2014,** *136*, 4881-4884.

68. Bevilacqua, V.; King, M.; Chaumontet, M.; Nothisen, M.; Gabillet, S.; Buisson, D.; Puente, C.; Wagner, A.; Taran, F., *Angew. Chem. Int. Edit.* **2014,** *53*, 5872-5876.

69. Smith, A. P.; Lamba, J. J. S.; Fraser, C. L. *Org. Synth.* **2002**, *78*, 82-90.

70. Gaydou, M.; Moragas, T.; Julia-Hernandez, F.; Martin, R., Site-Selective Catalytic Carboxylation of Unsaturated Hydrocarbons with CO_2 and Water. *J. Am. Chem. Soc.* **2017,** *139*, 12161-12164.

71. Fogler, E.; Balaraman, E.; Ben-David, Y.; Leitus, G.; Shimon, L. J. W.; Milstein, D., *Organometallics* **2011,** *30*, 3826-3833.

72. Zhang, Z. Y.; Yang, Y.; Sun, H. Y.; Cao, R., *Inorg. Chim. Acta.* **2015,** *434*, 158-171.

73. Zeng, F. L.; Yu, Z. K., *J. Org. Chem.* **2006,** *71*, 5274-5281.

74. Grieco, G.; Blacque, O.; Berke, H., A facile synthetic route to benzimidazolium salts bearing bulky aromatic N-substituents. *Beilstein J. Org. Chem.* **2015,** *11*, 1656-1666.

75. Vazquez-Serrano, L. D.; Owens, B. T.; Buriak, J. M., Catalytic olefin hydrogenation using N-heterocyclic carbene-phosphine complexes of iridium. *Chem. Commun.* **2002,** 2518-2519.

76. Mao, R. Z.; Balon, J.; Hu, X. L., Decarboxylative C(sp^3)-O Cross-Coupling. *Angew. Chem. Int. Ed.* **2018,** *57*, 13624-13628.

77. For the characterization references, see: (a) Shen, A.; Hu, Y. C.; Liu, T. T.; Ni, C.; Luo, Y.; Cao, Y. C., *Tetrahedron Lett.* **2016,** *57*, 2055-2058. (b) Li, Y. B.; Wang, J. R.; Wang, Z. W.; Huang, M. M.; Yan, B. Q.; Cui, X. L.; Wu, Y. S.; Wu, Y. J., *Rsc Adv.* **2014,** *4*, 36262-36266. (c) Denmark, S. E.; Butler, C. R. *Org. Lett.* **2006**, *8*, 63-66. (d) Wu, D.; Wang, Z. X., *Org. Biomol. Chem.* **2014,** *12*, 6414-6424. (e) Liu, Q. X.; Cai, K. Q.; Zhao, Z. X., *Rsc. Adv.* **2015,** *5*, 85568-85578. (f) Zhang, G. *Synthesis* **2005**, 537-542.

78. For the characterization references, see: (a) Moulton, B. E.; Whitwood, A. C.; Duhme-Klair, A. K.; Lynam, J. M.; Fairlamb, I. J. S. *J. Org. Chem.* **2011**, *76*, 5320-5334. (b) Ho, K. Y. T.; Aissa, C. *Chem. Eur. J.* **2012**, *18*, 3486-3489. (c) Baralle, A.; Yorimitsu, H.; Osuka, A. *Chem. Eur. J.* **2016**, *22*, 10768-10772. (d) Melzig, L.; Metzger, A.; Knochel, P. *Chem. Eur. J.* **2011**, *17*, 2948-2956. (e) Kim, H.; Lee, P. H. *Adv. Synth. Catal.* **2009**, *351*, 2827-2832. (f) Feuerstein, M.; Doucet, H.; Santelli, M. *J. Mol. Catal. A: Chem.* **2006**, *256*, 75-84. (g) Panteleev, J.; Huang, R. Y.; Lui, E. K. J.; Lautens, M. *Org. Lett.* **2011**, *13*, 5314-5317.

79. For the characterization references, see: (a) Kantam, M. L.; Redddy, P. V.; Srinivas, P.; Venugopal, A.; Bhargava, S.; Nishina, Y. *Catal. Sci. Technol.* **2013**, *3*, 2550-2554. (b) Stern, T.; Ruckbrod, S.; Czekelius, C.; Donner, C.; Brunner, H. *Adv. Synth. Catal.* **2010**, *352*, 1983-1992. (c) Alt, I. T.; Plietker, B. *Angew. Chem., Int. Ed.* **2016**, *55*, 1519-1522. (d) Wei, Y. L.; Li, Y.; Chen, Y. Q.; Dong, Y.; Yao, J. J.; Han, X. Y.; Dong, Y. B. *Inorg. Chem.* **2018**, *57*, 4379-4386. (e) Udumula, V.; Tyler, J. H.; Davis, D. A.; Wang, H.; Linford, M. R.; Minson, P. S.; Michaelis, D. J. *ACS Catal.* **2015**, *5*, 3457-3462. (f) Cahiez, G.; Gager, O.; Lecomte, F. *Org. Lett.* **2008**, *10*, 5255-5256. (g) Prukała, W.; Majchrzak, M.; Pietraszuk, C.; Marciniec, B. *J. Mol. Catal. A: Chem.* **2006**, *254*, 58-63. (h) Borate, H. B.; Dumbre, D. K.; Wakharkar, R. D.; Choudhary, V. R. *J. Chem. Res.* **2008**, 495-499. (i) Bandari, R.; Höche, T.; Prager, A.; Dirnberger, K.; Buchmeiser, M. R. *Chem. Eur. J.* **2010**, *16*, 4650-4658.